Brage Høyem Amundsen

Myocardial function quantified by speckle tracking and tissue Doppler echocardiography – Validation and application in exercise testing and training

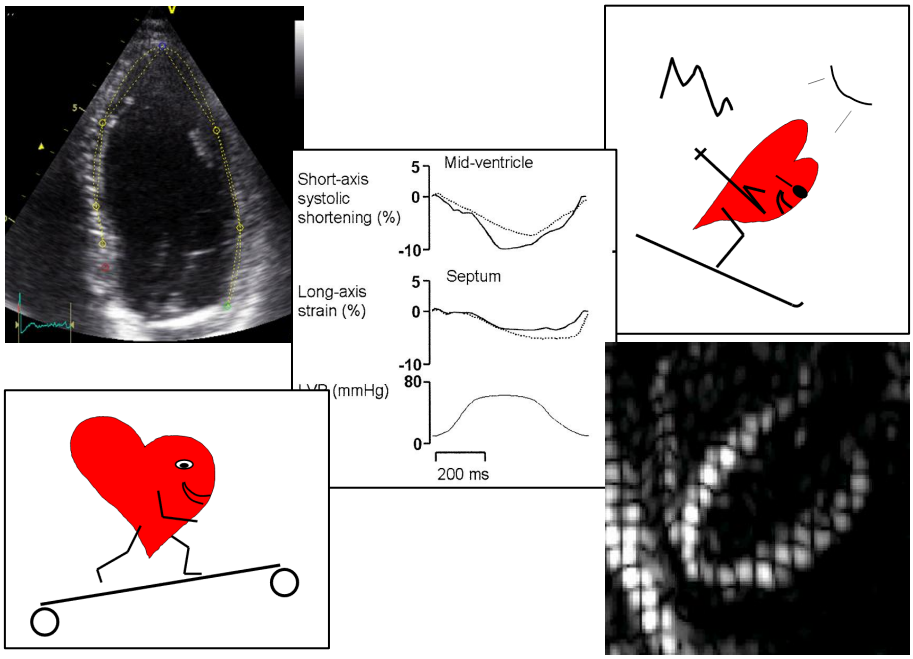

Thesis for the degree of philosophiae doctor

Trondheim October 2007

Department of Circulation and Medical Imaging
Faculty of Medicine
Norwegian University of Science and Technology

NTNU
Norwegian University of Science and Technology

Måling av hjertemuskelfunksjon med ultralyd vevs-Doppler og mønsterfølging (speckle tracking)
– Validering og bruk under arbeidsbelastning og trening

Ultralyd av hjertet (ekkokardiografi) er en relativt rimelig og lett tilgjengelig undersøkelse, og brukes ofte for å vurdere hvor mye de ulike delene av hjertet trekker seg sammen, og dermed hvor mye de bidrar til hjertet sin samlede pumpekraft. Hos pasienter med angina pectoris og hjerteinfarkt (koronarsykdom) er påvisning av skadde og svekkede områder viktig for riktig diagnose og behandling. De seneste årene har man, blant annet ved NTNU, utviklet flere nye metoder som kan gjøre slike målinger. I denne avhandlingen har vi undersøkt hvor nøyaktige og robuste disse metodene er, blant annet ved å sammenligne måleresultatene med tilsvarende målinger ved hjelp av magnet resonans tomografi (MR). Den ene metoden (vevs-Doppler) er basert på Doppler-prinsippet, mens den andre metoden (speckle tracking) er basert på å følge spesielle mønstre (speckle) i ultralydbildet ved hjelp av bildeanalyse-programmer. Studiene vi har gjort viser at metoder som bruker speckle tracking virker lovende, og kan ha fordeler i forhold til vevs-Doppler. Imidlertid trengs videre forbedring, særlig fordi variasjonen i målingene fortsatt er betydelig. Vi mener at ulike kombinasjoner av de to metodene bør studeres nærmere.

Som en del av avhandlingen har vi også brukt disse metodene for å studere hvordan hjertet arbeider under fysisk belastning (sykling), og hvordan dette endrer seg når hjertet er skadet etter et hjerteinfarkt. Vi fant at det særlig var forskjell i hvor godt de friske og skadde hjertene slappet av og sugde inn nytt blod i de korte pausene mellom hver sammentrekning (hvert hjerteslag). Dette kan sannsynligvis være en del av forklaringen på hvorfor pasientene merker at de orker mindre fysisk aktivitet enn før. Vi studerte også effekten av trening med ulik intensitet på hjertets funksjon hos pasienter med koronarsykdom. Trening på tredemølle med relativt høy intensitet så ut til å bedre hjertet sin evne til å slappe av og dermed suge inn blod mer effektivt mellom hvert hjerteslag. Det så ikke ut til at trening med moderat intensitet hadde den samme effekten. Samlet viser dette at ultralyd kan gi ny viten om hvordan hjertet jobber under belastning, og hvordan det tilpasser seg ulike typer trening. Selv om flere studier trengs, vil denne kunnskapen forhåpentligvis kunne bidra til at flere pasienter med hjertesykdom får mer effektiv behandling, særlig i form av riktig trening.

Brage Høyem Amundsen
Institutt for sirkulasjon og bildediagnostikk, NTNU
Hovedveileder: Stig A. Slørdahl
Biveiledere: Asbjørn Støylen og Hans Torp
Finansieringskilder: NTNU (SUP2) og St.Olavs Hospital

Ovennevnte avhandling er funnet verdig til å forsvares offentlig for graden philosophiae doctor i medisinsk teknologi.
Disputas finner sted i Auditoriet i Laboratoriesenteret (LA21), St. Olavs Hospital torsdag 24. januar 2008 kl. 12.15.

Contents

1. Acknowledgements

I would like to thank the Norwegian University of Science and Technology for giving me a scholarship in the SUP 2-programme from 2003 to 2006. The work has been carried out at the Department of Circulation and Medical Imaging, and I highly appreciate the extraordinary good colleagues I have had during these years. I am also grateful to the Department of Cardiology at St. Olavs Hospital, who gave me half a year scholarship in 2003, and GE Vingmed Ultrasound for valuable technical assistance and access to their hard- and software.

Stig A. Slørdahl has been my main supervisor. He was the one who guided me into cardiovascular ultrasound when I got interested in doing research, and I really appreciate the knowledge and enthusiasm you have demonstrated during these years. You are a good teacher in many ways. Asbjørn Støylen has been my co-supervisor, and both before, and especially after, Stig became the dean of the faculty, you have been a very important man for me. You're almost annoyingly full of knowledge, both in the fields of echocardiography and cardiology, but also in a lot of other topics that are most of the times relevant, and always interesting.

On the technical side, I have been lucky to have Hans Torp as my co-supervisor. He is the one to blame, or actually honour, for the times I have been mistaken for being an engineer. I am very grateful to you for the technological insight you have given me in the field of ultrasound.

Jonas Crosby has been an important co-worker in this thesis, and his skills have impressed me several times. Although he is accusing me of having a lemon-shaped left ventricle, I miss him now when he has moved south. Svein Arne Aase has also done an impressive job with the analysis-tools. Lene Anette Rustad did an honest piece of work with study III. I really look forward to continuing working with you all.

I would also like to express my gratitude to Thomas Helle-Valle, Thor Edvardsen, Otto Smiseth and their colleagues at the Department of Surgical Research at Rikshospitalet in Oslo. Without the cooperation with them, paper I would not have been possible. I hope we can do that again.

Per Arvid Steen at the Dept. of Medical Imaging at St. Olavs Hospital did the MRI-acquisitions in study II. I would also like to thank the Dept. of Medical Imaging at St. Olavs Hospital for employing me as a civilian national serviceman, and give me the opportunity to work with cardiac MRI. The research nurses at the Department of Cardiology, Eli Granviken and Ann-Elise Antonsen helped us with recruiting patients to the studies. Thank you very much.

Øivind Rognmo and Ulrik Wisløff also deserve mentioning. I have shared offices with both of you, which has been very nice, and an important reason why I have always been

looking forward to going to work. I wonder if we will ever share a three-person hotel room in a suburban area outside Vienna again.

My mother and father, thank you for being so supportive and for teaching me both theory and practice. Silje and Asbjørn, thank you for the opportunity to test it out☺

Finally, I would like to thank you, Cathrine, for being who you are, and for being so patient with me during the work with this thesis. You are the most important person for me, but now have to share that position with Erling, who gives us so much joy and surprises. He has been very lucky with his choice of mother.

2. List of papers

Paper I
Amundsen BH, Helle-Valle T, Edvardsen T, Torp H, Crosby J, Lyseggen E, Støylen A, Ihlen H, Lima JAC, Smiseth OA, Slørdahl SA. Non-invasive Myocardial strain measurement by speckle tracking echocardiography – validation against sonomicrometry and tagged magnetic resonance imaging. J Am Coll Cardiol. 2006;47:789-93.

Paper II
Amundsen BH, Crosby J, Steen PA, Torp H, Slørdahl SA, Støylen A. Regional myocardial long-axis strain and strain rate measured by different tissue Doppler and speckle tracking echocardiography methods –a comparison with tagged magnetic resonance imaging. Submitted.

Paper III
Rustad LA, Amundsen BH, Slørdahl, SA, Støylen, A. Upright bicycle exercise echocardiography in patients with myocardial infarction shows lack of diastolic, but not systolic, reserve – a tissue Doppler study. Submitted.

Paper IV
Amundsen BH, Rognmo Ø, Hatlen-Rebhan G, Slørdahl SA. High-intensity aerobic exercise improves diastolic function in coronary artery disease. Published ahead of print in *Scandinavian Cardiovascular Journal* 13.11.2007. DOI: 10.1080/14017430701744477.

3. Abbreviations and definitions

2D Strain	Speckle tracking application (GE Vingmed Ultrasound)
A_{SR}	Peak late diastolic strain rate
A_m	Peak late diastolic mitral annular velocity
AVC	Aortic valve closure
CO	Cardiac output
CAD	Coronary artery disease
COR	Coefficient of repeatability
COV	Coefficient of variation
E	Early mitral filling velocity
E_{SR}	Peak early diastolic strain rate
E_m	Peak early diastolic mitral annular velocity
EF	Left ventricular ejection fraction
HR	Heart rate
LOA	Limits of agreement
LV	Left ventricle
MI	Myocardial infarction
MRI	Magnetic resonance imaging
ROI	Region of interest
SD	Standard deviation
SR	Strain rate
S_{SR}	Peak systolic strain rate
S_m	Peak systolic mitral annular velocity
ST-7P	Speckle tracking (GcMat application, 7 kernels)
TDI	Tissue Doppler Imaging
TDI+ST	Method combining TDI and speckle tracking (segment length)
TDI-VG	Strain/-rate calculated from tissue Doppler velocity gradients
VO_{2max}	Maximal oxygen consumption
VO_{2peak}	Peak oxygen consumption
WMS	Wall motion score

4. Background

4.1. Tissue Doppler Imaging

The Doppler equation states that the velocity (v) of a moving reflector is given by

$$v = \frac{f_d \cdot c}{2 \cdot f_0 \cdot \cos\theta}$$

where f_0 is the emitted frequency, f_d is the Doppler shift, c is the velocity of sound in the medium and θ is the angle between the direction of the emitted sound and the direction of the moving object. In echocardiography this equation can be applied to both blood and tissue. McDicken et al published the first paper on myocardial velocity measurements by tissue Doppler in 1992 (1). Tissue velocities can be measured both with the pulsed wave (PW) method and the colour Doppler method. In PW tissue Doppler the whole frequency spectrum of the Doppler shift is displayed, while in colour tissue Doppler only the mean frequency of the Doppler shift is shown. Since 1992 tissue Doppler imaging (TDI) (or Doppler tissue imaging, Doppler Myocardial imaging, tissue velocity imaging) has become a widely used method, and a Pubmed search for the years 1992 – 2007 yields over 1300 hits for these terms.

Two velocity curves from the septum in a normal subject are showed in Figure 1A. Higher velocities are found near the mitral annulus, demonstrating the base-to-apex velocity gradient. A PW trace of blood velocities between the mitral and aortic valves is included below to show the timing of aortic valve closure (AVC), which defines end-systole, and mitral valve opening, which defines the end of the isovolumic relaxation period and the start of left ventricular (LV) filling (Figure 1B).

4.1.1. Limitations of TDI

Diagnosis of coronary artery disease (CAD) can be done by echocardiography by looking at regional differences in myocardial function in the LV during pharmacological or exercise stress. In most hospitals the assessment of regional function is made by looking at wall thickening (wall motion score, WMS), which is a semi-quantitative method with moderate inter-observer agreement (2). An important advantage for TDI is that it is a quantitative and more objective method. However, there are some important limitations:

- Tethering

Tethering exists when one part of myocardium pulls on a neighbour part of myocardium. This will give the neighbour tissue a velocity which is not necessarily due to its own contraction. Tethering will cause problems in diagnosis of CAD because regions with impaired contractile function might have normal velocity due to tethering.

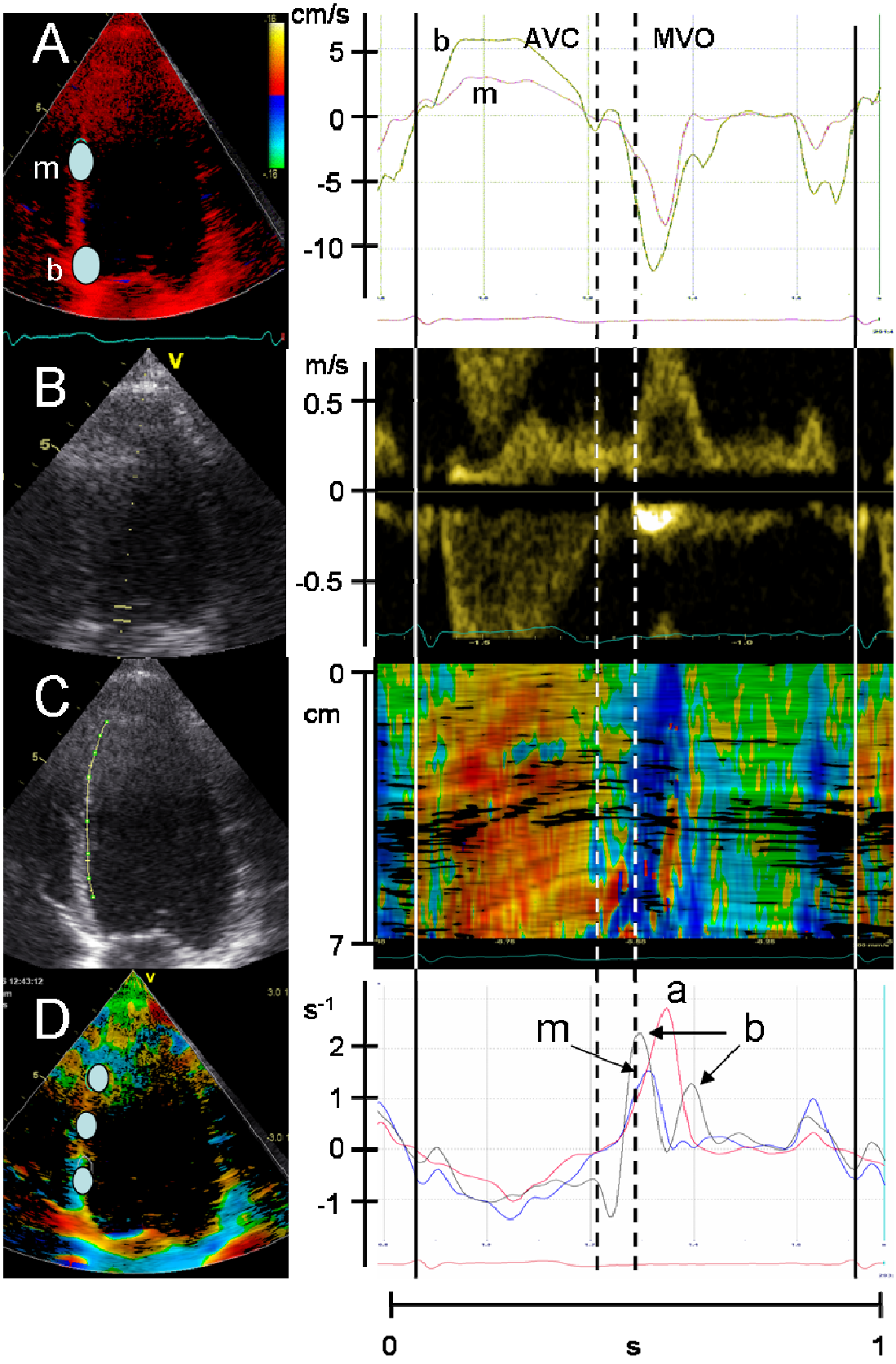

Figure 1.

Figure 1A. Tissue Doppler velocity curves from the basal (b) and mid-ventricular (m) parts of the interventricular septum in a young healthy subject. Higher velocities are seen near the base during all cardiac phases. Aortic valve closure (AVC) and mitral valve opening (MVO) are derived from the PW blood flow trace recorded between the mitral and aortic valves for determination of the isovolumic relaxation time in Figure **1B**. An anatomical M-mode of strain rate (SR) in the septum is shown in Figure **1C**. Yellow and red colours mean shortening; green means no deformation and blue means elongation. Systolic shortening starts nearly simultaneously, while early and late diastolic relaxation mainly spread as a wave starting from the basis. In the last part of the early phase a smaller wave travelling in the opposite direction can be seen. These two waves present as two peaks in the early diastolic phase of the SR tracing from the basal segment, while only one peak is present in the apical segment (Figure **1D**). The second wave might represent a reflection of the first wave from the apex, or a continuation of the first wave from the opposite wall (3). Note the relatively similar systolic SR values in the different segments (a=apical, m=midventricular, b=basal).

- Aliasing

Aliasing occurs when the sampling rate is not high enough relative to the actual velocity to be measured. According to the Nyquist-theorem the maximal measurable Doppler shift frequency can be half the sampling rate before aliasing occurs. Sampling rate equals the pulse repetition frequency in PW Doppler. Aliasing presents as a wrap-around effect; the velocities that are too high relative to the pulse repetition frequency are shown on the opposite side of the scale. Aliasing is prevented by increasing the pulse repetition frequency (sampling rate). An example of aliasing can be seen in the PW flow velocity curve in Figure 1B during systole (flow in the LV outflow tract).

- Global heart motion

Global motion of the heart during systole and diastole influences the regional velocities, but will not be linked to regional function, and will therefore not differ between normal and dysfunctional segments.

- Translation in the image plane

As the tissue Doppler sample volume is stationary, different parts of myocardium will be imaged during the cardiac cycle. Manual or automated tracking of the sample volume can be used to avoid this. A drawback with the automated alternative is that tissue Doppler information does not allow tracking in the lateral direction.

- Angle dependency

Only one of the three velocity components can be measured by using the Doppler-effect. Therefore, velocity measurements by ultrasound Doppler are sensitive to misalignment between the direction of motion of the object and the direction of the ultrasound wave. The error is the same in blood and tissue velocity measurements, and is proportional to the *cosine* of the angle. Thus, the error is below 10 % for deviations less than 25°, but will be larger if the measurements are used to calculate pressure gradients (blood, not tissue Doppler), or velocity gradients (see below). Angle correction can be applied in blood velocity measurements in vessels because the flow

direction can be predicted from the vessel geometry, and because the flow direction is constant during the cardiac cycle. Angle correction can not be applied in tissue Doppler because the direction of tissue velocities is difficult to predict, and also varies considerably during the cardiac cycle.

- Drop-outs

Loss of signal in a part of the image is most often due to ribs or lung tissue. Tissue velocity signal may still be picked up in regions with low signal, but these signals are probably not from the area with low signal, but from nearby regions with stronger reflectors. This can be explained by wide beams (low lateral resolution) and the presence of sidelobes.

- Sidelobes

Sidelobes are an acoustic phenomenon caused by focusing of the ultrasound wave (Figure 2). The sidelobes are present at certain positions lateral to the main lobe, and if this part of the wave is reflected, these echoes will be handled by the scanner as if they were from the main lobe. Consequently, they will appear in the image as if they were positioned in the field of the main lobe.

- Low lateral resolution

If frame rate is set too high, fewer and wider beams will be used to cover the image sector. Wide beams decrease the lateral resolution, and the lateral parts of these broad beams might be reflected by strongly reflecting tissue as explained above. This is relevant for instance in relation to the pericardium, which is a strong reflector, but not the tissue of interest.

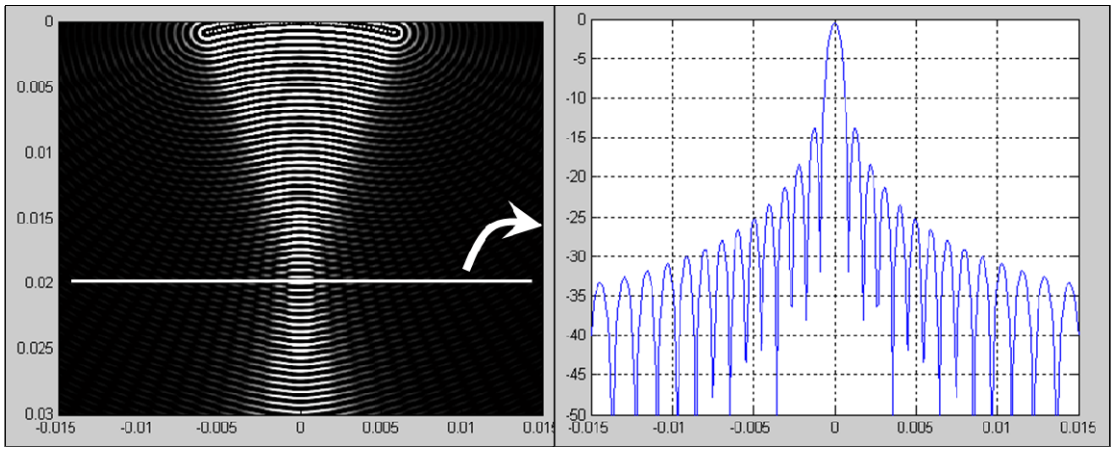

Figure 2. Illustration of the beam formed by a linear transducer, showing the sidelobes next to the main beam. The intensity across the field at the level of the focus depth is shown to the right. Simulation tool made by Hans Torp.

- Reverberations

An important artefact is stationary reflections called reverberations. They arise from sound pulses travelling several times between the probe and strong reflectors, especially between the probe and the chest wall. In PW tissue Doppler reverberations can be

separated from the true tissue velocity because all frequencies in the Doppler shift are displayed, and reverberations generally appear as a constant and low-velocity signal. In colour tissue Doppler this is not possible, as only the mean Doppler shift frequency is displayed.

- Through-plane motion

Through-plane motion causes two limitations of the Doppler velocity measurements. First, the tissue velocity components with direction out of the image plane cannot be measured by tissue Doppler. Second, through plane motion leads to errors if the velocity of the tissue that enters the image differs from the velocity of the tissue that is replaced.

4.2. Strain Rate Imaging

The first papers proposing that the myocardial velocity gradient could be used to quantify regional myocardial function were published in the middle of the 1990-s (4-7). A real-time application called strain rate imaging (SRI) was developed at the Dept. of Physiology and Biomedical Engineering at NTNU by Andreas Heimdal *et al* in the end of the 1990-s (8-10). SRI was designed to overcome some of the most important problems in TDI for evaluation of regional myocardial function (11). The main idea is to use the velocity gradient along the LV wall as it is shown in Figure 1A, under the assumption that reduced regional function in a segment of myocardium would cause a lower velocity gradient in this area. This approach eliminates the errors introduced by tethering and global heart motion in evaluation of regional myocardial function. Euler strain rate (SR) is defined as the velocity gradient, and is given by the following formula:

$$SR = \frac{v(x) - v(x + \Delta x)}{\Delta x}$$

where $v(x)$ and $v(x+\Delta x)$ are myocardial velocities in two points of myocardium along the ultrasound beam, separated by a distance Δx. The noise in SR measurements can be reduced by calculating the slope of the linear regression line fitted to all pixel velocities along a segment with length Δx. The SR values calculated in this way will be more robust because a higher number of measurements are averaged. Typical SR traces from the basal, midventricular and apical septum in a healthy subject is shown in Figure 1D. The most important difference relative to the tissue velocity traces is the relatively similar value for peak systolic SR in segments at different levels of the LV. SR is by convention negative for tissue shortening, and positive for tissue elongation.

SR can be integrated over time to give Lagrangian strain (ε), which is relative elongation, and given by the formula

$$\varepsilon = \frac{L_1 - L_0}{L_0}$$

where L_0 is tissue length at time=0 and L_1 is length at a certain time=1 afterwards. Negative strain values indicate tissue shortening Regional myocardial strain

measurements from TDI has been validated against sonomicrometry and MRI tagging (12,13). From a physiological point of view, both peak systolic SR and end-systolic strain are linked to myocardial contractile function, but end-systolic strain is more influenced by load and related to stroke volume (SV) (14).

4.2.1. Limitations of SRI

Strain and SR measurements by tissue Doppler velocity gradients have been shown to be equal or superior to tissue Doppler velocities and WMS for diagnosis of myocardial ischemia in experimental settings, and for significant coronary artery stenosis in clinical settings (15-20). SRI can also improve the accuracy in determination of myocardial viability (21,22). The prognostic significance of SR measurements on a global LV level during dobutamine stress echocardiography has recently been demonstrated (23).

Even with this track record, SRI has not become a standard tool for the common cardiologist. This is due to large random measurement errors, and frequent occurrence of artefacts which can only be fully recognised by expert readers (24). The artefacts discussed under TDI also occur in SRI, but some of them have different consequences when SR is calculated from the tissue Doppler data (Figure 3):

- Tethering

Tethering is not a problem in SRI because the regional deformation is calculated from the difference between velocities in the actual region. This is a major advantage of the method compared to TDI.

- Aliasing

Calculation of SR in regions with both aliased and non-aliased velocities is possible if the scanner has been programmed to use the velocity estimate which is compatible with the measured Doppler shift, and at the same time most likely according to the velocity measured at the previous time point. SR will be correctly calculated when all velocities within a region are aliased.

- Global heart motion

As for tethering, the velocity gradient principle will remove the effects of global heart motion on the SR calculations.

- Translation

Translation is a problem for SRI in the same way as for TDI.

- Angle-dependency

Angle dependency can lead to larger errors in SRI than in TDI. This is due to the three-dimensional deformation of the myocardium; the wall thickens transmurally as it gets shorter in the long-axis direction. For measurements of long-axis SR, angle misalignment between the ultrasound beam and the LV wall will lead to a larger component of the wall thickening being picked up, and give too low values for SR in the long-axis direction. The size of the error depends not only on the angle, but also on

the relation between long-axis shortening and wall thickening in the region (25). An error of 25 ° will in most cases give an error in the SR estimate of at least 30 %.

- Reverberations

A stationary echo in the image is interpreted as stationary tissue. For measurements of longitudinal SR in an apical image, a reverberation in a region of normal tissue will result in too high SR values calculated on the basal side, where tissue moves against the reverberation, and too low SR values on the apical side, where tissue moves away from the reverberation. In the SR anatomical M-mode the presence of a reverberation can be seen as a region with an abrupt transition between horizontally aligned bands of highly positive and highly negative strain rates.

- Through-plane motion

This is a problem in SRI in the same way as in TDI.

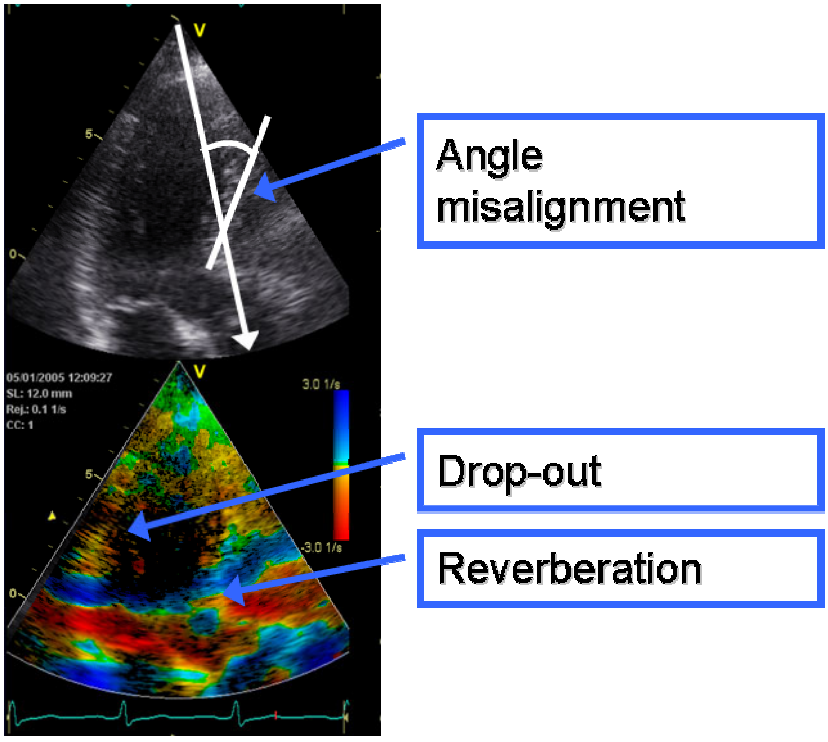

Figure 3. Illustration of some important artefacts in SRI. For long-axis measurements the angle misalignment is measured between the long-axis of the LV wall and the ultrasound beam direction. It is important to emphasise that this only quantifies the angle misalignment in one of three directions, and that such angle quantifications cannot be used to do angle correction. Drop-outs are seen as low signal intensity in the B-mode image. Reverberations are seen as abrupt transitions between opposite colours in the SR image, and as grey bands across the image in the background B-mode image.

4.3. Speckle tracking echocardiography

Ultrasound speckles are brightness-patterns in the ultrasound image originating from reflections and interference of sound from or between a large number of scatterers at different distance from the transducer. Therefore, the speckle pattern is tissue specific, but does not mimic the real tissue structure. In addition, images of myocardium will also contain signal from larger-size reflectors, due to tissue sheath structures, connective tissue and blood vessels. Variations in reflectivity due to different fibre angles relative to the ultrasound beam will contribute to the variation in signal intensity. A speckle pattern can also be seen in the blood in the LV cavity if the image quality is good and the frequency is somewhat higher then the standard 1.5-2.0 MHz. This pattern is thought to originate from reflections and interference between conglomerates of red blood cells. The origin of the speckle pattern is illustrated in Figure 4.

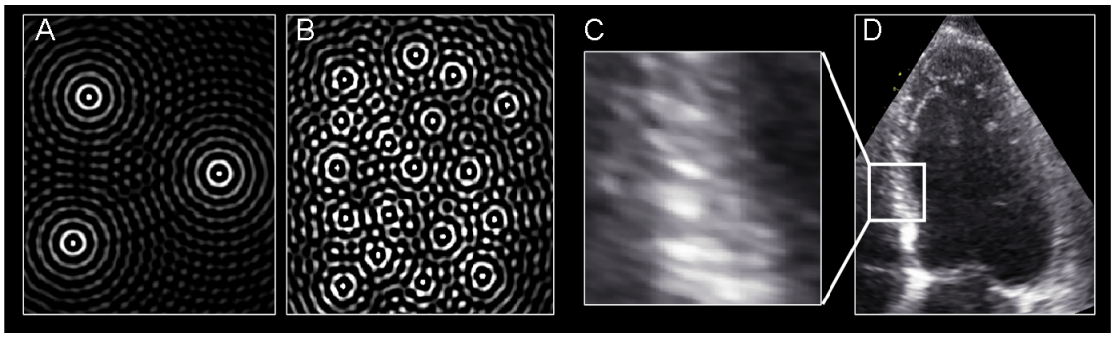

Figure 4. Illustration of the nature of the speckle pattern. The regular interference pattern created by sound waves from three sources (scatterers) is shown in the simulated image in A. The addition of more scatterers in image B results in an irregular interference pattern, which is more like the speckle pattern (C) in the septum in a four-chamber view (D). Simulation tool created by Hans Torp.

Speckle tracking was designed to recognise speckle patterns and measure velocities in moving tissue, including blood, in an angle-independent manner (26). It is based on the assumption that the pattern is characteristic for a specific region of myocardium or blood, and that it is constant from frame to frame, so that the displacement of the region can be followed in time from one frame to the next.

The principle of speckle tracking is illustrated in Figure 2 in paper I. A region (kernel) is selected in the image at time point t_0. The size of the kernel is selected as a compromise between spatial resolution and tracking robustness. In the next image, at time t_1, a larger region is defined around the position of the kernel, this is the search area. The size of the search area should be defined by using *a priori* knowledge of the amplitude and direction of motion of the region that was included in the kernel at t_0. Setting correct size of the search area is essential; if the area is too small it will lead to incorrect tracking and underestimation of the velocities, while a too large area will lead to waste of computational time. In the search area, regions with the same size as the kernel are defined, and the properties in each one of them are compared to same

properties in the kernel from t_0. After the region with the best match has been found, displacement and velocity can be estimated, and the process is repeated in the next frame. The main advantage of speckle tracking methods is that they are less angle dependent than tissue Doppler methods. This results from the ability of the algorithms to track displacement in both dimensions of a two-dimensional image; both along and perpendicular to the ultrasound beam.

Due to the relatively small aperture of the probe and the relatively long distance from the outside of the chest wall to the heart, the lateral resolution in the image is inherently lower than the radial resolution (beam direction). Radial resolution (Δr_z) is given by the formula

$$\Delta r_z = \frac{\lambda}{2} \cdot \frac{1}{Bw(\%)}$$

where λ is the wave length and *Bw(%)* is the bandwidth of the received signal relative to the center frequency. For a cardiac transducer using second harmonic imaging (f=3 MHz and Bw(%)=30 %), radial resolution can be calculated like this:

$$\Delta r_z = \frac{\lambda}{2} \cdot \frac{1}{Bw(\%)} = \frac{0.5\,mm}{2} \cdot \frac{1}{0.3} = 0.83\,mm$$

Lateral resolution (Δr_x) is given by

$$\Delta r_x = F\# \cdot \lambda$$

where $F\#$ is the *F*-number, which is given by the ratio between focal depth and aperture (*F*#=depth/aperture). For the same transducer with an aperture of 2 cm the lateral resolution at depth = 7 cm will be:

$$\Delta r_x = F\# \cdot \lambda = \frac{7\,cm}{2\,cm} \cdot 0.5\,mm = 1.75\,mm$$

This difference in resolution means that tracking will be less accurate in the lateral than in the radial direction. As lateral resolution is depth-dependent, lateral tracking will be less accurate in the deeper parts of the image. Reductions of effective probe aperture by ribs or lung tissue will further reduce the lateral resolution.

The variables that determine the relationship between the lateral and radial resolution can be found by dividing Δr_x by Δr_z:

$$\frac{\Delta r_x}{\Delta r_z} = \left(F\# \cdot \lambda\right) / \left(\frac{\lambda}{2} \cdot \frac{1}{Bw(\%)}\right) = 2 \cdot F\# \cdot Bw(\%)$$

Several different speckle tracking algorithms have been published lately (27-30). One of them used image data in the raw format (RF-data). This is more computational demanding, but in general allows higher temporal resolution than algorithms using B-mode images.

4.3.1. Tracking by sum-of-absolute-differences (SAD)

The formula for the SAD between two regions in images X and Y is

$$SAD_{m,n} = \sum_{i=1}^{l}\sum_{j=1}^{k}\left[X_{i,j} - Y_{i+m,j+n}\right]$$

where *i* and *j* are coordinates of the kernel in image *X*, *m* and *n* are the coordinates of the trial kernel-matching region in image *Y*, and *l* and *k* defines the search area (26). In words, possible matching regions are compared to the original kernel by subtracting pixel intensities, and the region in the search area which has the lowest SAD is taken as the best match. The SAD method is in general less computationally demanding than the cross-correlation method, and has been shown to have similar accuracy for flow and moderate tissue velocities (26).

4.3.2. The cross-correlation method

The formula for calculation of the cross-correlation coefficient between two corresponding image regions in *X* and *Y*, where $\overline{X}$ and $\overline{Y}$ are the mean pixel values of the corresponding image regions, is

$$\rho_{m,n} = \frac{\sum_{i=1}^{l}\sum_{j=1}^{k}\left(X_{i,j} - \overline{X}\right)\left(Y_{i+m,j+n} - \overline{Y}\right)}{\sqrt{\sum_{i=1}^{l}\sum_{j=1}^{k}\left(X_{i,j} - \overline{X}\right)^2 \sum_{i=1}^{l}\sum_{j=1}^{k}\left(Y_{i+m,j+n} - \overline{Y}\right)^2}}$$

where *i* and *j* are coordinates of the region in image *X*, *m* and *n* are the coordinates of the trial kernel-matching region in image *Y*, and *l* and *k* defines the search area. The best match is the region with the highest $\rho_{m,n}$ (26).

4.4. GcMat-application

In the work included in this thesis, a speckle tracking algorithm ("tissuetrack") developed by Hans Torp was implemented in a software toolbox called GcMat (GE Vingmed Ultrasound, Horten, Norway) (31), running under Matlab (MathWorks, Natic, Massachusetts, USA). The implementation allowed speckle tracking to be used alone or in combination with tissue Doppler data.

4.5. 2D Strain

GE Vingmed Ultrasound has introduced a speckle tracking tool called 2D Strain (28). The tool uses both SAD- and correlation-algorithms in the tracking of speckle patterns, and in addition selects regions with special features that are stable through the cardiac cycle. The motion of these regions is tracked, and smoothing is applied by fitting the motion to polynomials.

4.6. Automated analysis

Interpretation of strain and SR curves involves evaluation of both the shape of the curve and registration of the amplitude and timing of specific events, like peak systolic SR and peak systolic strain. When strain and SR are analysed manually in tissue Doppler images, the user has to position the region of interest (ROI) and mark the selected features in the curves. This process can be automated, and this has been done both in GcMat and 2D Strain. This reduces the time for analysis substantially (32), and also increases the objectivity of the measurements.

4.7. Sonomicrometry

Sonomicrometry is an invasive ultrasound method, and has been widely used in experimental models to measure myocardial deformation (33), and has served as a reference method in validation studies for new techniques (12,34,35). The method is based on implanting small ultrasonic crystals into myocardial tissue. These crystals can act both as transmitters and receivers of ultrasound, and are small enough to follow the motion of the surrounding tissue. Thus, the method gives measurements of tissue deformation with high temporal resolution and high accuracy. The method can only be performed in open-chest preparations, and this might alter cardiovascular physiology and mechanics. However, the method serves as a good reference for comparison with ultrasound methods.

4.8. MRI tagging

Magnetic resonance imaging (MRI) is a non-invasive imaging modality based on transmitting and receiving radio frequency signals from atomic nuclei (hydrogen in medical imaging) that are spinning in a strong magnetic field. By setting up additional weaker magnetic fields within this strong field, two-dimensional images with any three-dimensional orientation can be recorded. MRI normally operates with an in-plane pixel size of about 1-2 mm, while the slice thickness for functional cardiac imaging is about 6-10 mm. The major advantage of MRI is image quality, which is generally better than in echocardiography, and also equal in all parts of the image (no difference in lateral resolution with depth). Due to good differentiation between blood and myocardium, MRI is considered the gold standard for measurements of LV volume and ejection fraction (EF), and this is done by acquiring a stack of short axis slices which covers the whole left and right ventricles. Presumed that the patient can lie still during the exam,

and holds his/her breath in the same diaphragmatic position during every recording, the three-dimensional coordinates of the slices are known, and can be used in three-dimensional reconstruction. Larger three-dimensional volumes can also be acquired.

MRI is used rather infrequently in cardiac patients, at least compared to echocardiography. The main reasons are that it is more time-, and staff consuming, it is not portable, and the costs are higher than for echocardiography. There are a few methodological limitations. First of all, MRI is contraindicated in patients with some kinds of metallic implants. MRI in patients with implanted defibrillators or pacemakers is currently a topic under investigation. Some patients may need anxiolytic medication due to claustrophobia, and children may need sedation. Accurate ECG-triggering is absolutely necessary to get good cardiac recordings, and this might be a problem in some patients. Arrhythmias are also a problem, but can be reduced by medication in some cases. The examination of cardiac anatomy and function also generally needs to be done during breath-hold, which might be a problem for patients with dyspnea, reduced hearing or unable to cooperate. An important disadvantage compared to some echocardiographic applications is the low temporal resolution.

For patients with CAD, MRI can be used for several purposes. One is the measurement of volumes, EF and regional WMS, and WMS can also be done during dobutamine stress to diagnose viability and ischemia. During the last decade the development of the so-called delayed- or late-enhancement method has made an important contribution to the diagnostic toolbox in CAD. After injection of a standard Gadolinium-containing MRI contrast agent, myocardial perfusion can be assessed during the first-pass phase. If imaging is delayed for 10-15 min, the extracellular contrast agent will show brighter areas in regions with increased proportion of extracellular space, as in infarcted, inflamed or fibrotic tissue. The method is being increasingly used to detect and estimate the size of myocardial infarctions (MI), and to differentiate between different causes of myocardial damage, both in clinical practice and scientific studies (36,37).

MRI can provide quantitative measurements of myocardial deformation by a technique called tagging. Tagging is done by applying a grid or line-pattern of demagnetisation to myocardial tissue at the beginning of the QRS-complex, and acquire a series of images which show how the lines of demagnetisation move with the tissue in the different regions of the heart. Any image orientation can be selected, so, in principle, all components of myocardial deformation can be measured. Until a few years ago, analysis of tagging images to extract quantitative information was very time-consuming, and this limited the applicability of the method (38). Recently, a method has been introduced which can analyse motion in a more automated manner, based on the phase information in the images (39,40). The method is called harmonic phase analysis (HARP) and is based on analysis of the harmonic peaks in the backward Fourier transformed image (39,41-44).

MRI tagging has been chosen as a reference method in several studies of new echocardiographic deformation-measuring methods for two main reasons: It is a different modality, and it is non-invasive. It is normally used as a two-dimensional technique, but can also be used to gather three-dimensional data (45). Alternatively, the

motion information gathered from the two-dimensional images can be put together in three dimensions because the three-dimensional orientation of the image planes is known (46).

4.9. Coronary artery disease

Occlusive disease of the coronary arteries due to formation of atherosclerotic plaques is an important cause of death in the industrialised part of the world, and increasingly important also in less developed countries (47,48). Total occlusion is often a result of a thrombus arising due to plaque rupture, and leads to sudden death or MI. Chronic occlusion results in ischemia at rest or during exercise, depending mainly on the grade of occlusion. In addition, a period of ischemia might induce stunning; a kind of temporarily reduced contractile function in viable myocardium. Stunning has usually resolved one week after an infarction, and this is the reason why echocardiography to estimate infarct size is not performed during the first few days after the infarction (49). There might also be parts of myocardium next to the infarct core that are at risk of necrosis due to limited blood supply (area at risk). Hibernation is a somewhat similar condition to stunning; and is defined as myocardium that is viable, but has reduced contractile function, and regains function after revascularisation. In hibernation, the cause of the dysfunction is a chronically reduced blood supply, not a sudden short-lived period of ischemia as in stunning.

4.9.1. Echocardiography in myocardial infarction

Infarct size determined by wall motion analysis in echocardiographic images is an important prognostic variable after an MI (50). Such visual analysis is performed using the categorical WMS system. The advantage of this system is its simplicity; it requires no special software or post-processing of data. The limitations are: Limited sensitivity for small reductions in function, subjectivity and experience dependency, limited inter-observer reproducibility and the fact that assessment is mainly based on wall thickening, not long-axis shortening (2).

Can echocardiographic assessment of function contribute in therapeutic decisions in patients with MI? According to several studies it can. The presence of viable myocardium determined by improvement of WMS during dobutamine stress echocardiography is a significant predictor of the effect of revascularisation therapy (51). The presence of many viable, but dysfunctional, segments also suggests that such therapy should not be postponed (52). The relationship between viable myocardium and improved function after revascularisation or after the early phase of an infarction has also been demonstrated on a segmental level using gadolinium-contrast late-enhancement MRI (53-57). SR measurements have been shown to increase the predictive value of WMS for improvement of function after revascularisation when the two methods were combined, but they came out equal when compared head-to-head (21).

After an MI, increased LV end-diastolic volume (EDV), a process known as remodelling, occurs in a substantial number of patients, and can lead to development of

clinical symptoms of heart failure. This remodelling can be reduced by beta-blockers, angiotensin-converting enzyme-inhibitors/angiotensin receptor blockers and exercise training (58-60). Echocardiographic evaluation of LV function by reduced EF has been used both to guide inclusion and to evaluate the effect of therapy in these trials.

4.9.2. Ischemia (Angina pectoris)

Detection of ischemia is a major activity in any cardiology department, and can be done with different non-invasive methods: Echocardiography, SPECT, MRI, and CT. Dobutamine or exercise stress echocardiography and stress MRI aim at detecting the result of ischemia, which is reduced or worsened wall deformation. Perfusion during adenosine or exercise can be assessed by echocardiography, MRI or SPECT, while computerised tomography (CT) is a parallel method to invasive contrast angiography, aiming at anatomical definition of stenosis severity. In addition to these methods, positron emission tomography (PET) can also be used, but has very limited availability, and high cost.

Automated quantitative measurements of regional myocardial deformation has been tested in the setting of dobutamine stress echocardiography, and found to improve accuracy or be equal to manual analysis of WMS for detection of significant stenoses (16,17). There have been some discordant findings regarding which parameter is the most accurate. While the previously mentioned studies suggested that peak systolic SR was the more accurate, an earlier study found that post-systolic strain was better (15).

4.10. Myocardial function and exercise capacity

Fick's equation describes the relationship between cardiac output (CO), arterial and venous O_2-content (O_{2Art} and O_{2Ven}) and oxygen consumption (VO_2):

$$CO = \frac{VO_2}{O_{2\,Art} - O_{2Ven}}$$

This can be rewritten to illustrate the determinants of VO_2, with stroke volume (SV) and heart rate (HR) substituted for CO:

$$VO_2 = HR \cdot SV \cdot (O_{2\,Art} - O_{2Ven})$$

This equation is the basis for discussions of factors that determines VO_{2max}.

4.10.1. Acute hemodynamic changes during exercise

During exercise with large muscle groups (walking, running, cycling, rowing) at sea level, the main factor limiting exercise capacity is CO; the ability of the heart to pump blood to the exercising muscles (61). Maximal CO is determined by maximal HR and maximal SV. During exercise with progressively increasing intensity, HR increases linearly with the increasing exercise intensity and oxygen uptake. The relation between

intensity and SV has been subject for debate; the traditional view has been that SV increases with intensity up to about 50 % of VO_{2max}, and then levels off. However, recent studies have suggested that in well-trained athletes, SV can continue to increase up to VO_{2max} (62,63). The increase of SV is determined by three factors: 1) increased filling (preload) due to increased venous return caused by the muscle pump; 2) increased contractility (para-/ sympathetic nervous system, circulating catecholamines and HR (Bowditch effect)) and 3) decreased peripheral resistance. The decreased peripheral resistance is due to vasodilation in the exercising muscles. The increase in CO leads to a marked increase of systolic blood pressure, while the diastolic pressure increases less or not at all, due to the reduced total peripheral resistance.

In patients with CAD, the present consensus is that SV levels off at about 50-60 % of VO_{2max} (64). A number of studies have looked at the response in end-diastolic (EDV) and end-systolic volume (ESV), and reached very different conclusions. The most widely used methods have been radionuclide ventriculography and echocardiography. Both of these have limitations during exercise, especially at higher intensities. Most of the studies have found an increase of EDV and a progressive decrease in ESV during exercise (65). This suggests that patients with CAD utilize the Frank-Starling mechanism to increase SV during exercise. The increased EF might also be due to lower peripheral resistance during exercise.

4.10.2. Chronic adaptations to exercise training

Maximal HR changes only minimally by training (66-68). Thus, to increase CO, which is the most important determinant of VO_{2max}, the only opportunity is to increase SV. An increase in SV can be accomplished by changing any of the three factors mentioned above: increased preload, increased cardiac contractility or reduced peripheral resistance. Increased plasma volume, which is a frequent finding after exercise training, might contribute to the increase of SV by improving LV filling (preload) (69). Increased SV during exercise has been shown after training in healthy subjects, allowing work at the same submaximal load to be performed at a lower HR. A thorough review and study of the effects of exercise of different intensity and duration on VO_{2max} in young healthy moderately fit subjects has recently been presented by Helgerud et al (70). Their study showed that high intensity exercise was superior to moderate intensity exercise for increasing VO_{2max}, thus demonstrating that intensity cannot be replaced by duration of exercise. The study also showed that the increase of VO_{2max} was paralleled by an increase of SV measured at an intensity very close to VO_{2max}. An increased SV at submaximal load after training has also been demonstrated by echocardiography in young females (71).

In patients with CAD, exercise training can increase VO_{2max} as much as in healthy subjects. However, the mechanisms behind this increase seem to be less clear than in healthy subjects. Some studies have found improved cardiac contractile function during exercise after training (72-75), while others have found that the improvements of VO_{2max} can be explained by peripheral changes leading to a larger arterio-venous O_2-difference (66). Only two studies have directly compared the effects of exercise training at different intensities, one showed that higher intensity elicited the largest improvement

(74), while the other found no difference for VO_{2max}, but an increase in EF during heavy exercise only in the high-intensity group (75).

Cross-sectional studies suggest that athletes have altered cardiac morphology compared to sedentary subjects. Endurance athletes have larger EDV and increased wall thickness, and this is to some extent reversed by de-training (76,77). Strength-trained athletes have been found to have slightly higher wall thickness and lower end-diastolic dimensions than endurance-trained athletes (78). Two months of high-intensity exercise training causes LV mass to increase in young females (71), and even two hours bicycling for six-days have been shown to increase EDV during exercise (79). Interestingly, endurance exercise training, especially with high aerobic intensity, seems to reverse LV dilatation in patients with post-infarction heart failure (60,80).

4.10.3. Exercise capacity and cardiac function

Even though there seems to be a close relation between CO and VO_{2max}, there is no clear relation between EF at rest and VO_{2max} in healthy subjects (81). In the previously mentioned study showing that SV does not plateau during incremental cycling exercise, the results suggested that differences in diastolic function (filling rate) were more likely than systolic function (rate of emptying) to explain the different SV-pattern in the sedentary and elite athlete subjects (63). Echocardiographic measurements made during exercise support this (78).

In patients with cardiac disease, EF is an important marker of LV systolic function, with prognostic value in patients with MI (82) and heart failure (83). However, the relation to exercise capacity is not very close here either (83,84). In a population of patients refereed for exercise echocardiography, indices of diastolic function (LV mitral annular early diastolic velocity, E_m) and LV filling pressure (the ratio between early mitral filling and mitral annular velocity (E/E_m)) were more closely linked to exercise capacity than systolic indices like LV EF (85). A recent study from a cardiac rehabilitation program for patients with CAD supports this; training improved only early diastolic, and not systolic mitral annular velocities (67). In a subgroup with abnormal relaxation pattern, the improvement of E_m was related to the improvement of VO_{2max}.

4.10.4. Tissue Doppler and exercise hemodynamics

Tissue Doppler recorded mitral annular velocities are good markers of global LV systolic and diastolic function (86). An important advantage of these measurements is that they allow systolic and diastolic LV function to be evaluated with the same method (84,87,88). The ratio E/E_m has been taken into widespread clinical use as a marker of LV filling pressure, and has been validated for measurements both at rest and during exercise (89-92). As mentioned above, tissue Doppler velocities are influenced by global heart motion, and a resent study has proposed that global LV SR during isovolumic relaxation can be an alternative measurement that avoids this problem (93).

5. Aims of study

Study I
To validate speckle tracking echocardiography as a method for angle-independent measurement of regional myocardial strain, using sonomicrometry and MRI tagging as reference methods.

Study II
To compare four different automated echocardiographic methods, based on TDI and speckle tracking alone or combined, for regional myocardial long-axis strain measurements, using MRI tagging as reference method.

Study III
To compare systolic and diastolic LV function during upright bicycle exercise in patients with chronic MI, and compare the results to an age- and sex matched control group.

Study IV
To study the effect of aerobic treadmill exercise training with different intensity on LV myocardial function in patients with stable CAD, using strain rate- and tissue Doppler imaging.

6. Material and methods

6.1. Study subjects

6.1.1. Study I

In the experimental part we included experiments performed in nine mongrel dogs, at Dept. of Surgical Research, Rikshospitalet, Oslo, Norway. The study protocol was approved by the National Animal Experimental Board. The animals were sedated by thiopentone 25 mg/kg body weight and morphine 100 mg IV, followed by infusion of morphine 50 to 100 mg/h IV and pentobarbital 50 mg IV every hour. The animals were artificially ventilated through a cuffed endotracheal tube with room air with 20 % to 50 % oxygen. All measurements were made during apnoea.

The eleven subjects in study I were recruited from Johns Hopkins University Hospital (Baltimore, USA). Seven had sustained an MI, and were included because quantification of the size of an MI might be an important application of regional myocardial strain measurements. Four healthy subjects were also included.

6.1.2. Study II

The healthy controls were recruited among university students. Exclusion criteria were smoking, known heart disease, diabetes mellitus or hypertension. A standard echocardiographic examination was performed to exclude significant pathology.

The patients were recruited from a population that had recently been admitted to St. Olavs University Hospital and diagnosed with MI. They had a median EF of 41 (range 19 – 58). Patients with arrhythmias were excluded due to the problems this gives for the deformation measurements, especially MRI tagging. All examinations were performed >3 weeks after the infarction. The safety of the implanted stents was checked for the 3.0 Tesla magnetic field (94).

6.1.3. Study III

The patients in this study were recruited among the population admitted to St. Olavs Hospital and diagnosed with an acute MI >3 months earlier. The patients had relatively well preserved EF (46±7 %). The findings in this group were compared to those in an age-and sex-matched control group (no history of heart disease and no risk factors). The subjects in the control group were recruited among university staff and by advertisements at public places.

6.1.4. Study IV

The patients in this study were recruited among subjects undergoing routine coronary angiography at St. Olavs Hospital. The angiographic inclusion criterion was presence of at least one significant coronary artery stenosis. All patients in addition had clinical

signs or symptoms of CAD (ischemia or typical chest pain during exercise testing, previous MI, or had undergone percutan coronary intervention, coronary artery bypass surgery).

Poor image quality was not an exclusion criterion in any of the studies. Of the total 52 patients and 33 controls included in the four studies, eight (15 %) and eleven (33 %), respectively, were female. No adverse events occurred during the studies.

6.2. Image acquisition and analyses

6.2.1. Echocardiography

6.2.1.1. Study I

In the experimental part of study I, three B-mode cardiac cycles in the apical four-chamber view were acquired using a Vivid 7 scanner and a phased array 2.0 MHz transducer (GE Vingmed Ultrasound). The image orientation was matched to the position of the ultrasonic crystals.

The analyses were performed by GcMat. The end-diastolic distance between the crystals measured by sonomicrometry was used to guide the position of the ROIs for speckle tracking in the images, and was also used to reject images with a clear deviation of orientation relative to the position of the crystals. If the crystals were visible in the image, the ROIs were placed beside, and not on them, to avoid artificially good tracking.

In the clinical part of study I, four- and two chamber B-mode images were acquired with a System Five scanner (GE Vingmed Ultrasound) with a 2.0 MHz probe. The images were acquired with relatively high frame rate (84±18 s^{-1}). In pilot studies we found that this was necessary for the tracking algorithm to work properly.

6.2.1.2. Study II, III and IV

In these studies echocardiography was done with a Vivid 7 scanner, and an M3S phased array 2.0 MHz probe (GE Vingmed Ultrasound). Images were acquired during end-expiration. This was particularly stressed in study II to achieve the same conditions as during the MRI examination. Both B-mode and TDI were acquired in the four-, two- and apical long-axis views. TDI frame rate was about 120-130 s^{-1} in all studies. B-mode frame rate in study II was 82±8 s^{-1}. In study III we also acquired images during upright rest and upright incremental bicycle exercise (25, 50 and 75 W). On each stage tissue Doppler images in the four- and two-chamber views were acquired, in addition to the mitral inflow velocity profile by PW Doppler. Three of 42 subjects were excluded from analysis in this study due to poor image quality in the upright position.

6.2.1.3. GcMat-analyses

The GcMat application was used in all studies included in this thesis. The code for the tracking algorithm has been written mainly by Prof. Hans Torp at the Department of Circulation and Medical Imaging at NTNU, and various features have later been added by him or PhD–students at the department. Some of these, especially the valuable feature allowing automated analysis and extraction of relevant variables, has been described by Ingul et al (17,32,95,96). In this thesis the method has been used in a somewhat different manner, and this is described below.

The algorithm provides a framework for comparing analysis of regional myocardial deformation based on two basic principles; TDI and speckle tracking. Thus, both B-mode and combined colour tissue Doppler- and B-mode data can be used. When analysing tissue Doppler images, the user can also select to use only the B-mode data, which is sampled with a lower frame rate than TDI-data (1:3). If the TDI-data are used, the user can select to use speckle tracking in both the lateral (in plane, perpendicular to the beam) and the radial direction (beam direction). If TDI is used in the radial direction, speckle tracking is only needed in the lateral direction to make the measurements angle-independent (in the image plane), and this also saves computation time. When analysing B-mode data, speckle tracking is performed in both the radial and lateral directions.

Some important parameters in the algorithm are:

ROI lat: defines the ROI size (in mm) in the lateral direction (depends on image depth). Default in this thesis: 5 mm.
ROI rad: defines the ROI size (in mm) in the radial direction. Default in this thesis: 5 mm. Based on pilot experiments.
Vmax rad: defines the radial size of the search area used in speckle tracking. Must be specified according to *a priori* knowledge about myocardial velocities in the region. Is given in cm/s, and then adjusted for frame rate. Default in this thesis: 16 cm/s (20 in some healthy young subjects). If tissue Doppler data was used, this parameter was set to 0.
Vmax lat: same as Vmax rad, but for lateral size of the search area. Default 8 cm/s.
Use TDI: If checked TDI-data is used to track the ROI in the radial direction.
Apex fixed: holds the apex fixed, does not track motion either by TDI or speckle tracking. Not used in the present thesis.
Corr: Sets the lower threshold (correlation coefficient) for when the kernel should not be moved to the area with the best match (by SAD) in the next frame. Set to 0 in the present thesis. If set at e.g. 0.5, the kernel would not be moved if the correlation coefficient between the kernel at t_0 and the best SAD-match at t_1 was below this, e.g. 0.44.

When using B-mode data, the only way to analyse strain and SR in the GcMat-application is to measure the change of length between pairs of kernels during the cardiac cycle. When using tissue Doppler images there are two possibilities. One is similar to the method used in B-mode analysis, but the tracking of the kernel in the radial direction is done only by using tissue Doppler data. Strain and SR are calculated

from the change of length between pairs of kernels. This method was called TDI+ST, and was one of the four echo methods used in study II. TDI+ST was used for strain and SR measurements in study III and IV. The second method is more similar to the way strain and SR are analysed manually in EchoPac (GE Vingmed Ultrasound). Here, the same seven kernels on the segment boundaries are tracked first, by using tissue Doppler data in the radial direction and speckle tracking in the lateral direction. Then, six ROIs are positioned between pairs of kernels, in the middle of each of the six myocardial segments in each view. Strain and SR are calculated from the velocity gradient along the beam within this ROI. By using the tracked positions of the kernels on the segment boundaries, the ROI for the velocity gradient can be made to follow the approximate same myocardial tissue during the cardiac cycle. This method was called TDI-VG (tissue Doppler imaging-velocity gradient), and was only used in study II. In TDI-VG segments were excluded if the angle between the beam and the long-axis of the segment was > 30°.

Workflow in analyses:

1. Open an image, and select the appropriate view.
2. Select the end-diastolic frame
3. Mark the position of the seven kernels on the segment boundaries, to define six LV segments.
4. Initiate tracking of the kernels.
5. The algorithm searches for regions similar to each of the seven kernels in the next frame, using the SAD algorithm. TDI-use and size of search area are defined in advance. The algorithm also performs the same tracking backwards through the cine loop. The results from the backward and forward tracking are then subject to a weighted average, so that the forward tracking is emphasised in the start of the cycle, while the backward tracking is emphasised towards the end.
6. After tracking, the “Track-inspector”-window appears. The correlation coefficients from kernel to kernel during the cardiac cycle are displayed, together with the mean and standard deviation (SD) of the distance between the forward and backward tracking paths. The two paths are also graphically displayed, together with their weighted average, for all the seven kernels (Figure 5).
7. If the tracking result is not satisfactory, the position of the kernels is adjusted, and tracking performed again.
8. When a good result is obtained, the toolbox “AVCtiming” is chosen, and the timing of AVC (end-systole) is performed automatically (97).
9. The toolbox “tissuetrack” is chosen again. The proper analysis method is chosen, and the analysis performed. The results are displayed as strain and SR curves for each of the six segments.
10. The position of the marker for AVC and the other selected curve variables are visually inspected, and adjusted if necessary.
11. The parameters are saved to file.

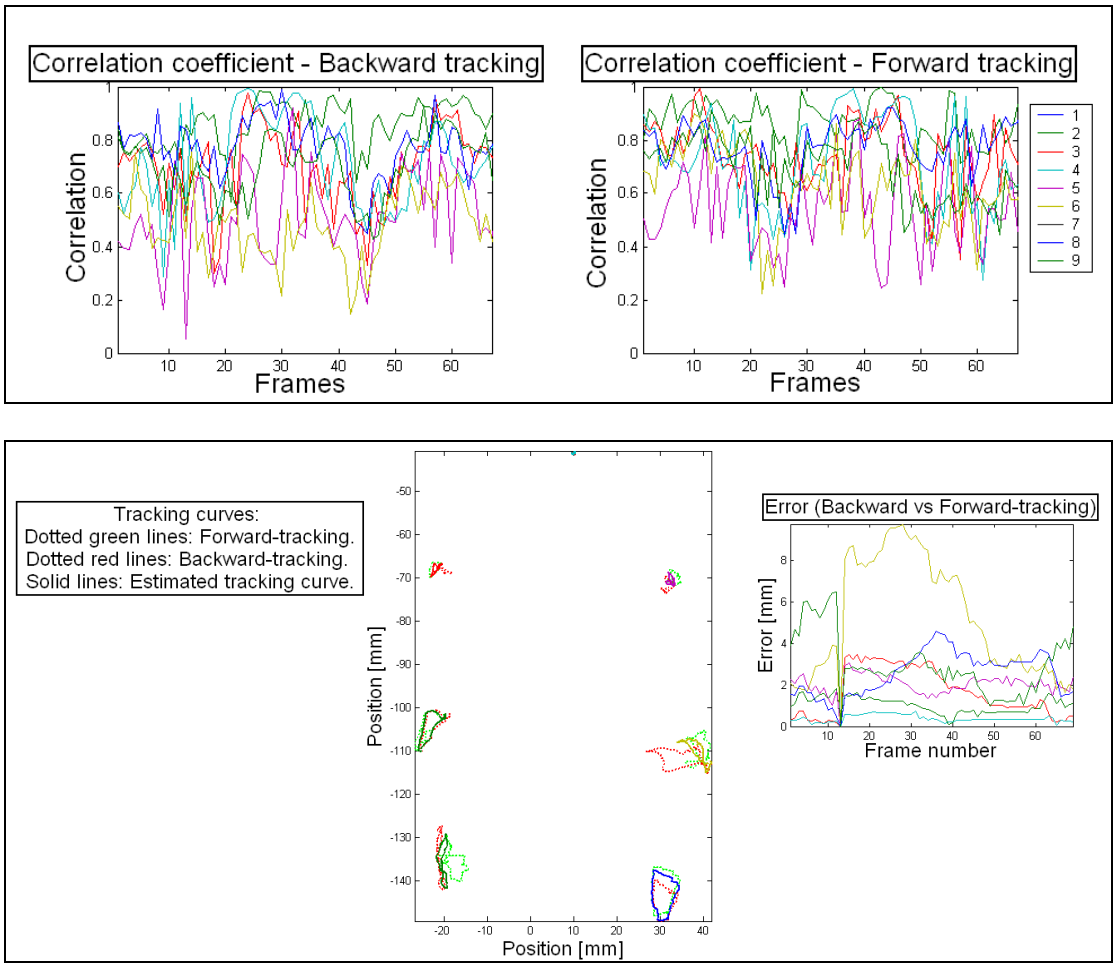

Figure 5. Illustration of the output from the track-inspector function. A graphic presentation of the correlation coefficients between the tracked regions is shown in the upper panel, for both forward and backward tracking. The forward and backward tracking paths are shown in the lower panel, together with the error between them during the cycle. Tracking was started at frame nr 13 in this example. Program code was written by Jonas Crosby.

6.2.2. Sonomicrometry

The sonomicrometry crystals used in study I (Sonometrics Corp., London, Ontario, Canada) were implanted in the subepicardium of the beating heart, and fixed with sutures. Afterwards the pericardium was adopted with sutures. The crystals emitted and received ultrasound pulses at a rate of 200 s^{-1}, and the signals were coded so that many crystals could be used simultaneously. In the experiments 16 crystals were implanted in the walls of the LV, to be able to measure LV rotation and twist in addition to long- and short-axis deformation. For the validation of the speckle tracking algorithm, only the four crystals positioned in the plane of the four-chamber view were used. By implanting the crystals like Figure 1 in study I shows, we were able to measure long-axis strain in the septum and lateral wall, and to confirm the accuracy of lateral tracking by simultaneously measuring LV short axis diameter change at the apical and

midventricular levels of the LV. The traces were analysed in SonoVIEW (Sonometrics Corp.), and exported to Matlab for calculation of strain and diameter change.

6.2.3. MRI tagging

In study I, tagged MRI images were recorded using a 1.5 T magnet with a phased-array cardiac coil (Signa, GE Healthcare, Waukesha, Wisconsin) using an ECG-triggered segmented k-space fast gradient-echo sequence (DANTE-SPAMM) (13,98). Four to five contiguous short-axis images (double oblique) were prescribed from base to apex, and six long-axis slices (double oblique) were prescribed radially every 30°. The motion of the myocardial tags was analysed, and adjusted by a displacement field-fitting method to give a 3D-map of radial, circumferential and longitudinal strain. Long-axis Lagrangian strain values were calculated for the basal, mid, and apical segments of the septum, lateral, anterior and inferior walls, to cover the same segments as in echocardiography (99).

In study II, tagged MRI images were recorded using a 3.0 T Philps Intera magnet and a six channels SENSE cardiac coil. Two separate acquisitions with parallel tag lines orthogonal to each other were acquired by complementary spatial modulation of magnetization (C-SPAMM) using a multi-phase ECG-triggered T_1-Fast Field Echo sequence (100). The acquisitions generally required a breath-hold time of about 15 s each, and were performed in end-expiration. The four-, two-chamber and apical long-axis views were acquired to cover the same segments as in echocardiography.

The two acquisitions with different tagging angle were combined, and exported in a complex data format for off-line analysis in TagTrack (Gyrotools Ltd, Zurich, Switzerland) using a peak-combination harmonic phase algorithm (44). The tracked contour was exported to Matlab, where seven points along the contour were selected, corresponding to the segment boundaries, and segmental strain and SR calculated from the change of length between pairs of points. Segmental results were excluded if the tracking was poor or if the curves were obviously wrong.

6.2.4. Lagrangian vs. Euler strain/SR

Strain and SR can be calculated by two different methods; the Lagrangian and the Euler (Natural) method. The basic difference is that the Lagrangian method uses the initial length of the object as a reference, while the Euler method calculates instantaneous strain in relation to the instantaneous length. It has been accepted as a standard to report strain as Lagrangian strain, and SR as Eulerian SR. In the speckle tracking methods in this thesis, Lagrangian strain was calculated from the change of length of a region of myocardium. This was also the case for the MRI tagging data in study II. A simple temporal derivation would give Lagrangian SR, so a correction was applied to get the Eulerian values (24).

6.2.5. Timing of events in the cardiac cycle

In the echocardiographic analyses in study II-IV we used an automatic algorithm developed at our department by Aase *et al*, which detects AVC, and thus end-systole, with high accuracy in apical tissue Doppler images (97). This method was also used in analysis of the B-mode images by ST-7P. We also used the same landmark in the annular velocity curves in 2D Strain.

The timing problem was avoided in study I, as we measured only peak strain, with no attempt to distinguish between systolic and post-systolic values. In study II, we measured the peak systolic strain by both echocardiography and MRI tagging. Timing of AVC by the same principle as in echocardiography was not possible in the MRI images due to low temporal resolution, therefore the positioning of AVC in the traces was guided by the AVC found by echocardiography, and by inspection of the shape of the strain and SR traces from the MRI analyses, especially looking for the small notch that can sometimes be seen in the strain curves at AVC. This unblinding was done strictly for the AVC results, no information of patient status or deformation results was revealed.

6.3. Statistics

Values are reported as mean ± SD or median (range). Paired or independent samples t-test, or Mann Whitney U-test and Wilcoxon signed rank test were used to compare measurements within or between groups. One-way analysis of variance was used to compare values from more than two methods. Bonferroni post-hoc adjustment of p-values was used in study I and III, but not in study II, as it is known to be very conservative when multiple comparisons are made. Relationship between variables was determined by Pearson's or Spearman's correlation/rank coefficient. Agreement between different methods was assessed using linear regression analysis and Bland-Altman statistics, with calculation of the 95 % limits of agreement (LOA) (101,102). In study II agreement for SR was illustrated by scatter plots with the line of identity, as agreement was unequal over the range of measurements, which violates the conditions for regular Bland-Altman analysis. Reproducibility (inter- and intraobserver) was determined by the coefficient of repeatability (COR) (102) or coefficient of variation (COV). In study IV, we also calculated the correlation coefficient between pre- and post-test values to estimate the reproducibility and/or the biological variation of the different measurements (103). In study III we used a general linear model for repeated measurements to test the differences in exercise responses in the two groups. A two-sided $p<0.05$ was regarded as a marker of statistical significance.

7. Summary of results

Study I

In this study the accuracy of the GcMat speckle tracking application (ST-7P) in B-mode images was confirmed using sonomicrometry and MRI tagging as reference methods. In the experimental part, we found that speckle tracking agreed well with sonomicrometry for measurements of myocardial strain and LV short-axis diameter change (95 % LOA (-4.4 – 5.0 %) and (-5.6 to 5.1 %), respectively). In the clinical part, we found low bias but a somewhat wider 95 % LOA-interval for the comparison with MRI tagging for long-axis measurements of segmental peak strain (95 % LOA (-9.1 – 8.0 %)). The feasibility for segmental analysis was 80 %.

Study II

In this study we compared segmental deformation measurements by different echocardiography methods to similar measurements by MRI tagging. In 21 subjects (10 with recent MI) we measured peak systolic strain and systolic (S_{SR}) and early diastolic (E_{SR}) SR by four different echo methods. Method number one and two used B-mode images, while method number three and four used tissue Doppler images: 1) 2D Strain (speckle tracking application in EchoPac (GE Vingmed Ultrasound)); 2) Speckle tracking of segment end-points (ST-7P); 3) Combined tissue Doppler (radial tracking) and speckle tracking (lateral tracking) (TDI+ST) ; 4) Strain and SR estimated from regional tissue velocity gradients, as in traditional manual analysis, but implemented in GcMat (TDI-VG). The 95 % LOA-intervals for the echo methods compared to MRI tagging were relatively wide, with a wider 95 % LOA-interval for strain for method 4. 2D Strain measured more negative strains than MRI tagging and the other echocardiography methods. Reproducibility was best for 2D Strain. 80-83 % of all segments were analysable for each method, except for method 4 (63 %).

Study III

In this study we compared systolic and diastolic LV function during upright bicycle exercise in patients with MI, and compared the results to those of a healthy age- and sex-matched control group. The patients had relatively well preserved LV function. At rest mitral annular systolic (S_m), but not E_m, was lower in the MI patients. During exercise S_m, but not E_m, increased in the patients, while both increased in the healthy subjects. E increased in both groups, thus the E/E_m-ratio, a marker of LV filling pressure, increased during exercise only in the MI group. HR was similar in both groups.

Study IV

In this study we investigated the effect of aerobic treadmill exercise training with different intensity on LV function, quantified by strain/SR and tissue Doppler mitral annular velocities, in patients with stable CAD. Seventeen patients were randomly assigned to either moderate (50-60 % of peak oxygen uptake (VO_{2peak})) or high intensity exercise (80-90 % of VO_{2peak}) for 10 weeks. The increase of VO_{2peak} was significantly larger in the high intensity group (17 vs. 8.0 %, p=0.01). Mean LV E_{SR} increased in the high, but not in the moderate, intensity group. For S_{SR} or mitral annular velocities there were no changes after training in either group.

8. Discussion

8.1. New methods for quantifying regional myocardial function

In study I and II in the present thesis we tested new algorithms for myocardial strain and SR measurements based on speckle tracking, both alone or combined with TDI. In the experimental part of study I, where we used only ST-7P, we showed that the method can detect changes in function due to ischemia and increased load. In the clinical part we showed that the method also works in patients. In study II we again used MRI tagging as a reference method to validate measurements by speckle tracking alone or combined with tissue Doppler data.

8.1.1. Choice of reference methods

We chose to validate the new echocardiographic methods described in this thesis against MRI tagging and sonomicrometry because they are accepted reference methods for regional myocardial strain measurements. We also compared the measurements against "pure" tissue Doppler-derived deformation measurements in study II, but using a different imaging modality is preferred to get an independent assessment of the accuracy of the new method.

We could have used other methods to evaluate the clinical value of the new methods. The essential question is: what property of the heart, or myocardium, is it that we really want to measure, for instance in patients with MI? Is deformation more important than the amount of viable myocardium in % of segmental myocardial mass?

In patients with MI, determination of myocardial viability is important to make correct decisions on revascularisation therapy. MRI with gadolinium late enhancement imaging has become a widely used tool for viability assessment, due to its high spatial resolution and generally high image quality. However, viability determined by WMS in low-dose dobutamine MRI seems to have better accuracy compared to late-enhancement MRI in predicting recovery of function, especially in segments with intermediate scar transmurality (104,105). This would mean that even though MRI late enhancement is considered to be the "gold standard" for viability/scar-assessment, WMS during low-dose dobutamine MRI works better when it comes to the main purpose of the assessment for these patients; the prediction of recovery of function. A problem with both studies is that the same method (WMS on MRI cineloops) was used to detect both viability and recovery. In other words; it is not that surprising that function is a better predictor of recovery of function, than information on the amount of scar. The two methods for prediction of recovery (MRI late enhancement and MRI/Echo low-dose dobutamine test) could have been compared in a randomised study looking at hard endpoints (morbidity/mortality) in patients who were candidates for revascularisation, but such method-comparison studies are seldom performed.

In relation to the work in paper I and II, the discussion above shows that validation of the new method against MRI tagging might have been as relevant as to evaluate its accuracy using MRI late enhancement. On the other hand, long-axis strain and SR is not equivalent to the wall thickening-based WMS, which was used in the study mentioned above, although the two methods seem to give relatively similar information (9). One possible advantage of MRI late enhancement is the good reproducibility and image quality relative to tagging. To summarise, this thesis is a basic validation of the new speckle tracking methods, but we have not compared them to old methods in a diagnostic or prognostic setting where they might be used, for instance in dobutamine stress echocardiography. Generally, such studies should be performed before new technology is taken into clinical use.

8.1.1.1. Sonomicrometry

While sonomicrometry has adequate temporal and spatial resolution to serve as a good reference method, the positioning of the crystals is vital for accurate measurements. There are some important sources of error when comparing measurements by sonomicrometry to measurements by two-dimensional echocardiography. First, correct alignment of the echocardiography image plane with the position of the crystals is vital. Second, the 2D echocardiography methods are not able to measure tissue motion out of the image plane, while this is possible in sonomicrometry because the crystals follow the three-dimensional motion of the tissue. Third, the positioning of the crystals relative to the endo- and epicardium is important, especially for the short-axis measurements. While the epicardium is almost still, the endocardium moves substantially, and this probably explained why the 95 % LOA-interval was somewhat wider for short-axis compared to long-axis measurements. Finally, the open-chest preparation is well suited for direct comparison studies, but induces circulatory and mechanical changes that must be taken into account when comparing the results with clinical studies.

8.1.1.2. MRI tagging

The tagging methods used in study I and II were different. In study I, several short- and long-axis images were combined to give a three-dimensional deformation map of the LV. The large number of images gave good spatial resolution and thus probably more robust deformation measurements, but simultaneously gave lower temporal resolution due to averaging over many cardiac cycles and breath-holds. In study II the measurements were made in two-dimensional images acquired in the same position as the echo images. The three-dimensional nature of the measurements in study I introduced some of the same problems as those mentioned for sonomicrometry. The MRI tagging method in study II had relatively high temporal resolution. The CSPAMM sequence also gave better and more sustained tag contrast (100). Tag duration was also improved by the longer T1-relaxation constant of myocardial tissue at 3.0 T compared to 1.5 T. Therefore, we were able to measure E_{SR} as well as S_{SR} in this study.

8.1.2. Feasibility

The feasibility for ST-7P was equal in study I and II (80 %). In study II 2D Strain and TDI+ST had feasibility in the same range (81 and 83 %, respectively), while the feasibility for TDI-VG was lower (64 %). These numbers were very similar to the ones found in the first study describing the automated approach (32). Angle dependency was found to be an important limitation of TDI-VG, causing 14 percentage points of the 36 % of segments excluded. Others have found slightly higher feasibility rates for 2D Strain (106,107). The feasibility for MRI tagging in study II was 83 %, which was lower than previously reported (108). This could be due to the type of sequence and the higher field strength used in study II, causing susceptibility artefacts and eddy current-effects.

8.1.3. Agreement – Speckle tracking

In study I the width of the 95 % LOA-interval was smaller in the experimental than in the clinical part. This could partly be explained by better image quality, but also by lower absolute values in the experimental part. The measurement bias was similar. The 95 % LOA-interval in the experimental part was similar to the agreement found for an RF-tracking algorithm in an experimental study by Langeland *et al* (29). Toyoda *et al* obtained slightly better results, but they measured only radial strain (30), and their good results were probably explained by the positioning of the crystals at the epi- and endocardium, where pattern tracking is probably better due to stronger reflections at the tissue surfaces.

The 95 % LOA-interval for the comparison between ST-7P and MRI tagging was narrower in study I than in study II. This was probably due to the use of a more comprehensive MRI method in study I, both in terms of acquisition and analysis. A very similar study to ours found 95 % LOA for 2D Strain vs. MRI tagging in the same range as we did. However, the bias was in the other direction, with more negative strain values being measured by MRI tagging than 2D Strain (108). In our study 2D Strain measured more negative strain values than both MRI tagging and the other echo methods. The explanation might be the different shape of the ROI in the different methods; in 2D Strain the ROI follows the curvature, while the segment is handled as a straight line in the other methods. The bias might also be due to the curve fitting implemented in the 2D Strain application. The kind of bias demonstrated in study II has been reported for 2D Strain previously (109).

Few studies have looked at longitudinal SR with MRI tagging and speckle tracking methods before, especially during diastole. Early diastolic circumferential SR has been measured by MRI tagging in an experimental study, and was found to be reduced in segments at risk after reperfusion, while S_{SR} was normal in the same regions (110). Diastolic SR measurements have also been used to calculate LV filling pressure (93). 2D Strain seemed to agree better with MRI tagging than ST-7P for both systolic and diastolic SR measurements, although all three methods probably underestimated the early diastolic values due to inadequate temporal resolution.

8.1.4. Agreement – Tissue Doppler

The TDI-VG method showed little bias compared to MRI tagging, but the 95 % LOA-interval was wider for the TDI-VG method compared to the other echo methods in study II. This was probably due to a high level of noise in the tissue Doppler data and angle deviations <30 °. A very similar study which also used MRI tagging as a reference method, also found a wider 95 % LOA-interval for strain by velocity gradients than for strain by 2D Strain (108). A previous study of strain by tissue Doppler compared to MRI tagging found slightly better agreement in terms of 95 % LOA-width than we did (13). Another possible explanation for the wider 95 % LOA-interval for TDI-VG vs. MRI tagging in study II was the basic difference in the methods; TDI-VG used the velocity gradients, while MRI tagging, and the speckle tracking methods (2D Strain, ST-7P, TDI+ST), tracked regions of myocardium.

8.1.5. Speckle tracking vs. Tissue Doppler methods

2D Strain measured more negative peak systolic strain relative to the other echo methods. As mentioned above the shape of the ROI might explain this. When strain is measured along the middle of a curved ROI which gets thicker during systole, the length of the middle line will decrease not only due to myocardial shortening but also because the middle line is displaced inwards. The range of values for peak systolic strain in the healthy subjects was narrower for 2D Strain, and this was mostly due to a more negative upper value (Table 1). The values are similar to values found in normal subjects in other studies, using 2D Strain (111) and tissue Doppler velocity gradients (112).

Table 1. Peak systolic strain in healthy subjects in study II.

Peak Strain (%)	Mean	SD	Range	Minimum	Maximum
MRI tagging	-19	4.4	22	-30	-8
2D Strain	-21	2.8	15	-29	-14
ST-7P	-19	3.8	19	-30	-11
TDI-VG	-19	5.9	28	-36	-8
TDI+ST	-18	3.2	19	-30	-11

In patients with MI, slightly different results have been obtained regarding the ability of longitudinal systolic strain measurements by 2D Strain to differentiate between normal, subendocardial and transmural (>50 % scar) infarcted segments. The optimal cut-off for transmural infarction seems to lie around -13 %, but there is considerable overlap (111,113). In a study where strain was calculated by the velocity gradient method, segmental values for peak systolic strain in normal and infarcted segments in patients with MI were similar to those obtained in the two studies using 2D Strain mentioned above (112). From these data, one might suspect that there were factors specific to the GcMat application that affected the values in ST-7P, TDI+ST and TDI-VG, and caused the bias relative to 2D Strain. However, a similar bias was found for 2D Strain versus MRI tagging.

The bias was different when comparing SR values; more negative S_{SR} values were found by ST-7P than by 2D Strain. This could have been an effect of less temporal smoothing, but this explanation does not fit with the observation that 2D Strain tended to measure higher E_{SR} (Fig 4, paper II). The values for S_{SR} and E_{SR} in the normal subjects in study II are shown in Table 2 and 3.

Table 2. Peak systolic SR in normal subjects in study II

Systolic SR (s^{-1})	Mean	SD	Range	Minimum	Maximum
MRI tagging	-1.3	0.3	1.8	-2.4	-0.7
2D Strain	-1.2	0.3	1.9	-2.6	-0.7
ST-7P	-1.3	0.4	1.9	-2.6	-0.7
TDI-VG	-1.4	0.5	2.6	-3.2	-0.5
TDI+ST	-1.3	0.3	1.7	-2.4	-0.7

Table 3. Peak early diastolic SR in normal subjects in study II

Early diastolic SR (s^{-1})	Mean	SD	Range	Minimum	Maximum
MRI tagging	1.8	0.7	3.7	0.6	4.3
2D Strain	2.0	0.7	3.7	0.7	4.4
ST-7P	2.0	0.7	4.3	0.7	5.0
TDI-VG	2.4	1.0	4.9	0.8	5.7
TDI+ST	1.8	0.6	3.3	0.5	3.7

Compared to tissue Doppler data from groups of healthy, but considerably older, subjects, the S_{SR} values in normal subjects in study II were equal or somewhat less negative, and the E_{SR} somewhat higher (114,115). Segmental S_{SR} by speckle tracking (2D Strain) and tissue Doppler has been compared in one previous study, and found to be equal, but slightly less negative than in study II (106). The problem with this study is that SR by tissue Doppler was calculated by adding tissue Doppler data to the same model where speckle information was also used, along with curve fitting and smoothing.

8.1.6. The combined segment-length method

The TDI+ST method is very similar to the ST-7P method. The main difference is that TDI-images are used, and that the kernel is moved in the radial direction according to the measured tissue velocities. When compared to MRI tagging, TDI+ST came out with similar width of the 95 % LOA-interval as 2D Strain and ST-7P for peak systolic strain. For SR, the agreement evaluated by the correlation coefficient seemed slightly better for 2D Strain than for TDI+ST, while ST-7P agreed less well with MRI. As speckle tracking was only performed in the lateral direction in TDI+ST, the method was less computational demanding than ST-7P. An advantage of the TDI+ST method compared to TDI-VG is that the user can assess the quality of the tissue Doppler data as the motion of the kernel is showed during analysis. A drawback of TDI+ST is the low B-mode frame rate, which might make speckle tracking difficult in some cases. The ratio

between B-mode and tissue Doppler frames can be adjusted in the scanner setup, and other settings should be tested to see if it might improve tracking quality. A related problem which is specific to the TDI+ST method used in the present thesis, is that the tissue Doppler data for the three samples between each B-mode sample were averaged before they were used to move the kernel. This solution was chosen to avoid moving the kernel in the radial direction when there was no information on the motion in the lateral direction. However, it results in temporal smoothing, and is probably why TDI+ST measured lower E_{SR} values than TDI-VG.

8.1.7. Reproducibility

2D Strain was better than MRI tagging and the other echo methods in all aspects of reproducibility (Fig 6, paper II), in line with previous results (16). The reproducibility was not tested in different acquisitions made on separate days, which would have been the situation most relevant to clinical use. However, analyses of a different cardiac cycle were made with all modalities. The intra-observer reproducibility for analyses of these images showed that 2D Strain had approximately half the variation of the other methods. The superiority of 2D Strain was probably due to a more standardised positioning of the ROI, and that the ROI consisted of many small kernels. The applied curve fitting and smoothing probably also contributed; the more smoothing applied, the lower variability. It is somewhat surprising that this advantage in reproducibility did not result in a narrower 95 % LOA-interval for 2D Strain vs. MRI.

No consistent differences were observed between the two TDI methods, except for slightly higher intra-observer different-cycle variability for TDI-VG. Higher variability for TDI-VG than for TDI+ST would be expected, as some temporal smoothing was applied in the TDI+ST algorithm. In addition, TDI+ST and ST-7P measured strain and SR over the entire segment, while TDI-VG used a shorter midsegmental region. This gave better spatial resolution in TDI-VG, at the cost of increased noise. In contrast to 2D Strain, there was no spatial smoothing across segments applied in the GcMat-based methods. ST-7P came out with similar values as the TDI-methods. The COV in study II were lower for both 2D Strain and the TDI-based methods compared to the results in a similar study (108).

In study IV we assessed the reproducibility of the average LV SR. In comparison to the values for segmental measurements in study II we found that the COV was reduced by a factor of 3-4, from about 12-14 to 3-4. The COV and COR were similar for systolic and diastolic measurements.

The reproducibility for MRI tagging was in the same range as the echo methods (not 2D Strain). The HARP-technology has till now been sparsely used for long-axis measurements, thus there are few studies to compare with. Today, most cardiac examinations are performed on 1.5 T systems, due to more artefacts and fewer available sequences at 3.0 T. It is possible that using a 1.5 T system in study II could have improved the reproducibility. On the other hand, tagging is one of the applications that might benefit from the longer T1-relaxation time at 3.0 T, because it gives less tag fading.

8.1.8. Timing of cardiac events

Accurate measurements of the strain, SR and tissue velocity variables used in the present thesis require accurate timing of the main cardiac events separating the different phases during the cardiac cycle. The onset of the QRS-complex in the ECG is an accepted standard for timing of end-diastole, but a method for timing of end-systolic has been more difficult to establish. Traces of LV outflow by PW Doppler can be used, but might be inaccurate as the measurements have to be made in a different cardiac cycle. AVC defines end-systole, but there has been no consensus on how to find AVC in tissue velocity or strain/-rate images. In the present thesis (paper II, III and IV) we used the automatic method proposed by Aase *et al* (97), which searches for a spike in the temporally derived mitral annular velocity curve, appearing in a predefined time-zone before the early diastolic relaxation (steepest up slope after first zero-crossing). The method has been validated in tissue Doppler images, but it was also used for ST-7P, and was found to work satisfactory.

Accurate timing is essential when comparing measurements like peak systolic strain between different methods, because post-systolic strain is common (approximately 1/3 of normal segments, more often in pathology). In study I we did not have adequate MRI-data to separate systole from early diastole, so peak strain was used. In study II we estimated AVC in the MRI tagging curves by using the AVC-time from the echo images, and adjusting it according to features in the strain curves: A small notch or a deflection in the down slope of the strain curve is often a marker of AVC. The accuracy of this approach was tested by calculating the correlation coefficients and 95 % LOA for peak strain (irrespective of systolic or post-systolic) between MRI tagging and the echo methods. The results were very similar to those obtained from the systolic measurements (≤1 percentage point difference in 95 % LOA-borders).

8.1.9. Frame rate vs. lateral resolution

In speckle tracking methods high frame rate is necessary to avoid impaired tracking caused by speckle decorrelation due to too high tissue deformation between frames. The necessary frame rate will therefore depend on the amount of deformation in the tissue under investigation. If the deformation rate is high, frame rate must be high. In addition to the ability to track the tissue, it is also a question whether frame rate is high enough to measure the true peak velocity or deformation rate. The drawback of increasing frame rate is that the reduced time between each frame reduces the amount of beams that can be sent out and received to build each image. When fewer beams can be used, their width must be increased so that there is no significant gap between each beam. Wider beams decrease the lateral resolution, and the image might look more smooth or smeared out. This will naturally affect the tracking accuracy in speckle tracking methods.

In pilot testing before study I we found that the optimal frame rate for GcMat speckle tracking (ST-7P) in full sector B-mode images was approximately 70-100, depending on LV size and depth from the probe. In study II we found that ST-7P probably

underestimated E_{SR}, and this was probably due to insufficiently high frame rate. This problem could have been addressed by making single-wall acquisitions, where frame rate can be over 150 s^{-1} with preserved lateral beam density. There seem to be no reasons why speckle tracking methods cannot resolve even short lived events, presumed the image acquisition setup is adjusted accordingly, but this needs to be tested. Future developments in probe technology and beam forming will give us better tools.

8.1.10. User-interaction and control

The beam density in the lateral direction leads the discussion to another important difference between tissue Doppler velocity gradient and speckle tracking methods. The emphasis put on temporal resolution has led to scanner setups with as few as 16 tissue Doppler beams covering the entire image in full-sector imaging of the LV. Including side-lobes, this causes each beam to have a large effective sector area, and this makes the inclusion of noise or signal from other tissue than myocardium more likely. In tissue Doppler the user would not notice this unless the curves don't look right, in terms of shape, or relative to the visually assessed wall motion. Speckle tracking reduces these problems: First, if the object is smeared out due to a low number of beams or a reduction in effective probe aperture, this can be seen in the B-mode image. Second, the quality of the tracking can be evaluated by checking that the kernel moves in the same way as the tissue. Importantly, this must be done at reduced playback speed due to limited capability of the human eye and brain to see short-lived events.

8.1.11. Automated quality assessment

In manual analysis of strain and SR in tissue Doppler data in EchoPac, the user has to search for an area with reasonable data quality, and which gives a trace that matches his/her visual assessment of regional function in the area in question. Thus, quality assessment is visual, subjective and experience dependent. In this thesis we investigated different alternatives for assessment of tracking quality by using variables that could be automatically extracted from the tracking algorithm. The quality assessment tool in the 2D Strain application incorporates many different scores to provide a "yes or no"-answer to whether the result in a segment should be regarded as valid. The sensitivity and specificity found for the 2D Strain tool was acceptable, but these numbers will vary according to the number of poor quality segments in a material. In the ST-7P GcMat application we looked more specifically at two possible markers of tracking quality: the correlation coefficient between successive kernels (this coefficient was not used for tracking), and the error between forward and backward tracking paths in the image. The analyses showed that the values for both markers were different in accepted and rejected segments, but that both markers will be difficult to use due to large overlap between included and different categories of excluded segments. Visual control of kernel tracking relative to wall motion was used as a gold standard, with its limitations.

8.1.12. Temporal resolution

The temporal resolution defines the accuracy of a method for defining specific events like AVC or E_m. It is mainly given by the frame rate, which was somewhat higher for

the tissue Doppler than the B-mode images. However, the resolution of events also depends on the amount of smoothing or averaging applied to the signal, as illustrated by the lower S_{SR} and E_{SR} found by TDI+ST compared to TDI-VG.

High frame rate is less important for strain than SR measurements. Frame rate as high as 300 s^{-1} has been suggested to be necessary to fully resolve the events during the isovolumic phases (116). However, inadequate frame rate might also affect strain measurements; if the peak velocities, especially in early diastole, are not sampled properly, this might lead to drifting in the curves. If this drift is linearly compensated for to make the curve return to zero at the next end-diastole, this will lead to incorrect measurements of for instance end-systolic strain.

The SR curves in 2D Strain look rather smooth, but the fact that the method measured higher E_{SR} than ST-7P, where no temporal smoothing is applied, suggests that this is likely to be an effect of spatial rather than temporal smoothing.

8.1.13. Spatial resolution

The spatial resolution in the images has already been commented on above. In ST-7P and TDI+ST strain and SR were measured by kernels positioned at the segment boundaries, thus the spatial resolution of the analysis tool was equal to the segment length. The methods can be used to measure strain and SR in considerably smaller regions, but this has not been tested yet, and will probably lead to increased variability.

In TDI-VG the ROI size was 10-15 mm. In 2D Strain, the software can calculate curves for 4-5 points per segment, but the average value per segment was used in study III. The true spatial resolution in 2D Strain is hard to define due to the spatial smoothing applied.

Some spatial averaging was also applied in the MRI tagging analysis. The degree of freedom for each of the small points along the drawn contour could be adjusted, and was set to allow relatively free motion. Strain and SR values were extracted from segment end-points here as well, so the resolution in the analysis tool was similar to the ST-7P and TDI+ST methods.

8.1.14. Clinical aspects

At present there are no established indications for using any of the quantitative methods for regional myocardial deformation measurements in daily clinical cardiology practice. The high level of random noise and the frequent occurrence of artefacts are significant obstacles, in addition to limited availability due to cost. They are used in stress echocardiography in some centres, but only by expert users.

The differences found between the methods tested in the present study are rather small compared to the large variation in the measurements. Their clinical significance is therefore uncertain, and must be determined in head-to-head comparison studies, preferably in the setting where they most likely will be used, for instance to measure

infarct size and prognosis and to detect ischemia. As an illustration of this, TDI-VG, which seemed to be inferior to the other methods in many of the aspects investigated in study II, came out with similar accuracy for diagnosis of significant coronary artery stenosis as TDI+ST in a recent study (17).

A similar study recently compared 2D Strain and manual analysis of strain/-rate from TDI for diagnosis of significant coronary artery stenosis. They found a similar diagnostic accuracy for 2D Strain and TDI-based measurements in the anterior segments, but lower accuracy in the posterior segments (16). In this study overall diagnostic accuracy was similar for WMS and the quantitative methods. 2D Strain had higher feasibility than TDI-strain at rest, but was inferior at peak stress. The study also found consistently higher cut-offs for peak stress systolic SR by 2D Strain than for TDI-based measurements, and these differences were slightly higher than the average difference between the methods. This might be related to the applied spatial smoothing in the 2D Strain algorithm. It should be noted that the group behind this study has a high level of expertise on tissue Doppler and WMS, so that different results might be obtained in less experienced centers.

For patients with MI there are a number of possible applications for regional deformation measurements, in addition to the use in stress echocardiography mentioned above: As a gate-keeper to acute invasive coronary angiography for patients admitted with chest pain, instead of ST-changes in the ECG; as a marker of reperfusion in patients who get thrombolysis because they are admitted to hospitals without an angio-lab; and as an assessment of improvement due to spontaneous recovery or the effect of medical and non-medical (e.g. exercise or intervention) therapy.

8.1.15. Limitations of speckle tracking

From the work with different speckle tracking applications in this thesis some comments can be made on the possible sources of error, with emphasis on the differences to SRI.

- Tethering

As in SRI, tethering is not a problem, as regional strain and SR is calculated from the difference in displacement between different regions.

- Aliasing

In contrast to TDI, there is no clear limit to the range of velocities that can be measured. The ability to measure such velocities depends on adequate temporal and spatial resolution. The velocities that are out of range will not appear on the opposite side of the scale, as in TDI. This might be a disadvantage, as this phenomenon makes it easy to detect aliasing in tissue Doppler images.

- Global heart motion

As for tethering, this will not affect regional strain and SR measurements by speckle tracking.

- Translation

Translation in the image plane is principally not a problem in speckle tracking methods because they are able to quantify tissue motion both in the radial (beam direction) and in the lateral direction in the image, and thus measure two of the three velocity components. This is in contrast to SRI, which only measures one of the three velocity components.

- Angle dependency

As discussed above, speckle tracking can quantify motion in the two dimensions of the image plane. It is therefore a less angle dependent method than SRI. However, as long as we are limited to speckle tracking in two-dimensional images, the methods will not be able to measure the velocity component out of the image plane, and will therefore still be angle dependent. In addition, the inherent difference between radial and lateral resolution will lead to less accurate tracking in the lateral direction, and consequently a certain angle dependency also in two-dimensional images. In contrast to SRI, this angle dependency will not be exaggerated by the simultaneous wall thickening because the orientation of the segment can be specified by the operator or found automatically, and taken into account in the calculations.

- Reverberations

Reverberations cause problems in speckle tracking in the same way as in SRI.

- Through-plane motion

Through-plane motion can cause errors by several mechanisms. As in SRI, there will be errors because the motion in this direction can not be quantified, and because the tissue that enters the image plane might have different function than the tissue that is replaced. Even in cases where the tissue which enters the plane might have similar function and velocity, the differences in tissue structure will lead to a change in the speckle pattern and risk of impaired tracking. This is in contrast to SRI, which will not be sensitive to changes in speckle pattern.

If the probe is positioned slightly lateral to the apex, wall motion in apical segment will cause tissue to enter the image plane. Dependent on the angle between the wall and the image plane, this wall motion will appear exaggerated in the image. A speckle tracking kernel positioned at the endocardial border might track this false wall motion and give wrong values.

Motion of strongly reflecting myocardial tissue through the image plane might cause problems in speckle tracking if the tissue structure runs obliquely through the image plane, and at the same time gives a similar speckle pattern or edge contour along its length. In this case displacement measured by speckle tracking might actually represent through plane motion, and not true displacement. In general, through-plane motion is a more important problem in short-axis than long-axis (apical) images.

8.1.16. Future developments

The clear impression from the analyses made in the present thesis is that image quality is a very important determinant of analysis accuracy, probably at least as important as

the choice of analysis method in most cases. Reverberations and drop-outs are important sources of error that restrict the applicability and accuracy of all the methods. Some anatomical limitations like ribs and lungs might be challenging, but spending time getting good images pays off in the analysis.

In the methods using tissue Doppler, the noise in the velocity estimates is considerable, and any improvement here would be very valuable to the techniques. With new and better probes we will hopefully get a higher number of beams/higher frame rate, which will be advantageous to both speckle tracking and tissue Doppler methods. The combination of the two seems to be a good alternative, and will need to be tested further, both with respect to acquisition setup and post-processing.

What about three-dimensional imaging? One of the options with the current GE Vingmed Ultrasound 3D probe (3V) is the acquisition of three planes simultaneously. This increases the likelihood of correct image orientation, which is vital in deformation studies. Speckle tracking in three dimensions has been a goal for years, as it will resolve the complex deformation pattern in the heart. This will reduce artefacts caused by through-plane motion, and possibly also allow analysis of deformation along the myocardial fiber direction, which is very interesting from a physiological point of view. Tracking might also be improved by having a three-, instead of two-dimensional pattern to follow. At present image quality and frame rate are too low for robust measurements, but these factors are likely to improve with future technological developments.

8.2. Myocardial function and exercise capacity

For patients with CAD, there is much truth in the saying "*heart disease is not a disease of rest, it is a disease of activity*". Reduced exercise capacity is an important symptom in CAD patients, with consequences for daily living. In fact, objectively measured reduced exercise capacity is more closely related to low self-reported health status than more specific markers of cardiac function (117). In addition, exercise capacity is a very powerful prognostic marker in CAD patients (118,119). Exercise therapy both increases exercise capacity and improves prognosis in CAD (120), but we know too little about the dose-response relationship.

The most obvious reason for the reduced exercise capacity is the heart itself. After an MI the amount of myocardium that can contribute to the pumping of blood is reduced, and this can be measured as reduced EF or systolic mitral annular velocities. However, there is no clear relation between EF at rest and exercise capacity (VO_{2peak}) (84,87). This suggests that other parts of the oxygen-transportation and –consuming system are affected as well in patients with CAD, and studies have shown that there is evidence of reduced function both in skeletal muscle and the perfusion-regulating endothelium that can contribute to the reduced exercise capacity (121,122).

8.2.1. Exercise in patients with MI – Study III

Patients who have had an MI are generally reported to have a VO_{2peak} that is 30-40 % lower than in healthy subjects of similar age (123). Some of this gap may be explained by reduced CO or peripheral changes associated with the MI, while some might also be due to lower VO_{2peak} before the MI, as low exercise capacity is a known risk factor for CAD (118).

In study III we wanted to study the possible mechanisms for the reduced exercise capacity in patients with MI. We compared the cardiac response to upright bicycle exercise in patients with MI and relatively well preserved EF, with the response in healthy age-matched controls. We found that early myocardial relaxation, measured by E_m, was not different between the two groups at rest, and that the healthy subjects, but not the MI patients, increased their E_m with increasing exercise intensity. Systolic contractile force, measured by S_m, was lower in MI patients both at rest and during exercise, but in contrast to E_m, S_m increased with increasing intensity. Thus, the MI patients lacked a diastolic reserve. From estimation of the E/E_m-ratio, which is a marker of LV filling pressure (89-91), it seemed that E increased during exercise due to increased LV filling pressure in the patients, but due to increased LV suction in the healthy subjects.

The E_m is mainly determined by left atrial pressure, LV active relaxation and LV recoil. One possible explanation to the lower E_m during exercise in the patients with MI might be that SV was lower with less recoiling forces present at the beginning of diastole. However, the difference in MAE, which is a marker of SV, was not larger during exercise than at rest, when there was no difference in E_m.

In a similar study Lele *et al* used radionuclide ventriculography to study the exercise response in patients with relatively small MIs during upright bicycling (124). They found that exercise capacity was most strongly related to LV filling rate and time to peak filling, but not to filling rate at rest or EF at rest or during exercise. These results are in line with our findings, but there were some differences between the studies. All the patients in the study by Lele at al had evidence of inducible ischemia. In our study four of 18 patients had significant stenoses still untreated at the time of the study. All these stenoses were in one of the non-culprit epicardial arteries. Their hemodynamic significance was not tested during angiography, but no new or worsening wall motion abnormalities were found during exercise, neither in those with nor without stenoses, suggesting that blood flow was adequate.

In study III we measured systolic and diastolic function with the same type of measurements (mitral annular velocities), while Lele at al used EF as a marker of systolic, and peak filling rate and time to peak filling rate as markers of diastolic function. While S_m, E_m and peak filling rates measure the highest rate of deformation or filling, EF is a measure of what has happened during the entire systole, and might therefore be less related to contractility and more affected by load. This might explain why EF was not related to exercise capacity. In the study by Lele *et al* the increase in peak filling rate during exercise was larger in the healthy group. In our study we found that early filling was preserved, but that this was not due to a higher E_m, but more likely due to increased filling pressure. Thus, tissue Doppler gave new information on the mechanisms of the diastolic dysfunction during exercise in these patients.

An important limitation of study III is that we did not measure VO_2 during exercise, neither did we test VO_{2peak}. This makes it difficult to estimate the importance of the detected differences between the groups. We compared the groups on the same absolute intensity, while Lele *et al* compared them at peak, which is a relative intensity description.

A second similar study was performed by Miyashita *et al*, who used supine exercise with simultaneously invasive LV manometry (125). This study included patients with no ischemia and similar EF to the patients in our study. Due to the invasive measurements, no control group was included. The study showed that maximum LV pressure rise (dP/dt_{max}) at peak exercise, but not at rest, was related to VO_{2peak}. This shows that systolic function is also related to exercise capacity, but that other measurements than EF is needed to discover it. Markers of LV early relaxation (dP/dt_{min} and peak negative LV pressure) were the only resting variables that were related to VO_{2peak}, and the relationships were slightly stronger when these were measured during peak exercise. End-diastolic pressure was related to VO_{2peak} at peak, but not at rest.

In athletes, Vinereanu *et al* found that E_m, but not S_m, immediately after exercise was related to VO_{2max}. ESV index at rest, but not after peak, was related to VO_{2max} (78). In a study by Støylen at al, also in athletes, both S_m and E_m during exercise were related to VO_{2max}, with no differences in the strength of the relations. EF was not measured (126). In patients with heart failure, EF after exercise, but not at rest, was weakly related to

VO_{2peak} (84). Systolic and diastolic annular velocities and the E/E_m ratio at rest were also weakly related to VO_{2peak}. Tissue Doppler variables were not measured after exercise in this study. Together, these studies demonstrate the limitations of resting measurements to predict what happens during exercise, at least in healthy subjects and patients with relatively well preserved function.

8.2.2. Cardiac volumes and tissue velocities during exercise

Many studies have looked at EDV, SV and CO during exercise in various populations of patients with heart disease and normal subjects. The results diverge, but an attempt to summarize the findings is presented below (Table 4).

Table 4. Cardiac function during exercise

	Normals/Athletes		**MI, NYHA I-II**		**CHF NYHA >II**	
Intensity	Subm	Peak	Subm	Peak	Subm	Peak
EDV	→/↑	→/↑	→	↑	→	→
ESV	↓	↓/↓↓	↓	↓	→	→
SV	↑	↑/↑↑	↑	↑	→	→
E_m	↑	↑↑	→	→	→	→/↓
S_m	↑	↑↑	↑	↑↑	→	→

- In normal sedentary subjects, EDV does not increase, because early diastolic relaxation (E_m) is sufficient to suck blood into the LV, and the systolic contractile force, measured by S_m, is sufficient to increase SV by decreasing ESV. EDV might increase in athletes (78,126-128).
- In patients with moderately reduced exercise capacity (like in study III), E_m is insufficient to increase suction, and S_m is reduced, and cannot keep up the SV at the same EDV. Thus the Frank-Starling mechanism must be used to maintain/increase SV, with an increase of LV filling pressure. Systolic function (S_m) increases during exercise and is sufficient to expel blood and maintain SV at a higher EDV, but ESV does not decrease as much as in normals ((124), study III).
- In patients with severely reduced exercise capacity, diastolic function is too reduced to allow an increase in EDV, thus the Frank-Starling mechanism is not used. In addition to impaired active relaxation, this might be due to low myocardial compliance, either due to dilatation as in post-infarction heart failure, or changes in myocardial tissue structure and -composition in non-dilated ventricles (129,130). Systolic power is low, so ESV is unchanged, and SV does not increase with increasing intensity. Increased HR is the main cause of increased CO (84).

The discussion of the EDV, SV and CO responses to exercise is difficult because these variables are difficult to measure with echocardiography during exercise, especially at higher intensity levels. In study III, we were able to measure EDV and mitral annular excursion (MAE), a marker of SV, but we could not measure EF reliably due to difficulties with ESV measurements during sitting bicycle exercise. MAE increased

from rest to low/moderate intensity, and then seemed to plateau. EDV was only found to increase in the patient group.

A further difficulty in comparison of studies is the different body positions used; supine or sitting. LV filling pressure, and thus load, is position dependent (131). A further source of variability in loading conditions is the type of exercise. Due to the muscle pump, bicycling with low and high pedal frequency might give different loading conditions. The importance of position and load was clearly demonstrated in study III, where annular velocities and MAE decreased from supine to sitting rest, while E increased slightly. The increase of E, together with a simultaneously reduced E_m, led to a significant increase of the E/E_m-ratio, suggesting an increased filling pressure from supine to sitting position. From previous invasive studies such an increase seems very unlikely (131,132), and the result therefore shows that the E/E_m-ratio has limitations as a marker of LV filling pressure. It is interesting to note that S_{SR} did not decrease from supine to sitting in this study. This is in line with previous results from stress echocardiography suggesting that SR is relatively load-insensitive (17).

8.2.3. Which cardiac properties are most closely linked to exercise capacity?

This question is not only interesting from a physiological point of view, but also from a clinical one, as the answer would tell us which variable(s) to focus on in diagnosis and treatment of patients with reduced exercise capacity. As exercise capacity is such a powerful prognostic variable, any variable closely related to it might also have prognostic information. From the discussion above it seems clear that exercise variables are the best candidates. However, a resting variable would be useful for clinical practice, as exercise echocardiography is performed rather infrequently.

It seems justified to choose a variable that describes the rate, and not the sum, of emptying or filling (dP/dt_{max} vs. EF). Furthermore, despite differences in measurement types in many studies, it also seems wise to select a diastolic variable. The variables describing the active, early, energy-demanding relaxation have been mostly used in the studies mentioned above. E_m, which is determined by the active myocardial relaxation, the atrio-ventricular pressure gradient and myocardial tissue properties (compliance/recoil), has been shown to a better predictor of exercise capacity than the deceleration time of E, which is considered a marker of LV compliance, the major determinant of passive relaxation. The E/E_m ratio was the best predictor in the study, which did not include measurements during exercise (85). One important reason why E was inferior to E_m is probably the pseudo-normalisation of peak E-velocity when diastolic function is poor (restrictive filling pattern), leading to a non-linear relationship between E (and E/A-ratio) and diastolic function. Dividing E by E_m sorts out those with a high E due to restrictive filling. Interestingly, E_m has incremental prognostic information when added to clinical data and standard echocardiographic variables (133).

E_{SR} has the same determinants as E_m, and might also be a candidate for linking cardiac function and exercise capacity. E_{SR} has been less investigated than S_{SR}, but carries patho-physiological information in relation to ischemia and reperfusion (110). Others

have suggested that E_{SR} is a better marker of viability than S_{SR}, and found it to be negatively correlated to regional myocardial stiffness (134). E_{SR} has also been found to be related to *tau*, the time constant of LV pressure decay during isovolumic relaxation, and to LV filling pressure (93,135). Interestingly, it has also been found to be preserved by physical activity in older subjects (136).

8.2.4. Diastolic vs. systolic function

In the discussion of exercise capacity and cardiac function it might seem somewhat artificial to handle systolic and diastolic function as two nearly separate aspects of cardiac function. Briefly, on the molecular level, diastolic relaxation rate is determined by the rate of calcium reuptake into the sarcoplasmic reticulum by the sarcoplasmic reticulum calcium ATP-ase (SERCA). The amount of calcium available in the sarcoplasmic reticulum for release with the next contraction determines the force in that contraction, together with the rate of calcium influx from extracellular space and the rate of the following efflux from SR. The amount of elastic recoil and tissue stiffness can be altered by changes in intracellular proteins (e.g. titin) and the extracellular matrix (137,138). The degree of relationship between the systolic and diastolic function has recently been a highly discussed matter in the debate on the pathophysiology of heart failure. Although accepted by some, the term "heart failure with normal EF" (or diastolic heart failure) seems somewhat unspecific, and it is based on a measurement of systolic function which has many limitations, especially in terms of reproducibility (88,137). It would seem more appropriate to diagnose and treat these patients according to the underlying disease causing their heart failure symptoms (129). At the same time, study III and IV, and others, show that diastolic function deserves attention on its own, and diastolic variables are probably as important as systolic ones in the search for a better diagnostic classification of patients with heart failure symptoms.

8.2.5. E_{SR} and exercise training – Study IV

In study IV we investigated the effects of aerobic endurance training with two different intensities, in an attempt to clarify the dose-response relationship for exercise therapy in patients with CAD. The study showed that the high-intensity group achieved a larger increase in VO_{2peak} than the moderate-intensity group. We also found that the high-intensity group increased their average LV E_{SR}, while the moderate-intensity group did not. E_m did not change after training, but was, in line with previous studies, related to VO_{2peak}. E_{SR} was not related to VO_{2peak} at baseline. The results suggest that improved relaxation gave improved VO_{2peak} through an effect on LV filling, SV and CO, but this can only be regarded as a hypothesis, mainly due to the low number of subjects included in the study, and that no measurements were made during exercise.

8.2.6. The relationship between E_m and E_{SR}

The fact that E_m, but not E_{SR}, was correlated to VO_{2peak} at baseline questions the use of E_{SR} to predict exercise capacity. What caused this discrepancy? One explanation is that E_{SR} is not simultaneous in all segments in a wall, and the degree of synchronicity therefore determines how closely related the two will be. The relative difference

between E_{SR} and E_m might be a marker of differences in early relaxation synchronicity in different populations. Another more likely explanation is that E_{SR} was not measured in all segments, but averaged from the segments where image quality was satisfactory, and then averaged. As the population included patients with regional dysfunction, the selected segments might not have been representative for the true LV value. The feasibility on the segmental level was low in the study (71 %), but, important for the reproducibility, 83 % of these segment were included both at pre- and posttest. This probably accounts for the high correlation we found between the pre- and posttest values for E_{SR}.

The matter of feasibility is relevant to studies that use the global SR, like Wang *et al* (93). They argue that global SR is better than annular velocities as SR avoids translation and tethering effects. This view might not be correct in the presence of significant artefacts, and needs to be tested. In this respect, averaging SR from the available segments might be a better alternative than using the global SR for the whole LV. This is the approach used in two studies using global strain to detect and measure the size of MIs (111,139).

One of the previous studies which have looked at the effects of training on LV function in patients with CAD and relatively well preserved LV EF, found improved E, and that this improvement was correlated to the increase of VO_{2peak} (67). We also found improved E in study IV, but no relation between this improvement and the improvement of VO_{2peak}. For systolic function we found no change in EF, S_m and S_{SR} at rest, which is in line with previous studies (72-74). In a similar study in patients with post-infarction heart failure, high-intensity exercise improved VO_{2peak} and E_m more than moderate-intensity exercise (80).

8.2.7. At what intensity should patients with CAD train?

There is convincing data on the positive effect of exercise training on prognosis in patients with CAD (140), but the interventions that have been used are so heterogeneous that specific recommendations are difficult to establish. In study IV the high-intensity group increased their VO_{2peak} more than the moderate group. This is in line with previous results in intensity-comparing studies both in patients with CAD (74,75), patients with heart failure (80) and healthy subjects (70). In a large prospective study Myers *et al* found that a 1 MET increase in exercise capacity, which was approximately the increase found in study IV, was equal to a 12 % increase in survival (118). Although the study was cross-sectional, and thus did not include a training intervention, it supports further investigation of the effects of high-intensity exercise training.

In addition to the effects on risk factors measured in short-term clinical trials, it is vital that the patients continue to exercise. In healthy subjects high-intensity training generally leads to larger improvements in VO_{2max} than moderate intensity training (141). If more and larger studies than study IV and those mentioned above should show that this holds true for patients with CAD as well, this might translate into improved long-term exercise compliance because of a larger perceived beneficial effect on exercise capacity in everyday-activities.

The safety data on high-intensity aerobic exercise are at present relatively sparse, and more data are needed. However, it is important that the focus on possible dangers associated with higher intensity does not leave the possible positive effects of such exercise unknown. In an important recent study, Noel *et al* prescribed exercise with an intensity corresponding to 1-2 mm ST-segment depression for 60 min to patients with CAD (142). They found no signs of myocardial injury, more frequent arrhythmias or LV dysfunction compared to a lower-intensity control group. Unfortunately, the applied six weeks training intervention did not increase VO_{2peak} in any of the groups. This questions the appropriateness of the applied training program, and is a weakness of the study.

Whereas previous guidelines recommended more strenuous activity (143), the European Society of Cardiology position paper for secondary prevention recommends exercise at moderate intensity (45–60 % of HR- or VO_2-reserve) (144). The guideline from the American Heart Association in 2001 recommends intensities from 40-85 % of HR- or VO_2-reserve (145). In practice these recommendations includes a wide range of intensities. It would be very interesting to see the result of studies that compared the compliance with such relatively unspecific advice with more specific and detailed recommendations, both on physician and patient levels. Also, individual prescription based on an exercise test with ECG-monitoring is emphasised in both papers. This seems sensible, but might not make the case any easier for the prescribing health care personnel. Consensus on a more specific training intervention probably would have been a good start in the process of determining the dose-response relationship of exercise, as new studies could have tested different exercise training protocols against this standard.

8.2.8. Future studies using echocardiography in exercise testing and therapy

Although small, study IV suggests that TDI-derived variables describing myocardial deformation are able to give new information on myocardial adaptations to exercise. There are a growing number of studies which relates these new indices of myocardial function to important fundamental properties of the myocardium, providing a basis for their application during exercise testing and monitoring of exercise therapy.

In relation to the present work, a recent study by Wang *et al* is interesting because it showed that global SR during the isovolumic relaxation interval is closely related to LV active relaxation and can improve prediction of LV filling pressure (93). The study leaves some important aspects of timing of the isovolumic time interval unanswered, but still suggest that we have much to learn about diastolic events, their relation to the active and passive relaxation of myocardium, their prognostic and therapeutic potential and their relation to exercise intolerance. The study also illustrates the importance of development of new methods, as they used one of the speckle tracking applications described in study II (2D Strain).

Speckle tracking can also be used to measure LV rotation and twist, but Notomi *et al* used an algorithm based on tissue Doppler velocities to study LV twist at rest and during exercise (146). They found that untwisting starts at end-systole and peaks before the peak of the intra-ventricular pressure gradient, the peak E and peak longitudinal and short-axis expansion, and also found that LV twist increased more than long-axis velocity during exercise. They concluded that LV untwisting is the main factor contributing to the intra-ventricular pressure gradient and thus early diastolic suction. Further, they suggested that untwisting is fuelled by release of potential energy stored during systole (titin-proteins connecting the actin and myosine-filaments), and thus constitutes a link between systolic and diastolic dysfunction. Exercise capacity was not measured, but studies using rotation and twist to predict exercise capacity and evaluate responses to training will certainly come. Some data from MRI tagging already exist, suggesting that early diastolic, but not systolic, rotation at rest is increased by a period of training (147).

There is probably also much to gain by evaluating the response to exercise training by looking at cardiac function during exercise, and not at rest. At least in patients with relatively well preserved LV function, the heart is not challenged at rest, and has a large reserve. This was shown in study III, where diastolic function in the two groups was equal at rest, but differed during exercise. Other methods than echocardiography are probably better suited for CO measurements, but as long as image quality is satisfactory, echocardiography can provide unique information of myocardial function.

9. Limitations

The patients selected for study I and II had MI. Other populations with altered wall motion could have been included to increase the validity of the result to other groups as well, e.g. patients with dilated and hypertrophic cardiomyopathy.

In study II, all analyses were done by a single operator. Care was therefore taken to achieve blinded measurements for all methods, with different id-numbers for the echo and MRI examinations.

Fully blinded analysis was not realistic in study III, as HR and regional wall motion abnormalities were visible in the images. Measurements of VO_{2peak} and maximum attainable bicycle load could have allowed more accurate evaluation of the relation between the different variables and exercise capacity.

In study III and IV there were patients with residual stenoses in major epicardial arteries. The patients were in this way representative of the CAD population. In study III we found no signs of regional ischemia in wall motion analysis, indicating that the stenoses were not flow-limiting, at least not at the exercise intensity used in the study. The results in the study were therefore probably not a result of ischemia during exercise. In study IV we did not investigate the extent of ischemia in the patients, and can therefore not exclude that this affected our results.

The number of patients was low, especially in study IV. This increases the possibility of type II errors, and means that we could have detected changes in other variables than E_{SR} and E if we had used a larger sample.

10. Conclusions

Study I and II show that automated measurement of regional myocardial systolic strain by speckle tracking methods is feasible. In an automated setting, speckle tracking alone or combined with TDI gives better agreement, in terms of 95 % LOA-interval, with MRI tagging than the velocity gradient approach. The clinical significance of this difference and the detected bias in 2D Strain needs further testing. The assessment of SR is less accurate compared to MRI tagging, but that might as well be due to limitations of the MRI method.

Study III and IV show that tissue Doppler alone or combined with speckle tracking seems to be well suited for studies of myocardial function during exercise, and of the myocardial response to exercise training. Study III shows that diastolic function is reduced in patients with MI, and suggests that this might be related to the reduced exercise capacity in this patient group. Although small, study IV suggests that exercise with high intensity can improve diastolic function in patients with CAD. Further studies should look more specifically at the different aspects of systolic and diastolic function, both at rest and especially during exercise, and relate them to exercise capacity and training.

11. References

1. McDicken WN, Sutherland GR, Moran CM, Gordon LN. Colour Doppler velocity imaging of the myocardium. Ultrasound Med Biol 1992; 18:651-4.

2. Hoffmann R, Lethen H, Marwick T, Arnese M, Fioretti P, Pingitore A et al. Analysis of interinstitutional observer agreement in interpretation of dobutamine stress echocardiograms. J Am Coll Cardiol 1996; 27:330-6.

3. Stoylen A, Slordahl S, Skjelvan GK, Heimdal A, Skjaerpe T. Strain rate imaging in normal and reduced diastolic function: comparison with pulsed Doppler tissue imaging of the mitral annulus. J Am Soc Echocardiogr 2001; 14:264-74.

4. Palka P, Lange A, Fleming AD, Fenn LN, Bouki KP, Shaw TR et al. Age-related transmural peak mean velocities and peak velocity gradients by Doppler myocardial imaging in normal subjects. Eur Heart J 1996; 17:940-50.

5. Nowicki A, Olszewski R, Etienne J, Karlowicz P, Adamus J. Assessment of wall velocity gradient imaging using a test phantom. Ultrasound Med Biol 1996; 22:1255-60.

6. Uematsu M, Miyatake K, Tanaka N, Matsuda H, Sano A, Yamazaki N et al. Myocardial velocity gradient as a new indicator of regional left ventricular contraction: detection by a two-dimensional tissue Doppler imaging technique. J Am Coll Cardiol 1995; 26:217-23.

7. Fleming AD, Xia X, McDicken WN, Sutherland GR, Fenn L. Myocardial velocity gradients detected by Doppler imaging. Br J Radiol 1994; 67:679-88.

8. Heimdal A, Stoylen A, Torp H, Skjaerpe T. Real-time strain rate imaging of the left ventricle by ultrasound. J Am Soc Echocardiogr 1998; 11:1013-9.

9. Stoylen A, Heimdal A, Bjornstad K, Wiseth R, Vik-Mo H, Torp H et al. Strain rate imaging by ultrasonography in the diagnosis of coronary artery disease. J Am Soc Echocardiogr 2000; 13:1053-64.

10. Stoylen A, Heimdal A, Bjornstad K, Torp HG, Skjaerpe T. Strain Rate Imaging by Ultrasound in the Diagnosis of Regional Dysfunction of the Left Ventricle. Echocardiography 1999; 16:321-9.

11. Hatle L, Sutherland GR. Regional myocardial function--a new approach. Eur Heart J 2000; 21:1337-57.

12. Urheim S, Edvardsen T, Torp H, Angelsen B, Smiseth OA. Myocardial strain by Doppler echocardiography. Validation of a new method to quantify regional myocardial function. Circulation 2000; 102:1158-64.

13. Edvardsen T, Gerber BL, Garot J, Bluemke DA, Lima JA, Smiseth OA. Quantitative assessment of intrinsic regional myocardial deformation by Doppler strain rate echocardiography in humans: validation against three-dimensional tagged magnetic resonance imaging. Circulation 2002; 106:50-6.

14. Weidemann F, Jamal F, Sutherland GR, Claus P, Kowalski M, Hatle L et al. Myocardial function defined by strain rate and strain during alterations in inotropic states and heart rate. Am J Physiol Heart Circ Physiol 2002; 283:H792-H799.

15. Voigt JU, Nixdorff U, Bogdan R, Exner B, Schmiedehausen K, Platsch G et al. Comparison of deformation imaging and velocity imaging for detecting regional inducible ischaemia during dobutamine stress echocardiography. Eur Heart J 2004; 25:1517-25.

16. Hanekom L, Cho GY, Leano R, Jeffriess L, Marwick TH. Comparison of two-dimensional speckle and tissue Doppler strain measurement during dobutamine stress echocardiography: an angiographic correlation. Eur Heart J 2007; 28:1765-72.

17. Ingul CB, Stoylen A, Slordahl SA, Wiseth R, Burgess M, Marwick TH. Automated analysis of myocardial deformation at dobutamine stress echocardiography: an angiographic validation. J Am Coll Cardiol 2007; 49:1651-9.

18. Skulstad H, Urheim S, Edvardsen T, Andersen K, Lyseggen E, Vartdal T et al. Grading of myocardial dysfunction by tissue Doppler echocardiography: a comparison between velocity, displacement, and strain imaging in acute ischemia. J Am Coll Cardiol 2006; 47:1672-82.

19. Skulstad H, Andersen K, Edvardsen T, Rein KA, Tonnessen TI, Hol PK et al. Detection of ischemia and new insight into left ventricular physiology by strain Doppler and tissue velocity imaging: assessment during coronary bypass operation of the beating heart. J Am Soc Echocardiogr 2004; 17:1225-33.

20. Edvardsen T, Skulstad H, Aakhus S, Urheim S, Ihlen H. Regional myocardial systolic function during acute myocardial ischemia assessed by strain Doppler echocardiography. J Am Coll Cardiol 2001; 37:726-30.

21. Hanekom L, Jenkins C, Jeffries L, Case C, Mundy J, Hawley C et al. Incremental value of strain rate analysis as an adjunct to wall-motion scoring for assessment of myocardial viability by dobutamine echocardiography: a follow-up study after revascularization. Circulation 2005; 112:3892-900.

22. Hoffmann R, Altiok E, Nowak B, Heussen N, Kuhl H, Kaiser HJ et al. Strain rate measurement by doppler echocardiography allows improved assessment of myocardial viability inpatients with depressed left ventricular function. J Am Coll Cardiol 2002; 39:443-9.

23. Bjork IC, Rozis E, Slordahl SA, Marwick TH. Incremental value of strain rate imaging to wall motion analysis for prediction of outcome in patients undergoing dobutamine stress echocardiography. Circulation 2007; 115:1252-9.

24. Stoylen A. Strain rate imaging. NTNU. http://folk.ntnu.no/stoylen/strainrate 2006. 6-6-2007.

25. Heimdal A. Angle Dependency of Systolic Strain Measurements using Strain Rate Imaging. http://folk.ntnu.no/stoylen/strainrate/mathemathics/Angledep.html . 1998. 10-10-2007.

26. Bohs LN, Trahey GE. A novel method for angle independent ultrasonic imaging of blood flow and tissue motion. IEEE Trans Biomed Eng 1991; 38:280-6.

27. Bohs LN, Friemel BH, Trahey GE. Experimental velocity profiles and volumetric flow via two-dimensional speckle tracking. Ultrasound Med Biol 1995; 21:885-98.

28. Rappaport D, Adam D, Lysyansky P, Riesner S. Assessment of myocardial regional strain and strain rate by tissue tracking in B-mode echocardiograms. Ultrasound Med Biol 2006; 32:1181-92.

29. Langeland S, D'hooge J, Wouters PF, Leather HA, Claus P, Bijnens B et al. Experimental validation of a new ultrasound method for the simultaneous assessment of radial and longitudinal myocardial deformation independent of insonation angle. Circulation 2005; 112:2157-62.

30. Toyoda T, Baba H, Akasaka T, Akiyama M, Neishi Y, Tomita J et al. Assessment of regional myocardial strain by a novel automated tracking system from digital image files. J Am Soc Echocardiogr 2004; 17:1234-8.

31. Ingul CB, Aase SA: Automated strain and strain rate; in: Marwick TH, Yu CM, Sun PS, (eds): Myocardial Imaging - Tissue Doppler and Speckle Tracking. Blackwell Publishing, 2007, pp 278-287.

32. Ingul CB, Torp H, Aase SA, Berg S, Stoylen A, Slordahl SA. Automated analysis of strain rate and strain: feasibility and clinical implications. J Am Soc Echocardiogr 2005; 18:411-8.

33. Hexeberg E, Birkeland S, Grong K, Matre K, Lekven J. Coronary artery stenosis provokes non-uniformity of two-dimensional deformation in the anterior wall of the feline left ventricle. Eur Heart J 1992; 13:981-9.

34. Helle-Valle T, Crosby J, Edvardsen T, Lyseggen E, Amundsen BH, Smith HJ et al. New noninvasive method for assessment of left ventricular rotation: speckle tracking echocardiography. Circulation 2005; 112:3149-56.

35. Lima JA, Jeremy R, Guier W, Bouton S, Zerhouni EA, McVeigh E et al. Accurate systolic wall thickening by nuclear magnetic resonance imaging with tissue

tagging: correlation with sonomicrometers in normal and ischemic myocardium. J Am Coll Cardiol 1993; 21:1741-51.

36. Kim RJ, Fieno DS, Parrish TB, Harris K, Chen EL, Simonetti O et al. Relationship of MRI delayed contrast enhancement to irreversible injury, infarct age, and contractile function. Circulation 1999; 100:1992-2002.

37. Bogaert J, Dymarkowski S. Delayed contrast-enhanced MRI: use in myocardial viability assessment and other cardiac pathology. Eur Radiol 2005; 15 Suppl 2:B52-B58.

38. Yeon SB, Reichek N, Tallant BA, Lima JA, Calhoun LP, Clark NR et al. Validation of in vivo myocardial strain measurement by magnetic resonance tagging with sonomicrometry. J Am Coll Cardiol 2001; 38:555-61.

39. Khalifa A, Youssef AB, Osman N. Improved Harmonic Phase (HARP) Method for Motion Tracking a Tagged Cardiac MR images. Conf Proc IEEE Eng Med Biol Soc 2005; 4:4298-301.

40. Osman NF, Kerwin WS, McVeigh ER, Prince JL. Cardiac motion tracking using CINE harmonic phase (HARP) magnetic resonance imaging. Magn Reson Med 1999; 42:1048-60.

41. Pan L, Prince JL, Lima JA, Osman NF. Fast tracking of cardiac motion using 3D-HARP. IEEE Trans Biomed Eng 2005; 52:1425-35.

42. Ryf S, Rutz AK, Boesiger P, Schwitter J. Is post-systolic shortening a reliable indicator of myocardial viability? An MR tagging and late-enhancement study. J Cardiovasc Magn Reson 2006; 8:445-51.

43. Ryf S, Schwitter J, Spiegel MA, Rutz AK, Luechinger R, Crelier GR et al. Accelerated tagging for the assessment of left ventricular myocardial contraction under physical stress. J Cardiovasc Magn Reson 2005; 7:693-703.

44. Ryf S, Tsao J, Schwitter J, Stuessi A, Boesiger P. Peak-combination HARP: a method to correct for phase errors in HARP. J Magn Reson Imaging 2004; 20:874-80.

45. Ryf S, Spiegel MA, Gerber M, Boesiger P. Myocardial tagging with 3D-CSPAMM. J Magn Reson Imaging 2002; 16:320-5.

46. Moore CC, O'Dell WG, McVeigh ER, Zerhouni EA. Calculation of three-dimensional left ventricular strains from biplanar tagged MR images. J Magn Reson Imaging 1992; 2:165-75.

47. Folkehelseinstituttet, Dødsårsaksregisteret. 2004: Stadig færre dør av infarkt. http://www.fhi.no/eway/default.aspx?pid=233&trg=MainArea_5661&MainArea_5661=5799:0:15,3409:1:0:0:::0:0 . 1-6-2006. 19-5-2007.

48. American Heart Association: Cardiovascular Disease Statistics. American Heart Association . 2007. 19-5-2007.

49. Ingul CB, Stoylen A, Slordahl SA. Recovery of stunned myocardium in acute myocardial infarction quantified by strain rate imaging: a clinical study. J Am Soc Echocardiogr 2005; 18:401-10.

50. Penco M, Sciomer S, Vizza CD, Dagianti A, Vitarelli A, Romano S et al. Clinical impact of echocardiography in prognostic stratification after acute myocardial infarction. Am J Cardiol 1998; 81:17G-20G.

51. Rizzello V, Poldermans D, Bax JJ. Assessment of myocardial viability in chronic ischemic heart disease: current status. Q J Nucl Med Mol Imaging 2005; 49:81-96.

52. Bax JJ, Schinkel AF, Boersma E, Rizzello V, Elhendy A, Maat A et al. Early versus delayed revascularization in patients with ischemic cardiomyopathy and substantial viability: impact on outcome. Circulation 2003; 108 Suppl 1:II39-II42.

53. Selvanayagam JB, Kardos A, Francis JM, Wiesmann F, Petersen SE, Taggart DP et al. Value of delayed-enhancement cardiovascular magnetic resonance imaging in predicting myocardial viability after surgical revascularization. Circulation 2004; 110:1535-41.

54. Gerber BL, Garot J, Bluemke DA, Wu KC, Lima JA. Accuracy of contrast-enhanced magnetic resonance imaging in predicting improvement of regional myocardial function in patients after acute myocardial infarction. Circulation 2002; 106:1083-9.

55. Beek AM, Kuhl HP, Bondarenko O, Twisk JW, Hofman MB, Van Dockum WG et al. Delayed contrast-enhanced magnetic resonance imaging for the prediction of regional functional improvement after acute myocardial infarction. J Am Coll Cardiol 2003; 42:895-901.

56. Kim RJ, Wu E, Rafael A, Chen EL, Parker MA, Simonetti O et al. The use of contrast-enhanced magnetic resonance imaging to identify reversible myocardial dysfunction. N Engl J Med 2000; 343:1445-53.

57. Sandstede JJ, Lipke C, Beer M, Harre K, Pabst T, Kenn W et al. Analysis of first-pass and delayed contrast-enhancement patterns of dysfunctional myocardium on MR imaging: use in the prediction of myocardial viability. AJR Am J Roentgenol 2000; 174:1737-40.

58. Moller JE, Dahlstrom U, Gotzsche O, Lahiri A, Skagen K, Andersen GS et al. Effects of losartan and captopril on left ventricular systolic and diastolic function after acute myocardial infarction: results of the Optimal Trial in Myocardial Infarction with Angiotensin II Antagonist Losartan (OPTIMAAL) echocardiographic substudy. Am Heart J 2004; 147:494-501.

59. Doughty RN, Whalley GA, Walsh HA, Gamble GD, Lopez-Sendon J, Sharpe N. Effects of carvedilol on left ventricular remodeling after acute myocardial infarction: the CAPRICORN Echo Substudy. Circulation 2004; 109:201-6.

60. Haykowsky MJ, Liang Y, Pechter D, Jones LW, McAlister FA, Clark AM. A meta-analysis of the effect of exercise training on left ventricular remodeling in heart failure patients: the benefit depends on the type of training performed. J Am Coll Cardiol 2007; 49:2329-36.

61. Wagner PD. New ideas on limitations to VO2max. Exerc Sport Sci Rev 2000; 28:10-4.

62. Zhou B, Conlee RK, Jensen R, Fellingham GW, George JD, Fisher AG. Stroke volume does not plateau during graded exercise in elite male distance runners. Med Sci Sports Exerc 2001; 33:1849-54.

63. Gledhill N, Cox D, Jamnik R. Endurance athletes' stroke volume does not plateau: major advantage is diastolic function. Med Sci Sports Exerc 1994; 26:1116-21.

64. Froelicher VF, Myers J: Exercise and the heart. ed 4th ed, Philadelphia, W.B. Saunders, 2000.

65. Froelicher VF, Myers J: Exercise and the heart. ed 5th ed, Philadelphia, Saunders Elsevier, 2006.

66. Ades PA, Waldmann ML, Meyer WL, Brown KA, Poehlman ET, Pendlebury WW et al. Skeletal muscle and cardiovascular adaptations to exercise conditioning in older coronary patients. Circulation 1996; 94:323-30.

67. Yu CM, Li LS, Lam MF, Siu DC, Miu RK, Lau CP. Effect of a cardiac rehabilitation program on left ventricular diastolic function and its relationship to exercise capacity in patients with coronary heart disease: experience from a randomized, controlled study. Am Heart J 2004; 147:e24.

68. Dubach P, Myers J, Dziekan G, Goebbels U, Reinhart W, Muller P et al. Effect of high intensity exercise training on central hemodynamic responses to exercise in men with reduced left ventricular function. J Am Coll Cardiol 1997; 29:1591-8.

69. Hagberg JM, Goldberg AP, Lakatta L, O'Connor FC, Becker LC, Lakatta EG et al. Expanded blood volumes contribute to the increased cardiovascular performance of endurance-trained older men. J Appl Physiol 1998; 85:484-9.

70. Helgerud J, Hoydal K, Wang E, Karlsen T, Berg P, Bjerkaas M et al. Aerobic high-intensity intervals improve VO2max more than moderate training. Med Sci Sports Exerc 2007; 39:665-71.

71. Slordahl SA, Madslien VO, Stoylen A, Kjos A, Helgerud J, Wisloff U. Atrioventricular plane displacement in untrained and trained females. Med Sci Sports Exerc 2004; 36:1871-5.

72. Ehsani AA, Biello DR, Schultz J, Sobel BE, Holloszy JO. Improvement of left ventricular contractile function by exercise training in patients with coronary artery disease. Circulation 1986; 74:350-8.

73. Hagberg JM, Ehsani AA, Holloszy JO. Effect of 12 months of intense exercise training on stroke volume in patients with coronary artery disease. Circulation 1983; 67:1194-9.

74. Oberman A, Fletcher GF, Lee J, Nanda N, Fletcher BJ, Jensen B et al. Efficacy of high-intensity exercise training on left ventricular ejection fraction in men with coronary artery disease (the Training Level Comparison Study). Am J Cardiol 1995; 76:643-7.

75. Adachi H, Koike A, Obayashi T, Umezawa S, Aonuma K, Inada M et al. Does appropriate endurance exercise training improve cardiac function in patients with prior myocardial infarction? Eur Heart J 1996; 17:1511-21.

76. Pelliccia A, Di Paolo FM, Maron BJ. The athlete's heart: remodeling, electrocardiogram and preparticipation screening. Cardiol Rev 2002; 10:85-90.

77. Pelliccia A, Maron BJ, De LR, Di Paolo FM, Spataro A, Culasso F. Remodeling of left ventricular hypertrophy in elite athletes after long-term deconditioning. Circulation 2002; 105:944-9.

78. Vinereanu D, Florescu N, Sculthorpe N, Tweddel AC, Stephens MR, Fraser AG. Left ventricular long-axis diastolic function is augmented in the hearts of endurance-trained compared with strength-trained athletes. Clin Sci (Lond) 2002; 103:249-57.

79. Goodman JM, Liu PP, Green HJ. Left ventricular adaptations following short-term endurance training. J Appl Physiol 2005; 98:454-60.

80. Wisloff U, Stoylen A, Loennechen JP, Bruvold M, Rognmo O, Haram PM et al. Superior cardiovascular effect of aerobic interval training versus moderate continuous training in heart failure patients: a randomized study. Circulation 2007; 115:3086-94.

81. Huonker M, Konig D, Keul J. Assessment of left ventricular dimensions and functions in athletes and sedentary subjects at rest and during exercise using echocardiography, Doppler sonography and radionuclide ventriculography. Int J Sports Med 1996; 17 Suppl 3:S173-S179.

82. St John SM, Pfeffer MA, Plappert T, Rouleau JL, Moye LA, Dagenais GR et al. Quantitative two-dimensional echocardiographic measurements are major predictors of adverse cardiovascular events after acute myocardial infarction. The protective effects of captopril. Circulation 1994; 89:68-75.

83. Tabet JY, Logeart D, Geyer C, Guiti C, Ennezat PV, Dahan M et al. Comparison of the prognostic value of left ventricular filling and peak oxygen uptake in patients with systolic heart failure. Eur Heart J 2000; 21:1864-71.

84. Smart N, Haluska B, Leano R, Case C, Mottram PM, Marwick TH. Determinants of functional capacity in patients with chronic heart failure: role of filling pressure and systolic and diastolic function. Am Heart J 2005; 149:152-8.

85. Skaluba SJ, Litwin SE. Mechanisms of exercise intolerance: insights from tissue Doppler imaging. Circulation 2004; 109:972-7.

86. Alam M, Wardell J, Andersson E, Samad BA, Nordlander R. Characteristics of mitral and tricuspid annular velocities determined by pulsed wave Doppler tissue imaging in healthy subjects. J Am Soc Echocardiogr 1999; 12:618-28.

87. Skaluba SJ, Bray BE, Litwin SE. Close coupling of systolic and diastolic function: combined assessment provides superior prediction of exercise capacity. J Card Fail 2005; 11:516-22.

88. Yip G, Wang M, Zhang Y, Fung JW, Ho PY, Sanderson JE. Left ventricular long axis function in diastolic heart failure is reduced in both diastole and systole: time for a redefinition? Heart 2002; 87:121-5.

89. Ommen SR, Nishimura RA, Appleton CP, Miller FA, Oh JK, Redfield MM et al. Clinical utility of Doppler echocardiography and tissue Doppler imaging in the estimation of left ventricular filling pressures: A comparative simultaneous Doppler-catheterization study. Circulation 2000; 102:1788-94.

90. Nagueh SF, Mikati I, Kopelen HA, Middleton KJ, Quinones MA, Zoghbi WA. Doppler estimation of left ventricular filling pressure in sinus tachycardia. A new application of tissue doppler imaging. Circulation 1998; 98:1644-50.

91. Burgess MI, Jenkins C, Sharman JE, Marwick TH. Diastolic stress echocardiography: hemodynamic validation and clinical significance of estimation of ventricular filling pressure with exercise. J Am Coll Cardiol 2006; 47:1891-900.

92. Ha JW, Oh JK, Pellikka PA, Ommen SR, Stussy VL, Bailey KR et al. Diastolic stress echocardiography: a novel noninvasive diagnostic test for diastolic dysfunction using supine bicycle exercise Doppler echocardiography. J Am Soc Echocardiogr 2005; 18:63-8.

93. Wang J, Khoury DS, Thohan V, Torre-Amione G, Nagueh SF. Global diastolic strain rate for the assessment of left ventricular relaxation and filling pressures. Circulation 2007; 115:1376-83.

94. MRIsafety.com. Institute for magnetic resonance safety, education, and research . 2007. 20-5-2007.

95. Bjork IC, Rozis E, Slordahl SA, Marwick TH. Incremental value of strain rate imaging to wall motion analysis for prediction of outcome in patients undergoing dobutamine stress echocardiography. Circulation 2007; 115:1252-9.

96. Ingul CB. Quantification of regional myocardial function by strain rate and strain for evaluation of coronary artery disease. 2006. Norwegian University of Science and Technology.

97. Aase SA, Stoylen A, Ingul CB, Frigstad S, Torp H. Automatic timing of aortic valve closure in apical tissue Doppler images. Ultrasound Med Biol 2006; 32:19-27.

98. O'Dell WG, Moore CC, Hunter WC, Zerhouni EA, McVeigh ER. Three-dimensional myocardial deformations: calculation with displacement field fitting to tagged MR images. Radiology 1995; 195:829-35.

99. Cerqueira MD, Weissman NJ, Dilsizian V, Jacobs AK, Kaul S, Laskey WK et al. Standardized myocardial segmentation and nomenclature for tomographic imaging of the heart: a statement for healthcare professionals from the Cardiac Imaging Committee of the Council on Clinical Cardiology of the American Heart Association. Circulation 2002; 105:539-42.

100. Fischer SE, McKinnon GC, Maier SE, Boesiger P. Improved myocardial tagging contrast. Magn Reson Med 1993; 30:191-200.

101. Bland JM, Altman DG. Measuring agreement in method comparison studies. Stat Methods Med Res 1999; 8:135-60.

102. Bland JM, Altman DG. Statistical methods for assessing agreement between two methods of clinical measurement. Lancet 1986; 1:307-10.

103. Vickers AJ, Altman DG. Statistics notes: Analysing controlled trials with baseline and follow up measurements. BMJ 2001; 323:1123-4.

104. Wellnhofer E, Olariu A, Klein C, Grafe M, Wahl A, Fleck E et al. Magnetic resonance low-dose dobutamine test is superior to SCAR quantification for the prediction of functional recovery. Circulation 2004; 109:2172-4.

105. Motoyasu M, Sakuma H, Ichikawa Y, Ishida N, Uemura S, Okinaka T et al. Prediction of regional functional recovery after acute myocardial infarction with low dose dobutamine stress cine MR imaging and contrast enhanced MR imaging. J Cardiovasc Magn Reson 2003; 5:563-74.

106. Leitman M, Lysyansky P, Sidenko S, Shir V, Peleg E, Binenbaum M et al. Two-dimensional strain-a novel software for real-time quantitative echocardiographic assessment of myocardial function. J Am Soc Echocardiogr 2004; 17:1021-9.

107. Becker M, Hoffmann R, Kuhl HP, Grawe H, Katoh M, Kramann R et al. Analysis of myocardial deformation based on ultrasonic pixel tracking to determine transmurality in chronic myocardial infarction. Eur Heart J 2006; 27:2560-6.

108. Cho GY, Chan J, Leano R, Strudwick M, Marwick TH. Comparison of two-dimensional speckle and tissue velocity based strain and validation with harmonic phase magnetic resonance imaging. Am J Cardiol 2006; 97:1661-6.

109. Korinek J, Wang J, Sengupta PP, Miyazaki C, Kjaergaard J, McMahon E et al. Two-dimensional strain--a Doppler-independent ultrasound method for quantitation of regional deformation: validation in vitro and in vivo. J Am Soc Echocardiogr 2005; 18:1247-53.

110. Azevedo CF, Amado LC, Kraitchman DL, Gerber BL, Osman NF, Rochitte CE et al. Persistent diastolic dysfunction despite complete systolic functional recovery after reperfused acute myocardial infarction demonstrated by tagged magnetic resonance imaging. Eur Heart J 2004; 25:1419-27.

111. Gjesdal O, Hopp E, Vartdal T, Lunde K, Helle-Valle T, Aakhus S et al. Global longitudinal strain by two-dimensional speckle tracking echocardiography is closely related to myocardial infarct size in chronic ischaemic heart disease. Clin Sci (Lond) 2007.

112. Sachdev V, Aletras AH, Padmanabhan S, Sidenko S, Rao YN, Brenneman CL et al. Myocardial strain decreases with increasing transmurality of infarction: a Doppler echocardiographic and magnetic resonance correlation study. J Am Soc Echocardiogr 2006; 19:34-9.

113. Chan J, Hanekom L, Wong C, Leano R, Cho GY, Marwick TH. Differentiation of subendocardial and transmural infarction using two-dimensional strain rate imaging to assess short-axis and long-axis myocardial function. J Am Coll Cardiol 2006; 48:2026-33.

114. Zhang Y, Chan AK, Yu CM, Yip GW, Fung JW, Lam WW et al. Strain rate imaging differentiates transmural from non-transmural myocardial infarction: a validation study using delayed-enhancement magnetic resonance imaging. J Am Coll Cardiol 2005; 46:864-71.

115. Jamal F, Kukulski T, Sutherland GR, Weidemann F, D'hooge J, Bijnens B et al. Can changes in systolic longitudinal deformation quantify regional myocardial function after an acute infarction? An ultrasonic strain rate and strain study. J Am Soc Echocardiogr 2002; 15:723-30.

116. Slordahl SA, Bjaerum S, Amundsen BH, Stoylen A, Heimdal A, Rabben SI et al. High frame rate strain rate imaging of the interventricular septum in healthy subjects. Eur J Ultrasound 2001; 14:149-55.

117. Sarkar U, Ali S, Whooley MA. Self-efficacy and health status in patients with coronary heart disease: findings from the heart and soul study. Psychosom Med 2007; 69:306-12.

118. Myers J, Prakash M, Froelicher V, Do D, Partington S, Atwood JE. Exercise capacity and mortality among men referred for exercise testing. N Engl J Med 2002; 346:793-801.

119. Kavanagh T, Mertens DJ, Hamm LF, Beyene J, Kennedy J, Corey P et al. Prediction of long-term prognosis in 12 169 men referred for cardiac rehabilitation. Circulation 2002; 106:666-71.

120. Taylor RS, Brown A, Ebrahim S, Jolliffe J, Noorani H, Rees K et al. Exercise-based rehabilitation for patients with coronary heart disease: systematic review and meta-analysis of randomized controlled trials. Am J Med 2004; 116:682-92.

121. Wilson JR, Mancini DM, Dunkman WB. Exertional fatigue due to skeletal muscle dysfunction in patients with heart failure. Circulation 1993; 87:470-5.

122. Walther C, Gielen S, Hambrecht R. The effect of exercise training on endothelial function in cardiovascular disease in humans. Exerc Sport Sci Rev 2004; 32:129-34.

123. Lele SS, Macfarlane D, Morrison S, Thomson H, Khafagi F, Frenneaux M. Determinants of exercise capacity in patients with coronary artery disease and mild to moderate systolic dysfunction. Role of heart rate and diastolic filling abnormalities. Eur Heart J 1996; 17:204-12.

124. Lele SS, Thomson HL, Seo H, Belenkie I, McKenna WJ, Frenneaux MP. Exercise capacity in hypertrophic cardiomyopathy. Role of stroke volume limitation, heart rate, and diastolic filling characteristics. Circulation 1995; 92:2886-94.

125. Miyashita T, Okano Y, Takaki H, Satoh T, Kobayashi Y, Goto Y. Relation between exercise capacity and left ventricular systolic versus diastolic function during exercise in patients after myocardial infarction. Coron Artery Dis 2001; 12:217-25.

126. Stoylen A, Wisloff U, Slordahl S. Left ventricular mechanics during exercise: a Doppler and tissue Doppler study. Eur J Echocardiogr 2003; 4:286-91.

127. Schairer JR, Stein PD, Keteyian S, Fedel F, Ehrman J, Alam M et al. Left ventricular response to submaximal exercise in endurance-trained athletes and sedentary adults. Am J Cardiol 1992; 70:930-3.

128. Sundstedt M, Hedberg P, Jonason T, Ringqvist I, Brodin LA, Henriksen E. Left ventricular volumes during exercise in endurance athletes assessed by contrast echocardiography. Acta Physiol Scand 2004; 182:45-51.

129. Sanderson JE. Heart failure with a normal ejection fraction. Heart 2007; 93:155-8.

130. Kass DA, Bronzwaer JG, Paulus WJ. What mechanisms underlie diastolic dysfunction in heart failure? Circ Res 2004; 94:1533-42.

131. Thadani U, West RO, Mathew TM, Parker JO. Hemodynamics at rest and during supine and sitting bicycle exercise in patients with coronary artery disease. Am J Cardiol 1977; 39:776-83.

132. Thadani U, Parker JO. Hemodynamics at rest and during supine and sitting bicycle exercise in normal subjects. Am J Cardiol 1978; 41:52-9.

133. Wang M, Yip GW, Wang AY, Zhang Y, Ho PY, Tse MK et al. Peak early diastolic mitral annulus velocity by tissue Doppler imaging adds independent and incremental prognostic value. J Am Coll Cardiol 2003; 41:820-6.

134. Park TH, Nagueh SF, Khoury DS, Kopelen HA, Akrivakis S, Nasser K et al. Impact of myocardial structure and function postinfarction on diastolic strain measurements: implications for assessment of myocardial viability. Am J Physiol Heart Circ Physiol 2006; 290:H724-H731.

135. Kato T, Noda A, Izawa H, Nishizawa T, Somura F, Yamada A et al. Myocardial velocity gradient as a noninvasively determined index of left ventricular diastolic dysfunction in patients with hypertrophic cardiomyopathy. J Am Coll Cardiol 2003; 42:278-85.

136. Palka P, Lange A, Nihoyannopoulos P. The effect of long-term training on age-related left ventricular changes by Doppler myocardial velocity gradient. Am J Cardiol 1999; 84:1061-7.

137. Paulus WJ, Tschope C, Sanderson JE, Rusconi C, Flachskampf FA, Rademakers FE et al. How to diagnose diastolic heart failure: a consensus statement on the diagnosis of heart failure with normal left ventricular ejection fraction by the Heart Failure and Echocardiography Associations of the European Society of Cardiology. Eur Heart J 2007; 28:2539-50.

138. Nagueh SF, Shah G, Wu Y, Torre-Amione G, King NM, Lahmers S et al. Altered titin expression, myocardial stiffness, and left ventricular function in patients with dilated cardiomyopathy. Circulation 2004; 110:155-62.

139. Vartdal T, Brunvand H, Pettersen E, Smith HJ, Lyseggen E, Helle-Valle T et al. Early prediction of infarct size by strain Doppler echocardiography after coronary reperfusion. J Am Coll Cardiol 2007; 49:1715-21.

140. Jolliffe JA, Rees K, Taylor RS, Thompson D, Oldridge N, Ebrahim S. Exercise-based rehabilitation for coronary heart disease. *Cochrane Database of Systematic Reviews* 2000, Issue 4. Art. No.: CD001800. DOI: 10.1002/14651858.CD001800

141. Wenger HA, Bell GJ. The interactions of intensity, frequency and duration of exercise training in altering cardiorespiratory fitness. Sports Med 1986; 3:346-56.

142. Noel M, Jobin J, Marcoux A, Poirier P, Dagenais GR, Bogaty P. Can prolonged exercise-induced myocardial ischaemia be innocuous? Eur Heart J 2007; 28:1559-65.

143. Lee IM. Dose-response relation between physical activity and fitness: even a little is good; more is better. JAMA 2007; 297:2137-9.

144. Giannuzzi P, Mezzani A, Saner H, Bjornstad H, Fioretti P, Mendes M et al. Physical activity for primary and secondary prevention. Position paper of the Working Group on Cardiac Rehabilitation and Exercise Physiology of the European Society of Cardiology. Eur J Cardiovasc Prev Rehabil 2003; 10:319-27.

145. Fletcher GF, Balady GJ, Amsterdam EA, Chaitman B, Eckel R, Fleg J et al. Exercise standards for testing and training: a statement for healthcare professionals from the American Heart Association. Circulation 2001; 104:1694-740.

146. Notomi Y, Martin-Miklovic MG, Oryszak SJ, Shiota T, Deserranno D, Popovic ZB et al. Enhanced ventricular untwisting during exercise: a mechanistic manifestation of elastic recoil described by Doppler tissue imaging. Circulation 2006; 113:2524-33.

147. Myers J, Wagner D, Schertler T, Beer M, Luchinger R, Klein M et al. Effects of exercise training on left ventricular volumes and function in patients with nonischemic cardiomyopathy: application of magnetic resonance myocardial tagging. Am Heart J 2002; 144:719-25.

Paper I

Journal of the American College of Cardiology
© 2006 by the American College of Cardiology Foundation
Published by Elsevier Inc.

Vol. 47, No. 4, 2006
ISSN 0735-1097/06/$32.00
doi:10.1016/j.jacc.2005.10.040

Noninvasive Myocardial Strain Measurement by Speckle Tracking Echocardiography

Validation Against Sonomicrometry and Tagged Magnetic Resonance Imaging

Brage H. Amundsen, MD,* Thomas Helle-Valle, MD,† Thor Edvardsen, PHD, MD,† Hans Torp, DRTECHN,* Jonas Crosby, MSC,* Erik Lyseggen, MD,† Asbjørn Støylen, MD, PHD,*‡ Halfdan Ihlen, MD, PHD,† João A. C. Lima, MD, FACC,§ Otto A. Smiseth, MD, PHD, FACC,† Stig A. Slørdahl, MD, PHD*‡

Trondheim and Oslo, Norway; and Baltimore, Maryland

OBJECTIVES The aim of this study was to validate speckle tracking echocardiography (STE) as a method for angle-independent measurement of regional myocardial strain, using sonomicrometry and magnetic resonance imaging (MRI) tagging as reference methods.

BACKGROUND Tissue Doppler imaging allows non-invasive measurement of myocardial strain in the left ventricle (LV), but is limited by angle dependency.

METHODS Strain measurements with STE were obtained by a custom-made program that allowed tracking of two-dimensional motion of speckle patterns in a B-mode image. In anesthetized dogs, we compared LV long- and short-axis measurements by STE to sonomicrometry during preload changes and regional myocardial ischemia. Measurements in the two orthogonal axes were obtained simultaneously in a single imaging plane. In human subjects, long-axis strain by STE and MRI tagging were compared in multiple segments of the LV.

RESULTS In the experimental study there was good correlation and agreement between STE and sonomicrometry for systolic strain in the long axis ($r = 0.90$, $p < 0.001$; 95% limits of agreement −4.4% to 5.0%) and systolic shortening in the short axis ($r = 0.79$, $p < 0.001$; −5.6% to 5.1%). In the clinical study, 80% of the segments could be analyzed, and correlation and agreement between STE and MRI tagging were good ($r = 0.87$, $p < 0.001$; −9.1% to 8.0%).

CONCLUSIONS Speckle tracking echocardiography provides accurate and angle-independent measurements of LV dimensions and strains and has potential to become a clinical bedside tool for quantifying myocardial strain. (J Am Coll Cardiol 2006;47:789–93) © 2006 by the American College of Cardiology Foundation

Myocardial strain calculated from tissue Doppler imaging (TDI) has been shown to be superior to myocardial velocities by TDI and wall motion score in assessment of ischemia in experimental and clinical studies (1–4). However, TDI-based strain measurements are angle dependent owing to use of the Doppler effect and simultaneous opposite deformation in the long and short axes (1,2). Speckle tracking is an echocardiographic method based on tracking of characteristic speckle patterns created by interference of ultrasound beams in the myocardium (5). As the tracking is based on grayscale B-mode images, it is in principle angle independent. Different speckle tracking methods have been applied in vivo previously, but systematic validation studies are sparse (6,7).

We have developed a speckle tracking echocardiography (STE) application for B-mode images that tracks the displacement of segment end points and calculates strain from the change of length between them. In contrast, a different speckle tracking application that has recently been made commercially available (2D Strain, GE Vingmed, Horten, Norway) tracks a larger number of small regions and averages their motion with spline interpolation before regional curves can be extracted (6). The aim of the present study was to validate STE against sonomicrometry in an experimental study and against magnetic resonance imaging (MRI) tagging in a clinical study.

METHODS

Experimental study. Nine mongrel dogs of either gender (23 ± 2 kg) were anesthetized and instrumented as previously described (2). Recordings were done at baseline ($n = 9$), during intravenous loading with 1,000 ml saline ($n = 9$), and during 5 to 15 min occlusion of the left anterior descending coronary artery (LAD) ($n = 9$). The study protocol was approved by the National Animal Experimental Board.

Sonomicrometry. Four ultrasonic crystals were implanted in the left ventricular (LV) wall (Sonometrics Corp., London, Ontario, Canada) to allow simultaneous measurements

From the *Department of Circulation and Medical Imaging, Norwegian University of Science and Technology, Trondheim, Norway; †Institute for Surgical Research/Department of Cardiology, Rikshospitalet University Hospital, Oslo, Norway; ‡Department of Cardiology, St. Olavs Hospital/Trondheim University Hospital, Trondheim, Norway; and §Department of Cardiology, Johns Hopkins University, Baltimore, Maryland. Dr. Amundsen and Mr. Crosby were recipients of grants from the Research Council of Norway, Oslo, Norway. Drs. Helle-Valle and Lyseggen were recipients of grants from the Norwegian Council of Cardiovascular Diseases, Oslo, Norway. Dr. Torp has received consultant fees from GE Vingmed Ultrasound, Norway.

Manuscript received April 15, 2005; revised manuscript received August 14, 2005, accepted October 3, 2005.

Abbreviations and Acronyms

COR = coefficient of repeatability
LAD = left anterior descending artery
LV = left ventricle/ventricular
MRI = magnetic resonance imaging
ROI = region of interest
STE = speckle tracking echocardiography
TDI = tissue Doppler imaging

of long-axis strain (in the septum and lateral wall) and LV short-axis systolic shortening (at the apical and mid-ventricular levels) (Fig. 1A). The traces were analyzed in SonoVIEW (Sonometrics Corp.). Lagrangian strain was calculated as: strain = $(L - L_0)/L_0$, where L_0 is segment length at the onset of the QRS.

Echocardiography. B-mode second-harmonic images (frame rate 68 ± 31 s^{-1}) were recorded from the apical four-chamber view (Vivid 7, 2.0 MHz transducer, GE Vingmed, Horten, Norway). The imaging plane was matched to the crystal positions. Images were analyzed in a Matlab-based custom-made program (MathWorks Inc., Natick, Massachusetts), which uses the "sum of absolute differences" method to find the most similar speckle pattern in two subsequent frames (5) (Fig. 2). Four 5 × 5 mm regions of interest (ROI) were placed corresponding to the crystal positions. Maximum tracking velocities were ±16 cm/s in the beam direction and ±12 cm/s laterally, and forward and backward tracking were averaged (weighted). Strain and shortening were calculated from the change of length between pairs of ROIs and averaged over three cycles. No temporal averaging was applied.

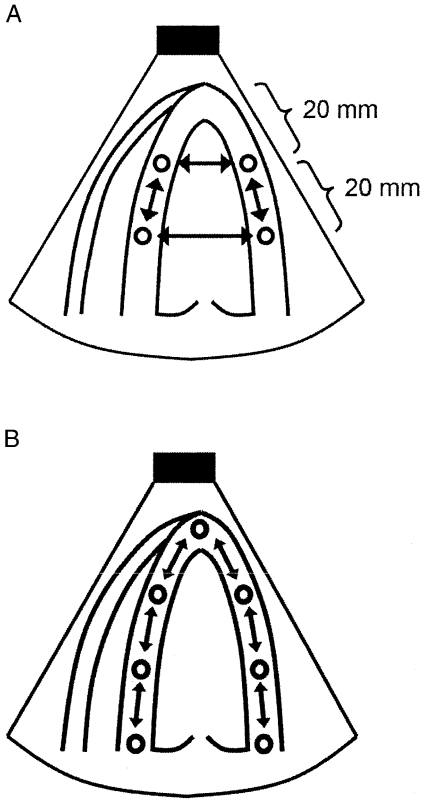

Figure 1. (A) Figure from the experimental study showing an apical four-chamber view with crystal positions **(circles)** and directions for strain and shortening measurements **(arrows)**. **(B)** Figure from the clinical study showing an apical four-chamber view with the positions of the seven regions of interest **(circles)** and **arrows** to indicate where strain was measured.

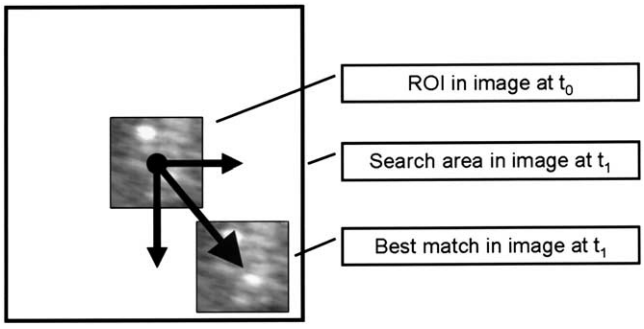

Figure 2. Speckle tracking: the motion of the region of interest (ROI) from one frame (t_0) to the next (t_1) can be quantified in two dimensions, allowing angle-independent measurements. t = time.

Clinical study. Eleven subjects, seven with previous myocardial infarction (65 ± 7 years) and four healthy volunteers (37 ± 13 years) were included after having given written informed consent. The study protocol was approved by the Institutional Review Board of the Johns Hopkins University.

MRI tagging. Tagged MRI images were recorded using a 1.5-T magnet with a phased-array cardiac coil (Signa, GE Healthcare, Waukesha, Wisconsin) applying an electrocardiogram-triggered segmented k-space fast gradient-echo sequence (DANTE-SPAMM) (8). Four to five contiguous stacks of short-axis images were prescribed from base to apex, and six long-axis slices were prescribed radially every 30°. Lagrangian strain was analyzed from this three-dimensional data using a displacement field-fitting method (8). Long-axis strain was measured in the basal, mid, and apical segments of the septum, lateral, anterior, and inferior walls (9).

Echocardiography. B-mode second-harmonic images (frame rate 84 ± 18 s^{-1}) were recorded from the apical two- and four-chamber views (System Five, 2.0 MHz transducer, GE Vingmed). Seven ROIs were positioned to measure strain in six segments in each image (Fig. 1B).

Statistics. Strain values were compared using paired-sample *t* test and by calculating the 95% limits of agreement (10). Bonferroni post-hoc correction of p values was used for comparison of baseline with loading and LAD occlusion values (number of comparisons = 2). Intra- and interobserver variability was measured by the coefficient of repeatability (COR) (10). A $p < 0.05$ was considered statistically significant. Values are reported as mean ± SD.

RESULTS

Experimental study. Long-axis strain measured by STE and sonomicrometry correlated well ($r = 0.90$, $p < 0.001$), as did the measurements of short-axis systolic

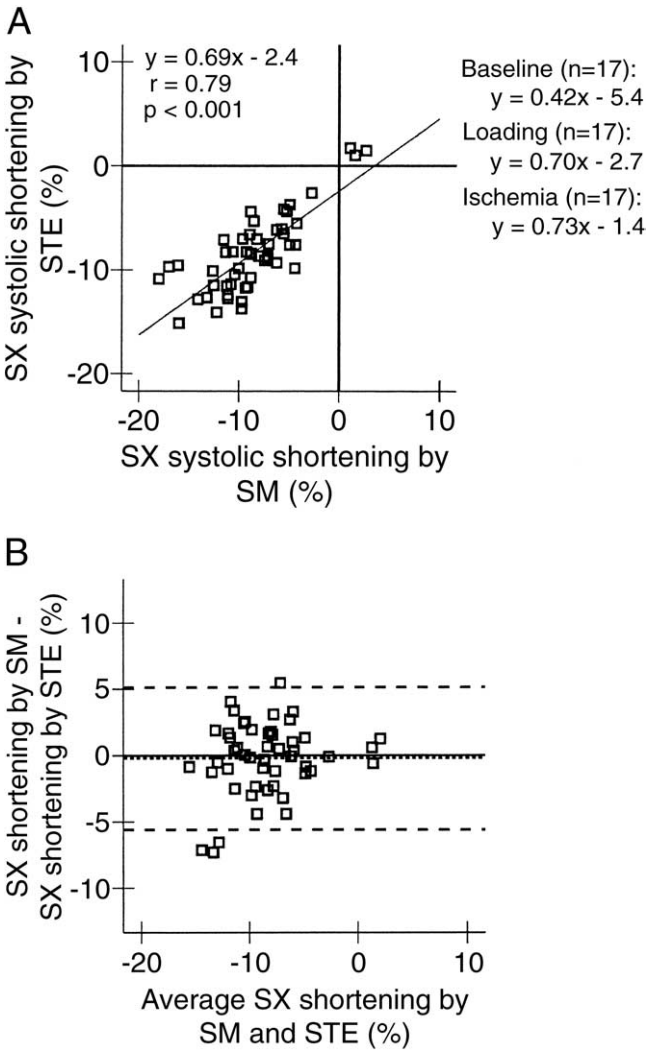

Figure 3. **(A)** Plot showing the relation between left ventricular short-axis (SX) shortening by sonomicrometry (SM) and speckle tracking echocardiography (STE). **(B)** Bland-Altman plot showing the mean difference **(dotted middle line)** and 95% limits of agreement **(dashed lines)**.

shortening ($r = 0.79$, $p < 0.001$) (Figs. 3A and 4A). The 95% limits of agreement for long- and short-axis measurements were not significantly different (−4.4 to 5.0% vs. −5.6 to 5.1%, respectively; $p = 0.28$) (Figs. 3B and 4B). Saline loading increased long-axis septal strain and midventricular systolic shortening, whereas LAD occlusion reduced apical short-axis shortening and lateral wall strain (Table 1). Speckle tracking echocardiography and sonomicrometry measurements were not significantly different in any of the measurement conditions. Intra- and interobserver COR for STE measurements were 4.6% and 7.0%, respectively, for shortening and 6.0% and 6.4%, respectively, for strain. A representative example of traces is shown in Figure 5.

Clinical study. Twenty-six of 132 segments (20%) were excluded from STE analysis (7 because of reverberations, 19 because of drop-outs). Strain measured by STE and MRI tagging correlated well ($r = 0.87$, $p < 0.001$) (Fig. 6A). The 95% limits of agreement were −9.1 to 8.0% (Fig. 6B). Intra- and interobserver COR for strain by STE was 5.2% and 8.6%, respectively. Heart rate was 84 ± 18 beats/min.

DISCUSSION

The present study demonstrates that STE can quantify regional myocardial deformation independent of insonation angle and thus simultaneously assess systolic long-axis strain and short-axis shortening. The accuracy of STE was confirmed using sonomicrometry and MRI tagging as reference methods.

A recent experimental study with a different speckle tracking application found agreement with sonomicrometry comparable to our results (7); however, the researchers used frequencies and depths that are less relevant for a clinical setting. In the experimental part of the present study, STE appeared to underestimate shortening at higher values of short-axis shortening (Figs. 3A and 3B). Poorer lateral than

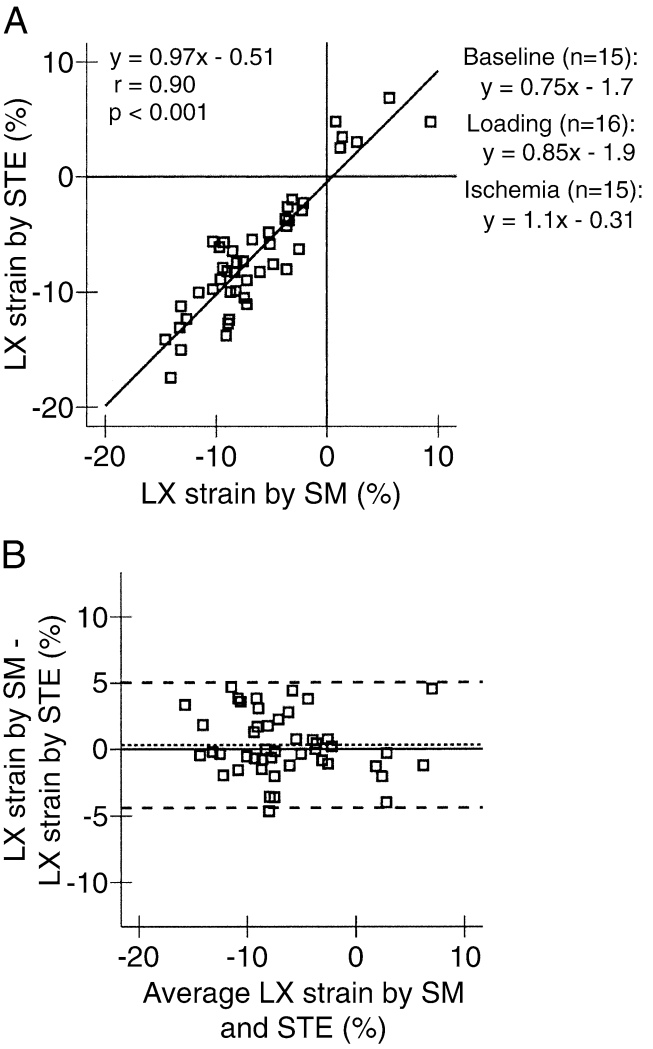

Figure 4. **(A)** Plot showing the relation between long-axis (LX) strain by sonomicrometry (SM) and speckle tracking echocardiography (STE). **(B)** Bland-Altman plot showing the mean difference **(dotted middle line)** and 95% limits of agreement **(dashed lines)**.

Table 1. Results From the Experimental Study

	Baseline	Loading	p Value	Ischemia	p Value
Long-axis strain (%)					
Septum					
STE	−9.0 ± 3	−12 ± 3*	0.032	−10 ± 2	1.0
SM	−9.4 ± 2	−12 ± 2*	0.034	−7.9 ± 2	0.27
Lateral wall					
STE	−5.1 ± 2	−5.9 ± 2	1.0	3.2 ± 3*	0.001
SM	−5.0 ± 2	−5.3 ± 3	1.0	2.5 ± 4*	0.003
Systolic shortening in LV short axis (%)					
Apex					
STE	−8.6 ± 3	−7.9 ± 3	0.81	−4.0 ± 5	0.13
SM	−8.1 ± 3	−8.2 ± 3	1.0	−4.0 ± 5	0.16
Mid-ventricle					
STE	−9.7 ± 2	−11 ± 3	0.13	−8.3 ± 3	0.46
SM	−10 ± 4	−12 ± 4*	0.016	−9.1 ± 4	1.0
Heart rate (min^{-1})	94 ± 13	106 ± 13*	0.042	108 ± 9*	0.042

All values are mean ± SD. The p values are for comparison with baseline values. All p values are adjusted for multiple comparisons (Bonferroni, n = 2). *Significantly different from baseline.
LV = left ventricle; SM = sonomicrometry; STE = speckle tracking echocardiography.

axial resolution might explain this, as there was no such trend in the long-axis strain measurements.

In the clinical study STE was tested against MRI tagging, which is currently the non-invasive gold standard for evaluation of systolic deformation (11). Reduced systolic strain was found in infarcted areas, whereas remote myocardium had normal values. The agreement was comparable to what has previously been reported for TDI-based strain and MRI tagging (8), as was the percentage of analyzed segments (3).

The number of beams covering the sector determines the lateral resolution, and in TDI recordings for strain measurements, this number is three to four times lower than in B-mode images, which are used in STE. Even though strain can be measured only in the beam direction with TDI methods, the lateral resolution is important, as lower resolution increases the likelihood for inclusion of noise from for instance the pericardium. In TDI-based

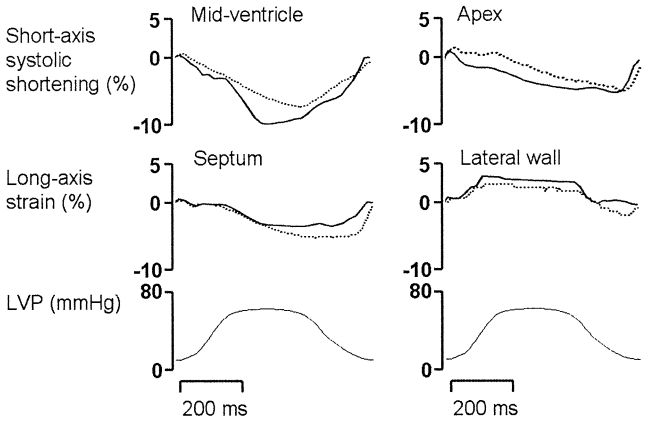

Figure 5. Recordings from a single experiment during left anterior descending artery occlusion. **(Upper panels)** Left ventricular (LV) short-axis shortening at mid-ventricular level **(left)** and apical level **(right)**. **(Middle panels)** Long-axis strain in the septum **(left)** and lateral wall **(right)**. **(Lower panels)** LV pressure (LVP) for timing. Reduced short-axis systolic shortening and lateral wall strain indicate ischemic dysfunction. **Dashed line** = sonomicrometry, **solid line** = speckle tracking echocardiography.

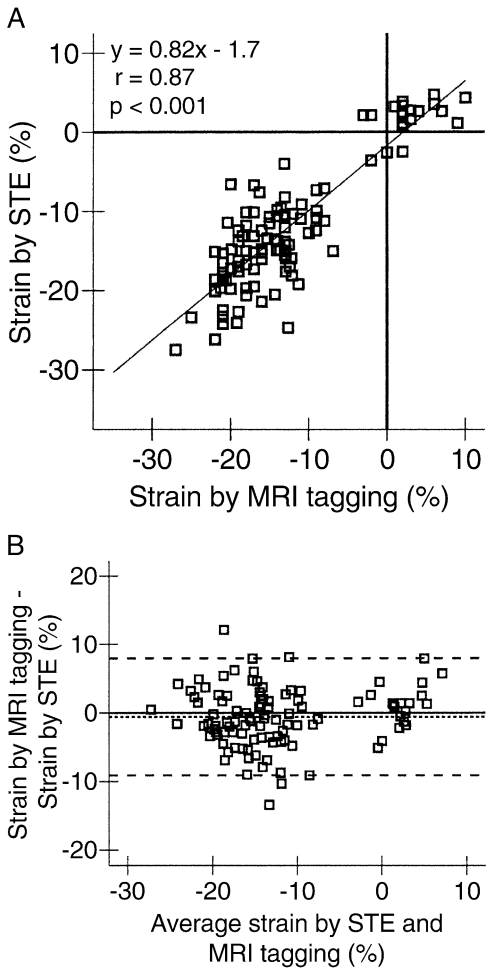

Figure 6. (A) Long-axis strains measured by magnetic resonance imaging (MRI) tagging and speckle tracking echocardiography (STE). **(B)** Bland-Altman plot showing the mean difference **(dotted middle line)** and 95% limits of agreement **(dashed lines)**.

methods, such noise can be included without the user's knowledge, whereas the accuracy of STE can be inspected by the user because the tracking result is displayed in the image.

Study limitations. Sonomicrometry measures the motion of material points in the myocardium, while STE measures motion in the image plane. Thus, misalignment between the ultrasound plane and the crystals and out-of-plane motion were probably the most important sources of variation between the methods. High B-mode frame rates were used to minimize speckle decorrelation.

In the clinical study, misaligned image planes and segment boarders in MRI tagging and STE might explain some of the variation. As strain by MRI tagging was calculated by a three-dimensional technique, whereas STE is two-dimensional, out-of-plane movement in STE could also have contributed to the variation.

The ROI size must be considerably larger than the image resolution to allow robust tracking, but also small enough to allow accurate positioning. We did not perform systematic comparisons of the effects of different ROI sizes on tracking quality, but preliminary testing showed that 5 × 5 mm was a reasonable compromise between robust tracking and accurate positioning.

The Vivid 7 scanner used in the experimental study has better resolution than the System Five scanner used in the clinical part, and using Vivid 7 in the clinical study as well might have improved our results.

Conclusions. The present study demonstrates that STE can provide accurate and angle-independent measurements of regional myocardial strain and has potential to become a clinical bedside tool to quantify regional myocardial function.

Reprint requests and correspondence: Dr. Brage H. Amundsen, Department of Circulation and Medical Imaging, NTNU, MTFS, N-7489 Trondheim, Norway. E-mail: brage.h.amundsen@ntnu.no.

REFERENCES

1. Støylen A, Heimdal A, Bjørnstad K, et al. Strain rate imaging by ultrasonography in the diagnosis of coronary artery disease. J Am Soc Echocardiogr 2000;13:1053–64.
2. Urheim S, Edvardsen T, Torp H, Angelsen B, Smiseth OA. Myocardial strain by Doppler echocardiography. Validation of a new method to quantify regional myocardial function. Circulation 2000; 102:1158–64.
3. Voigt JU, Nixdorff U, Bogdan R, et al. Comparison of deformation imaging and velocity imaging for detecting regional inducible ischaemia during dobutamine stress echocardiography. Eur Heart J 2004; 25:1517–25.
4. Edvardsen T, Skulstad H, Aakhus S, Urheim S, Ihlen H. Regional myocardial systolic function during acute myocardial ischemia assessed by strain Doppler echocardiography. J Am Coll Cardiol 2001;37:726–30.
5. Bohs LN, Trahey GE. A novel method for angle independent ultrasonic imaging of blood flow and tissue motion. IEEE Trans Biomed Eng 1991;38:280–6.
6. Leitman M, Lysyansky P, Sidenko S, et al. Two-dimensional strain-A novel software for real-time quantitative echocardiographic assessment of myocardial function. J Am Soc Echocardiogr 2004;17:1021–9.
7. Toyoda T, Baba H, Akasaka T, et al. Assessment of regional myocardial strain by a novel automated tracking system from digital image files. J Am Soc Echocardiogr 2004;17:1234–8.
8. Edvardsen T, Gerber BL, Garot J, Bluemke DA, Lima JA, Smiseth OA. Quantitative assessment of intrinsic regional myocardial deformation by Doppler strain rate echocardiography in humans: validation against three-dimensional tagged magnetic resonance imaging. Circulation 2002;106:50–6.
9. Cerqueira MD, Weissmann NJ, Dilsizian V, et al. Standardized myocardial segmentation and nomenclature for tomographic imaging of the heart. Circulation 2002;105:539–42.
10. Bland JM, Altman DG. Statistical methods for assessing agreement between two methods of clinical measurement. Lancet 1986;1:307–10.
11. Lima JA, Jeremy R, Guier W, et al. Accurate systolic wall thickening by nuclear magnetic resonance imaging with tissue tagging: correlation with sonomicrometers in normal and ischemic myocardium. J Am Coll Cardiol 1993;21:1741–51.

Paper II

Is not included due to copyright

Paper III

Is not included due to copyright

Paper IV

Is not included due to copyright

Dissertations at the Faculty of Medicine, NTNU

1977

1. Knut Joachim Berg: EFFECT OF ACETYLSALICYLIC ACID ON RENAL FUNCTION
2. Karl Erik Viken and Arne Ødegaard: STUDIES ON HUMAN MONOCYTES CULTURED *IN VITRO*

1978

3. Karel Bjørn Cyvin: CONGENITAL DISLOCATION OF THE HIP JOINT.
4. Alf O. Brubakk: METHODS FOR STUDYING FLOW DYNAMICS IN THE LEFT VENTRICLE AND THE AORTA IN MAN.

1979

5. Geirmund Unsgaard: CYTOSTATIC AND IMMUNOREGULATORY ABILITIES OF HUMAN BLOOD MONOCYTES CULTURED IN VITRO

1980

6. Størker Jørstad: URAEMIC TOXINS
7. Arne Olav Jenssen: SOME RHEOLOGICAL, CHEMICAL AND STRUCTURAL PROPERTIES OF MUCOID SPUTUM FROM PATIENTS WITH CHRONIC OBSTRUCTIVE BRONCHITIS

1981

8. Jens Hammerstrøm: CYTOSTATIC AND CYTOLYTIC ACTIVITY OF HUMAN MONOCYTES AND EFFUSION MACROPHAGES AGAINST TUMOR CELLS *IN VITRO*

1983

9. Tore Syversen: EFFECTS OF METHYLMERCURY ON RAT BRAIN PROTEIN.
10. Torbjørn Iversen: SQUAMOUS CELL CARCINOMA OF THE VULVA.

1984

11. Tor-Erik Widerøe: ASPECTS OF CONTINUOUS AMBULATORY PERITONEAL DIALYSIS.
12. Anton Hole: ALTERATIONS OF MONOCYTE AND LYMPHOCYTE FUNCTIONS IN REALTION TO SURGERY UNDER EPIDURAL OR GENERAL ANAESTHESIA.
13. Terje Terjesen: FRACTURE HEALING AN STRESS-PROTECTION AFTER METAL PLATE FIXATION AND EXTERNAL FIXATION.
14. Carsten Saunte: CLUSTER HEADACHE SYNDROME.
15. Inggard Lereim: TRAFFIC ACCIDENTS AND THEIR CONSEQUENCES.
16. Bjørn Magne Eggen: STUDIES IN CYTOTOXICITY IN HUMAN ADHERENT MONONUCLEAR BLOOD CELLS.
17. Trond Haug: FACTORS REGULATING BEHAVIORAL EFFECTS OG DRUGS.

1985

18. Sven Erik Gisvold: RESUSCITATION AFTER COMPLETE GLOBAL BRAIN ISCHEMIA.
19. Terje Espevik: THE CYTOSKELETON OF HUMAN MONOCYTES.
20. Lars Bevanger: STUDIES OF THE Ibc (c) PROTEIN ANTIGENS OF GROUP B STREPTOCOCCI.
21. Ole-Jan Iversen: RETROVIRUS-LIKE PARTICLES IN THE PATHOGENESIS OF PSORIASIS.
22. Lasse Eriksen: EVALUATION AND TREATMENT OF ALCOHOL DEPENDENT BEHAVIOUR.
23. Per I. Lundmo: ANDROGEN METABOLISM IN THE PROSTATE.

1986

24. Dagfinn Berntzen: ANALYSIS AND MANAGEMENT OF EXPERIMENTAL AND CLINICAL PAIN.
25. Odd Arnold Kildahl-Andersen: PRODUCTION AND CHARACTERIZATION OF MONOCYTE-DERIVED CYTOTOXIN AND ITS ROLE IN MONOCYTE-MEDIATED CYTOTOXICITY.
26. Ola Dale: VOLATILE ANAESTHETICS.

1987

27. Per Martin Kleveland: STUDIES ON GASTRIN.
28. Audun N. Øksendal: THE CALCIUM PARADOX AND THE HEART.
29. Vilhjalmur R. Finsen: HIP FRACTURES

1988

30. Rigmor Austgulen: TUMOR NECROSIS FACTOR: A MONOCYTE-DERIVED REGULATOR OF CELLULAR GROWTH.
31. Tom-Harald Edna: HEAD INJURIES ADMITTED TO HOSPITAL.
32. Joseph D. Borsi: NEW ASPECTS OF THE CLINICAL PHARMACOKINETICS OF METHOTREXATE.

33. Olav F. M. Sellevold: GLUCOCORTICOIDS IN MYOCARDIAL PROTECTION.
34. Terje Skjærpe: NONINVASIVE QUANTITATION OF GLOBAL PARAMETERS ON LEFT VENTRICULAR FUNCTION: THE SYSTOLIC PULMONARY ARTERY PRESSURE AND CARDIAC OUTPUT.
35. Eyvind Rødahl: STUDIES OF IMMUNE COMPLEXES AND RETROVIRUS-LIKE ANTIGENS IN PATIENTS WITH ANKYLOSING SPONDYLITIS.
36. Ketil Thorstensen: STUDIES ON THE MECHANISMS OF CELLULAR UPTAKE OF IRON FROM TRANSFERRIN.
37. Anna Midelfart: STUDIES OF THE MECHANISMS OF ION AND FLUID TRANSPORT IN THE BOVINE CORNEA.
38. Eirik Helseth: GROWTH AND PLASMINOGEN ACTIVATOR ACTIVITY OF HUMAN GLIOMAS AND BRAIN METASTASES - WITH SPECIAL REFERENCE TO TRANSFORMING GROWTH FACTOR BETA AND THE EPIDERMAL GROWTH FACTOR RECEPTOR.
39. Petter C. Borchgrevink: MAGNESIUM AND THE ISCHEMIC HEART.
40. Kjell-Arne Rein: THE EFFECT OF EXTRACORPOREAL CIRCULATION ON SUBCUTANEOUS TRANSCAPILLARY FLUID BALANCE.
41. Arne Kristian Sandvik: RAT GASTRIC HISTAMINE.
42. Carl Bredo Dahl: ANIMAL MODELS IN PSYCHIATRY.

1989

43. Torbjørn A. Fredriksen: CERVICOGENIC HEADACHE.
44. Rolf A. Walstad: CEFTAZIDIME.
45. Rolf Salvesen: THE PUPIL IN CLUSTER HEADACHE.
46. Nils Petter Jørgensen: DRUG EXPOSURE IN EARLY PREGNANCY.
47. Johan C. Ræder: PREMEDICATION AND GENERAL ANAESTHESIA IN OUTPATIENT GYNECOLOGICAL SURGERY.
48. M. R. Shalaby: IMMUNOREGULATORY PROPERTIES OF TNF-α AND THE RELATED CYTOKINES.
49. Anders Waage: THE COMPLEX PATTERN OF CYTOKINES IN SEPTIC SHOCK.
50. Bjarne Christian Eriksen: ELECTROSTIMULATION OF THE PELVIC FLOOR IN FEMALE URINARY INCONTINENCE.
51. Tore B. Halvorsen: PROGNOSTIC FACTORS IN COLORECTAL CANCER.

1990

52. Asbjørn Nordby: CELLULAR TOXICITY OF ROENTGEN CONTRAST MEDIA.
53. Kåre E. Tvedt: X-RAY MICROANALYSIS OF BIOLOGICAL MATERIAL.
54. Tore C. Stiles: COGNITIVE VULNERABILITY FACTORS IN THE DEVELOPMENT AND MAINTENANCE OF DEPRESSION.
55. Eva Hofsli: TUMOR NECROSIS FACTOR AND MULTIDRUG RESISTANCE.
56. Helge S. Haarstad: TROPHIC EFFECTS OF CHOLECYSTOKININ AND SECRETIN ON THE RAT PANCREAS.
57. Lars Engebretsen: TREATMENT OF ACUTE ANTERIOR CRUCIATE LIGAMENT INJURIES.
58. Tarjei Rygnestad: DELIBERATE SELF-POISONING IN TRONDHEIM.
59. Arne Z. Henriksen: STUDIES ON CONSERVED ANTIGENIC DOMAINS ON MAJOR OUTER MEMBRANE PROTEINS FROM ENTEROBACTERIA.
60. Steinar Westin: UNEMPLOYMENT AND HEALTH: Medical and social consequences of a factory closure in a ten-year controlled follow-up study.
61. Ylva Sahlin: INJURY REGISTRATION, a tool for accident preventive work.
62. Helge Bjørnstad Pettersen: BIOSYNTHESIS OF COMPLEMENT BY HUMAN ALVEOLAR MACROPHAGES WITH SPECIAL REFERENCE TO SARCOIDOSIS.
63. Berit Schei: TRAPPED IN PAINFUL LOVE.
64. Lars J. Vatten: PROSPECTIVE STUDIES OF THE RISK OF BREAST CANCER IN A COHORT OF NORWEGIAN WOMAN.

1991

65. Kåre Bergh: APPLICATIONS OF ANTI-C5a SPECIFIC MONOCLONAL ANTIBODIES FOR THE ASSESSMENT OF COMPLEMENT ACTIVATION.
66. Svein Svenningsen: THE CLINICAL SIGNIFICANCE OF INCREASED FEMORAL ANTEVERSION.
67. Olbjørn Klepp: NONSEMINOMATOUS GERM CELL TESTIS CANCER: THERAPEUTIC OUTCOME AND PROGNOSTIC FACTORS.

68. Trond Sand: THE EFFECTS OF CLICK POLARITY ON BRAINSTEM AUDITORY EVOKED POTENTIALS AMPLITUDE, DISPERSION, AND LATENCY VARIABLES.
69. Kjetil B. Åsbakk: STUDIES OF A PROTEIN FROM PSORIATIC SCALE, PSO P27, WITH RESPECT TO ITS POTENTIAL ROLE IN IMMUNE REACTIONS IN PSORIASIS.
70. Arnulf Hestnes: STUDIES ON DOWN´S SYNDROME.
71. Randi Nygaard: LONG-TERM SURVIVAL IN CHILDHOOD LEUKEMIA.
72. Bjørn Hagen: THIO-TEPA.
73. Svein Anda: EVALUATION OF THE HIP JOINT BY COMPUTED TOMOGRAMPHY AND ULTRASONOGRAPHY.

1992

74. Martin Svartberg: AN INVESTIGATION OF PROCESS AND OUTCOME OF SHORT-TERM PSYCHODYNAMIC PSYCHOTHERAPY.
75. Stig Arild Slørdahl: AORTIC REGURGITATION.
76. Harold C Sexton: STUDIES RELATING TO THE TREATMENT OF SYMPTOMATIC NON-PSYCHOTIC PATIENTS.
77. Maurice B. Vincent: VASOACTIVE PEPTIDES IN THE OCULAR/FOREHEAD AREA.
78. Terje Johannessen: CONTROLLED TRIALS IN SINGLE SUBJECTS.
79. Turid Nilsen: PYROPHOSPHATE IN HEPATOCYTE IRON METABOLISM.
80. Olav Haraldseth: NMR SPECTROSCOPY OF CEREBRAL ISCHEMIA AND REPERFUSION IN RAT.
81. Eiliv Brenna: REGULATION OF FUNCTION AND GROWTH OF THE OXYNTIC MUCOSA.

1993

82. Gunnar Bovim: CERVICOGENIC HEADACHE.
83. Jarl Arne Kahn: ASSISTED PROCREATION.
84. Bjørn Naume: IMMUNOREGULATORY EFFECTS OF CYTOKINES ON NK CELLS.
85. Rune Wiseth: AORTIC VALVE REPLACEMENT.
86. Jie Ming Shen: BLOOD FLOW VELOCITY AND RESPIRATORY STUDIES.
87. Piotr Kruszewski: SUNCT SYNDROME WITH SPECIAL REFERENCE TO THE AUTONOMIC NERVOUS SYSTEM.
88. Mette Haase Moen: ENDOMETRIOSIS.
89. Anne Vik: VASCULAR GAS EMBOLISM DURING AIR INFUSION AND AFTER DECOMPRESSION IN PIGS.
90. Lars Jacob Stovner: THE CHIARI TYPE I MALFORMATION.
91. Kjell Å. Salvesen: ROUTINE ULTRASONOGRAPHY IN UTERO AND DEVELOPMENT IN CHILDHOOD.

1994

92. Nina-Beate Liabakk: DEVELOPMENT OF IMMUNOASSAYS FOR TNF AND ITS SOLUBLE RECEPTORS.
93. Sverre Helge Torp: *erb*B ONCOGENES IN HUMAN GLIOMAS AND MENINGIOMAS.
94. Olav M. Linaker: MENTAL RETARDATION AND PSYCHIATRY. Past and present.
95. Per Oscar Feet: INCREASED ANTIDEPRESSANT AND ANTIPANIC EFFECT IN COMBINED TREATMENT WITH DIXYRAZINE AND TRICYCLIC ANTIDEPRESSANTS.
96. Stein Olav Samstad: CROSS SECTIONAL FLOW VELOCITY PROFILES FROM TWO-DIMENSIONAL DOPPLER ULTRASOUND: Studies on early mitral blood flow.
97. Bjørn Backe: STUDIES IN ANTENATAL CARE.
98. Gerd Inger Ringdal: QUALITY OF LIFE IN CANCER PATIENTS.
99. Torvid Kiserud: THE DUCTUS VENOSUS IN THE HUMAN FETUS.
100. Hans E. Fjøsne: HORMONAL REGULATION OF PROSTATIC METABOLISM.
101. Eylert Brodtkorb: CLINICAL ASPECTS OF EPILEPSY IN THE MENTALLY RETARDED.
102. Roar Juul: PEPTIDERGIC MECHANISMS IN HUMAN SUBARACHNOID HEMORRHAGE.
103. Unni Syversen: CHROMOGRANIN A. Phsysiological and Clinical Role.

1995

104. Odd Gunnar Brakstad: THERMOSTABLE NUCLEASE AND THE *nuc* GENE IN THE DIAGNOSIS OF *Staphylococcus aureus* INFECTIONS.
105. Terje Engan: NUCLEAR MAGNETIC RESONANCE (NMR) SPECTROSCOPY OF PLASMA IN MALIGNANT DISEASE.
106. Kirsten Rasmussen: VIOLENCE IN THE MENTALLY DISORDERED.
107. Finn Egil Skjeldestad: INDUCED ABORTION: Timetrends and Determinants.
108. Roar Stenseth: THORACIC EPIDURAL ANALGESIA IN AORTOCORONARY BYPASS SURGERY.

109. Arild Faxvaag: STUDIES OF IMMUNE CELL FUNCTION *in mice infected with* MURINE RETROVIRUS.

1996

110. Svend Aakhus: NONINVASIVE COMPUTERIZED ASSESSMENT OF LEFT VENTRICULAR FUNCTION AND SYSTEMIC ARTERIAL PROPERTIES. Methodology and some clinical applications.
111. Klaus-Dieter Bolz: INTRAVASCULAR ULTRASONOGRAPHY.
112. Petter Aadahl: CARDIOVASCULAR EFFECTS OF THORACIC AORTIC CROSS-CLAMPING.
113. Sigurd Steinshamn: CYTOKINE MEDIATORS DURING GRANULOCYTOPENIC INFECTIONS.
114. Hans Stifoss-Hanssen: SEEKING MEANING OR HAPPINESS?
115. Anne Kvikstad: LIFE CHANGE EVENTS AND MARITAL STATUS IN RELATION TO RISK AND PROGNOSIS OF CANSER.
116. Torbjørn Grøntvedt: TREATMENT OF ACUTE AND CHRONIC ANTERIOR CRUCIATE LIGAMENT INJURIES. A clinical and biomechanical study.
117. Sigrid Hørven Wigers: CLINICAL STUDIES OF FIBROMYALGIA WITH FOCUS ON ETIOLOGY, TREATMENT AND OUTCOME.
118. Jan Schjøtt: MYOCARDIAL PROTECTION: Functional and Metabolic Characteristics of Two Endogenous Protective Principles.
119. Marit Martinussen: STUDIES OF INTESTINAL BLOOD FLOW AND ITS RELATION TO TRANSITIONAL CIRCULATORY ADAPATION IN NEWBORN INFANTS.
120. Tomm B. Müller: MAGNETIC RESONANCE IMAGING IN FOCAL CEREBRAL ISCHEMIA.
121. Rune Haaverstad: OEDEMA FORMATION OF THE LOWER EXTREMITIES.
122. Magne Børset: THE ROLE OF CYTOKINES IN MULTIPLE MYELOMA, WITH SPECIAL REFERENCE TO HEPATOCYTE GROWTH FACTOR.
123. Geir Smedslund: A THEORETICAL AND EMPIRICAL INVESTIGATION OF SMOKING, STRESS AND DISEASE: RESULTS FROM A POPULATION SURVEY.

1997

124. Torstein Vik: GROWTH, MORBIDITY, AND PSYCHOMOTOR DEVELOPMENT IN INFANTS WHO WERE GROWTH RETARDED *IN UTERO*.
125. Siri Forsmo: ASPECTS AND CONSEQUENCES OF OPPORTUNISTIC SCREENING FOR CERVICAL CANCER. Results based on data from three Norwegian counties.
126. Jon S. Skranes: CEREBRAL MRI AND NEURODEVELOPMENTAL OUTCOME IN VERY LOW BIRTH WEIGHT (VLBW) CHILDREN. A follow-up study of a geographically based year cohort of VLBW children at ages one and six years.
127. Knut Bjørnstad: COMPUTERIZED ECHOCARDIOGRAPHY FOR EVALUTION OF CORONARY ARTERY DISEASE.
128. Grethe Elisabeth Borchgrevink: DIAGNOSIS AND TREATMENT OF WHIPLASH/NECK SPRAIN INJURIES CAUSED BY CAR ACCIDENTS.
129. Tor Elsås: NEUROPEPTIDES AND NITRIC OXIDE SYNTHASE IN OCULAR AUTONOMIC AND SENSORY NERVES.
130. Rolf W. Gråwe: EPIDEMIOLOGICAL AND NEUROPSYCHOLOGICAL PERSPECTIVES ON SCHIZOPHRENIA.
131. Tonje Strømholm: CEREBRAL HAEMODYNAMICS DURING THORACIC AORTIC CROSSCLAMPING. An experimental study in pigs.

1998

132. Martinus Bråten: STUDIES ON SOME PROBLEMS REALTED TO INTRAMEDULLARY NAILING OF FEMORAL FRACTURES.
133. Ståle Nordgård: PROLIFERATIVE ACTIVITY AND DNA CONTENT AS PROGNOSTIC INDICATORS IN ADENOID CYSTIC CARCINOMA OF THE HEAD AND NECK.
134. Egil Lien: SOLUBLE RECEPTORS FOR **TNF** AND **LPS**: RELEASE PATTERN AND POSSIBLE SIGNIFICANCE IN DISEASE.
135. Marit Bjørgaas: HYPOGLYCAEMIA IN CHILDREN WITH DIABETES MELLITUS
136. Frank Skorpen: GENETIC AND FUNCTIONAL ANALYSES OF DNA REPAIR IN HUMAN CELLS.
137. Juan A. Pareja: SUNCT SYNDROME. ON THE CLINICAL PICTURE. ITS DISTINCTION FROM OTHER, SIMILAR HEADACHES.
138. Anders Angelsen: NEUROENDOCRINE CELLS IN HUMAN PROSTATIC CARCINOMAS AND THE PROSTATIC COMPLEX OF RAT, GUINEA PIG, CAT AND DOG.

139. Fabio Antonaci: CHRONIC PAROXYSMAL HEMICRANIA AND HEMICRANIA CONTINUA: TWO DIFFERENT ENTITIES?
140. Sven M. Carlsen: ENDOCRINE AND METABOLIC EFFECTS OF METFORMIN WITH SPECIAL EMPHASIS ON CARDIOVASCULAR RISK FACTORES.

1999

141. Terje A. Murberg: DEPRESSIVE SYMPTOMS AND COPING AMONG PATIENTS WITH CONGESTIVE HEART FAILURE.
142. Harm-Gerd Karl Blaas: THE EMBRYONIC EXAMINATION. Ultrasound studies on the development of the human embryo.
143. Noèmi Becser Andersen:THE CEPHALIC SENSORY NERVES IN UNILATERAL HEADACHES. Anatomical background and neurophysiological evaluation.
144. Eli-Janne Fiskerstrand: LASER TREATMENT OF PORT WINE STAINS. A study of the efficacy and limitations of the pulsed dye laser. Clinical and morfological analyses aimed at improving the therapeutic outcome.
145. Bård Kulseng: A STUDY OF ALGINATE CAPSULE PROPERTIES AND CYTOKINES IN RELATION TO INSULIN DEPENDENT DIABETES MELLITUS.
146. Terje Haug: STRUCTURE AND REGULATION OF THE HUMAN UNG GENE ENCODING URACIL-DNA GLYCOSYLASE.
147. Heidi Brurok: MANGANESE AND THE HEART. A Magic Metal with Diagnostic and Therapeutic Possibilites.
148. Agnes Kathrine Lie: DIAGNOSIS AND PREVALENCE OF HUMAN PAPILLOMAVIRUS INFECTION IN CERVICAL INTRAEPITELIAL NEOPLASIA. Relationship to Cell Cycle Regulatory Proteins and HLA DQBI Genes.
149. Ronald Mårvik: PHARMACOLOGICAL, PHYSIOLOGICAL AND PATHOPHYSIOLOGICAL STUDIES ON ISOLATED STOMACS.
150. Ketil Jarl Holen: THE ROLE OF ULTRASONOGRAPHY IN THE DIAGNOSIS AND TREATMENT OF HIP DYSPLASIA IN NEWBORNS.
151. Irene Hetlevik: THE ROLE OF CLINICAL GUIDELINES IN CARDIOVASCULAR RISK INTERVENTION IN GENERAL PRACTICE.
152. Katarina Tunòn: ULTRASOUND AND PREDICTION OF GESTATIONAL AGE.
153. Johannes Soma: INTERACTION BETWEEN THE LEFT VENTRICLE AND THE SYSTEMIC ARTERIES.
154. Arild Aamodt: DEVELOPMENT AND PRE-CLINICAL EVALUATION OF A CUSTOM-MADE FEMORAL STEM.
155. Agnar Tegnander: DIAGNOSIS AND FOLLOW-UP OF CHILDREN WITH SUSPECTED OR KNOWN HIP DYSPLASIA.
156. Bent Indredavik: STROKE UNIT TREATMENT: SHORT AND LONG-TERM EFFECTS
157. Jolanta Vanagaite Vingen: PHOTOPHOBIA AND PHONOPHOBIA IN PRIMARY HEADACHES

2000

158. Ola Dalsegg Sæther: PATHOPHYSIOLOGY DURING PROXIMAL AORTIC CROSS-CLAMPING CLINICAL AND EXPERIMENTAL STUDIES
159. xxxxxxxxx (blind number)
160. Christina Vogt Isaksen: PRENATAL ULTRASOUND AND POSTMORTEM FINDINGS – A TEN YEAR CORRELATIVE STUDY OF FETUSES AND INFANTS WITH DEVELOPMENTAL ANOMALIES.
161. Holger Seidel: HIGH-DOSE METHOTREXATE THERAPY IN CHILDREN WITH ACUTE LYMPHOCYTIC LEUKEMIA: DOSE, CONCENTRATION, AND EFFECT CONSIDERATIONS.
162. Stein Hallan: IMPLEMENTATION OF MODERN MEDICAL DECISION ANALYSIS INTO CLINICAL DIAGNOSIS AND TREATMENT.
163. Malcolm Sue-Chu: INVASIVE AND NON-INVASIVE STUDIES IN CROSS-COUNTRY SKIERS WITH ASTHMA-LIKE SYMPTOMS.
164. Ole-Lars Brekke: EFFECTS OF ANTIOXIDANTS AND FATTY ACIDS ON TUMOR NECROSIS FACTOR-INDUCED CYTOTOXICITY.
165. Jan Lundbom: AORTOCORONARY BYPASS SURGERY: CLINICAL ASPECTS, COST CONSIDERATIONS AND WORKING ABILITY.
166. John-Anker Zwart: LUMBAR NERVE ROOT COMPRESSION, BIOCHEMICAL AND NEUROPHYSIOLOGICAL ASPECTS.
167. Geir Falck: HYPEROSMOLALITY AND THE HEART.

168. Eirik Skogvoll: CARDIAC ARREST Incidence, Intervention and Outcome.
169. Dalius Bansevicius: SHOULDER-NECK REGION IN CERTAIN HEADACHES AND CHRONIC PAIN SYNDROMES.
170. Bettina Kinge: REFRACTIVE ERRORS AND BIOMETRIC CHANGES AMONG UNIVERSITY STUDENTS IN NORWAY.
171. Gunnar Qvigstad: CONSEQUENCES OF HYPERGASTRINEMIA IN MAN
172. Hanne Ellekjær: EPIDEMIOLOGICAL STUDIES OF STROKE IN A NORWEGIAN POPULATION. INCIDENCE, RISK FACTORS AND PROGNOSIS
173. Hilde Grimstad: VIOLENCE AGAINST WOMEN AND PREGNANCY OUTCOME.
174. Astrid Hjelde: SURFACE TENSION AND COMPLEMENT ACTIVATION: Factors influencing bubble formation and bubble effects after decompression.
175. Kjell A. Kvistad: MR IN BREAST CANCER – A CLINICAL STUDY.
176. Ivar Rossvoll: ELECTIVE ORTHOPAEDIC SURGERY IN A DEFINED POPULATION. Studies on demand, waiting time for treatment and incapacity for work.
177. Carina Seidel: PROGNOSTIC VALUE AND BIOLOGICAL EFFECTS OF HEPATOCYTE GROWTH FACTOR AND SYNDECAN-1 IN MULTIPLE MYELOMA.

2001

178. Alexander Wahba: THE INFLUENCE OF CARDIOPULMONARY BYPASS ON PLATELET FUNCTION AND BLOOD COAGULATION – DETERMINANTS AND CLINICAL CONSEQUENSES
179. Marcus Schmitt-Egenolf: THE RELEVANCE OF THE MAJOR hISTOCOMPATIBILITY COMPLEX FOR THE GENETICS OF PSORIASIS
180. Odrun Arna Gederaas: BIOLOGICAL MECHANISMS INVOLVED IN 5-AMINOLEVULINIC ACID BASED PHOTODYNAMIC THERAPY
181. Pål Richard Romundstad: CANCER INCIDENCE AMONG NORWEGIAN ALUMINIUM WORKERS
182. Henrik Hjorth-Hansen: NOVEL CYTOKINES IN GROWTH CONTROL AND BONE DISEASE OF MULTIPLE MYELOMA
183. Gunnar Morken: SEASONAL VARIATION OF HUMAN MOOD AND BEHAVIOUR
184. Bjørn Olav Haugen: MEASUREMENT OF CARDIAC OUTPUT AND STUDIES OF VELOCITY PROFILES IN AORTIC AND MITRAL FLOW USING TWO- AND THREE-DIMENSIONAL COLOUR FLOW IMAGING
185. Geir Bråthen: THE CLASSIFICATION AND CLINICAL DIAGNOSIS OF ALCOHOL-RELATED SEIZURES
186. Knut Ivar Aasarød: RENAL INVOLVEMENT IN INFLAMMATORY RHEUMATIC DISEASE. A Study of Renal Disease in Wegener's Granulomatosis and in Primary Sjögren's Syndrome
187. Trude Helen Flo: RESEPTORS INVOLVED IN CELL ACTIVATION BY DEFINED URONIC ACID POLYMERS AND BACTERIAL COMPONENTS
188. Bodil Kavli: HUMAN URACIL-DNA GLYCOSYLASES FROM THE UNG GENE: STRUCTRUAL BASIS FOR SUBSTRATE SPECIFICITY AND REPAIR
189. Liv Thommesen: MOLECULAR MECHANISMS INVOLVED IN TNF- AND GASTRIN-MEDIATED GENE REGULATION
190. Turid Lingaas Holmen: SMOKING AND HEALTH IN ADOLESCENCE; THE NORD-TRØNDELAG HEALTH STUDY, 1995-97
191. Øyvind Hjertner: MULTIPLE MYELOMA: INTERACTIONS BETWEEN MALIGNANT PLASMA CELLS AND THE BONE MICROENVIRONMENT
192. Asbjørn Støylen: STRAIN RATE IMAGING OF THE LEFT VENTRICLE BY ULTRASOUND. FEASIBILITY, CLINICAL VALIDATION AND PHYSIOLOGICAL ASPECTS
193. Kristian Midthjell: DIABETES IN ADULTS IN NORD-TRØNDELAG. PUBLIC HEALTH ASPECTS OF DIABETES MELLITUS IN A LARGE, NON-SELECTED NORWEGIAN POPULATION.
194. Guanglin Cui: FUNCTIONAL ASPECTS OF THE ECL CELL IN RODENTS
195. Ulrik Wisløff: CARDIAC EFFECTS OF AEROBIC ENDURANCE TRAINING: HYPERTROPHY, CONTRACTILITY AND CALCUIM HANDLING IN NORMAL AND FAILING HEART
196. Øyvind Halaas: MECHANISMS OF IMMUNOMODULATION AND CELL-MEDIATED CYTOTOXICITY INDUCED BY BACTERIAL PRODUCTS
197. Tore Amundsen: PERFUSION MR IMAGING IN THE DIAGNOSIS OF PULMONARY EMBOLISM

198. Nanna Kurtze: THE SIGNIFICANCE OF ANXIETY AND DEPRESSION IN FATIQUE AND PATTERNS OF PAIN AMONG INDIVIDUALS DIAGNOSED WITH FIBROMYALGIA: RELATIONS WITH QUALITY OF LIFE, FUNCTIONAL DISABILITY, LIFESTYLE, EMPLOYMENT STATUS, CO-MORBIDITY AND GENDER
199. Tom Ivar Lund Nilsen: PROSPECTIVE STUDIES OF CANCER RISK IN NORD-TRØNDELAG: THE HUNT STUDY. Associations with anthropometric, socioeconomic, and lifestyle risk factors
200. Asta Kristine Håberg: A NEW APPROACH TO THE STUDY OF MIDDLE CEREBRAL ARTERY OCCLUSION IN THE RAT USING MAGNETIC RESONANCE TECHNIQUES

2002

201. Knut Jørgen Arntzen: PREGNANCY AND CYTOKINES
202. Henrik Døllner: INFLAMMATORY MEDIATORS IN PERINATAL INFECTIONS
203. Asta Bye: LOW FAT, LOW LACTOSE DIET USED AS PROPHYLACTIC TREATMENT OF ACUTE INTESTINAL REACTIONS DURING PELVIC RADIOTHERAPY. A PROSPECTIVE RANDOMISED STUDY.
204. Sylvester Moyo: STUDIES ON STREPTOCOCCUS AGALACTIAE (GROUP B STREPTOCOCCUS) SURFACE-ANCHORED MARKERS WITH EMPHASIS ON STRAINS AND HUMAN SERA FROM ZIMBABWE.
205. Knut Hagen: HEAD-HUNT: THE EPIDEMIOLOGY OF HEADACHE IN NORD-TRØNDELAG
206. Li Lixin: ON THE REGULATION AND ROLE OF UNCOUPLING PROTEIN-2 IN INSULIN PRODUCING ß-CELLS
207. Anne Hildur Henriksen: SYMPTOMS OF ALLERGY AND ASTHMA VERSUS MARKERS OF LOWER AIRWAY INFLAMMATION AMONG ADOLESCENTS
208. Egil Andreas Fors: NON-MALIGNANT PAIN IN RELATION TO PSYCHOLOGICAL AND ENVIRONTENTAL FACTORS. EXPERIENTAL AND CLINICAL STUDES OF PAIN WITH FOCUS ON FIBROMYALGIA
209. Pål Klepstad: MORPHINE FOR CANCER PAIN
210. Ingunn Bakke: MECHANISMS AND CONSEQUENCES OF PEROXISOME PROLIFERATOR-INDUCED HYPERFUNCTION OF THE RAT GASTRIN PRODUCING CELL
211. Ingrid Susann Gribbestad: MAGNETIC RESONANCE IMAGING AND SPECTROSCOPY OF BREAST CANCER
212. Rønnaug Astri Ødegård: PREECLAMPSIA – MATERNAL RISK FACTORS AND FETAL GROWTH
213. Johan Haux: STUDIES ON CYTOTOXICITY INDUCED BY HUMAN NATURAL KILLER CELLS AND DIGITOXIN
214. Turid Suzanne Berg-Nielsen: PARENTING PRACTICES AND MENTALLY DISORDERED ADOLESCENTS
215. Astrid Rydning: BLOOD FLOW AS A PROTECTIVE FACTOR FOR THE STOMACH MUCOSA. AN EXPERIMENTAL STUDY ON THE ROLE OF MAST CELLS AND SENSORY AFFERENT NEURONS

2003

216. Jan Pål Loennechen: HEART FAILURE AFTER MYOCARDIAL INFARCTION. Regional Differences, Myocyte Function, Gene Expression, and Response to Cariporide, Losartan, and Exercise Training.
217. Elisabeth Qvigstad: EFFECTS OF FATTY ACIDS AND OVER-STIMULATION ON INSULIN SECRETION IN MAN
218. Arne Åsberg: EPIDEMIOLOGICAL STUDIES IN HEREDITARY HEMOCHROMATOSIS: PREVALENCE, MORBIDITY AND BENEFIT OF SCREENING.
219. Johan Fredrik Skomsvoll: REPRODUCTIVE OUTCOME IN WOMEN WITH RHEUMATIC DISEASE. A population registry based study of the effects of inflammatory rheumatic disease and connective tissue disease on reproductive outcome in Norwegian women in 1967-1995.
220. Siv Mørkved: URINARY INCONTINENCE DURING PREGNANCY AND AFTER DELIVERY: EFFECT OF PELVIC FLOOR MUSCLE TRAINING IN PREVENTION AND TREATMENT
221. Marit S. Jordhøy: THE IMPACT OF COMPREHENSIVE PALLIATIVE CARE
222. Tom Christian Martinsen: HYPERGASTRINEMIA AND HYPOACIDITY IN RODENTS – CAUSES AND CONSEQUENCES
223. Solveig Tingulstad: CENTRALIZATION OF PRIMARY SURGERY FOR OVARAIN CANCER. FEASIBILITY AND IMPACT ON SURVIVAL

224. Haytham Eloqayli: METABOLIC CHANGES IN THE BRAIN CAUSED BY EPILEPTIC SEIZURES
225. Torunn Bruland: STUDIES OF EARLY RETROVIRUS-HOST INTERACTIONS – VIRAL DETERMINANTS FOR PATHOGENESIS AND THE INFLUENCE OF SEX ON THE SUSCEPTIBILITY TO FRIEND MURINE LEUKAEMIA VIRUS INFECTION
226. Torstein Hole: DOPPLER ECHOCARDIOGRAPHIC EVALUATION OF LEFT VENTRICULAR FUNCTION IN PATIENTS WITH ACUTE MYOCARDIAL INFARCTION
227. Vibeke Nossum: THE EFFECT OF VASCULAR BUBBLES ON ENDOTHELIAL FUNCTION
228. Sigurd Fasting: ROUTINE BASED RECORDING OF ADVERSE EVENTS DURING ANAESTHESIA – APPLICATION IN QUALITY IMPROVEMENT AND SAFETY
229. Solfrid Romundstad: EPIDEMIOLOGICAL STUDIES OF MICROALBUMINURIA. THE NORD-TRØNDELAG HEALTH STUDY 1995-97 (HUNT 2)
230. Geir Torheim: PROCESSING OF DYNAMIC DATA SETS IN MAGNETIC RESONANCE IMAGING
231. Catrine Ahlén: SKIN INFECTIONS IN OCCUPATIONAL SATURATION DIVERS IN THE NORTH SEA AND THE IMPACT OF THE ENVIRONMENT
232. Arnulf Langhammer: RESPIRATORY SYMPTOMS, LUNG FUNCTION AND BONE MINERAL DENSITY IN A COMPREHENSIVE POPULATION SURVEY. THE NORD-TRØNDELAG HEALTH STUDY 1995-97. THE BRONCHIAL OBSTRUCTION IN NORD-TRØNDELAG STUDY
233. Einar Kjelsås: EATING DISORDERS AND PHYSICAL ACTIVITY IN NON-CLINICAL SAMPLES
234. Arne Wibe: RECTAL CANCER TREATMENT IN NORWAY – STANDARDISATION OF SURGERY AND QUALITY ASSURANCE

2004

235. Eivind Witsø: BONE GRAFT AS AN ANTIBIOTIC CARRIER
236. Anne Mari Sund: DEVELOPMENT OF DEPRESSIVE SYMPTOMS IN EARLY ADOLESCENCE
237. Hallvard Lærum: EVALUATION OF ELECTRONIC MEDICAL RECORDS – A CLINICAL TASK PERSPECTIVE
238. Gustav Mikkelsen: ACCESSIBILITY OF INFORMATION IN ELECTRONIC PATIENT RECORDS; AN EVALUATION OF THE ROLE OF DATA QUALITY
239. Steinar Krokstad: SOCIOECONOMIC INEQUALITIES IN HEALTH AND DISABILITY. SOCIAL EPIDEMIOLOGY IN THE NORD-TRØNDELAG HEALTH STUDY (HUNT), NORWAY
240. Arne Kristian Myhre: NORMAL VARIATION IN ANOGENITAL ANATOMY AND MICROBIOLOGY IN NON-ABUSED PRESCHOOL CHILDREN
241. Ingunn Dybedal: NEGATIVE REGULATORS OF HEMATOPOIETEC STEM AND PROGENITOR CELLS
242. Beate Sitter: TISSUE CHARACTERIZATION BY HIGH RESOLUTION MAGIC ANGLE SPINNING MR SPECTROSCOPY
243. Per Arne Aas: MACROMOLECULAR MAINTENANCE IN HUMAN CELLS – REPAIR OF URACIL IN DNA AND METHYLATIONS IN DNA AND RNA
244. Anna Bofin: FINE NEEDLE ASPIRATION CYTOLOGY IN THE PRIMARY INVESTIGATION OF BREAST TUMOURS AND IN THE DETERMINATION OF TREATMENT STRATEGIES
245. Jim Aage Nøttestad: DEINSTITUTIONALIZATION AND MENTAL HEALTH CHANGES AMONG PEOPLE WITH MENTAL RETARDATION
246. Reidar Fossmark: GASTRIC CANCER IN JAPANESE COTTON RATS
247. Wibeke Nordhøy: MANGANESE AND THE HEART, INTRACELLULAR MR RELAXATION AND WATER EXCHANGE ACROSS THE CARDIAC CELL MEMBRANE

2005

248. Sturla Molden: QUANTITATIVE ANALYSES OF SINGLE UNITS RECORDED FROM THE HIPPOCAMPUS AND ENTORHINAL CORTEX OF BEHAVING RATS
249. Wenche Brenne Drøyvold: EPIDEMIOLOGICAL STUDIES ON WEIGHT CHANGE AND HEALTH IN A LARGE POPULATION. THE NORD-TRØNDELAG HEALTH STUDY (HUNT)
250. Ragnhild Støen: ENDOTHELIUM-DEPENDENT VASODILATION IN THE FEMORAL ARTERY OF DEVELOPING PIGLETS

251. Aslak Steinsbekk: HOMEOPATHY IN THE PREVENTION OF UPPER RESPIRATORY TRACT INFECTIONS IN CHILDREN
252. Hill-Aina Steffenach: MEMORY IN HIPPOCAMPAL AND CORTICO-HIPPOCAMPAL CIRCUITS
253. Eystein Stordal: ASPECTS OF THE EPIDEMIOLOGY OF DEPRESSIONS BASED ON SELF-RATING IN A LARGE GENERAL HEALTH STUDY (THE HUNT-2 STUDY)
254. Viggo Pettersen: FROM MUSCLES TO SINGING: THE ACTIVITY OF ACCESSORY BREATHING MUSCLES AND THORAX MOVEMENT IN CLASSICAL SINGING
255. Marianne Fyhn: SPATIAL MAPS IN THE HIPPOCAMPUS AND ENTORHINAL CORTEX
256. Robert Valderhaug: OBSESSIVE-COMPULSIVE DISORDER AMONG CHILDREN AND ADOLESCENTS: CHARACTERISTICS AND PSYCHOLOGICAL MANAGEMENT OF PATIENTS IN OUTPATIENT PSYCHIATRIC CLINICS
257. Erik Skaaheim Haug: INFRARENAL ABDOMINAL AORTIC ANEURYSMS – COMORBIDITY AND RESULTS FOLLOWING OPEN SURGERY
258. Daniel Kondziella: GLIAL-NEURONAL INTERACTIONS IN EXPERIMENTAL BRAIN DISORDERS
259. Vegard Heimly Brun: ROUTES TO SPATIAL MEMORY IN HIPPOCAMPAL PLACE CELLS
260. Kenneth McMillan: PHYSIOLOGICAL ASSESSMENT AND TRAINING OF ENDURANCE AND STRENGTH IN PROFESSIONAL YOUTH SOCCER PLAYERS
261. Marit Sæbø Indredavik: MENTAL HEALTH AND CEREBRAL MAGNETIC RESONANCE IMAGING IN ADOLESCENTS WITH LOW BIRTH WEIGHT
262. Ole Johan Kemi: ON THE CELLULAR BASIS OF AEROBIC FITNESS, INTENSITY-DEPENDENCE AND TIME-COURSE OF CARDIOMYOCYTE AND ENDOTHELIAL ADAPTATIONS TO EXERCISE TRAINING
263. Eszter Vanky: POLYCYSTIC OVARY SYNDROME – METFORMIN TREATMENT IN PREGNANCY
264. Hild Fjærtoft: EXTENDED STROKE UNIT SERVICE AND EARLY SUPPORTED DISCHARGE. SHORT AND LONG-TERM EFFECTS
265. Grete Dyb: POSTTRAUMATIC STRESS REACTIONS IN CHILDREN AND ADOLESCENTS
266. Vidar Fykse: SOMATOSTATIN AND THE STOMACH
267. Kirsti Berg: OXIDATIVE STRESS AND THE ISCHEMIC HEART: A STUDY IN PATIENTS UNDERGOING CORONARY REVASCULARIZATION
268. Björn Inge Gustafsson: THE SEROTONIN PRODUCING ENTEROCHROMAFFIN CELL, AND EFFECTS OF HYPERSEROTONINEMIA ON HEART AND BONE

2006

269. Torstein Baade Rø: EFFECTS OF BONE MORPHOGENETIC PROTEINS, HEPATOCYTE GROWTH FACTOR AND INTERLEUKIN-21 IN MULTIPLE MYELOMA
270. May-Britt Tessem: METABOLIC EFFECTS OF ULTRAVIOLET RADIATION ON THE ANTERIOR PART OF THE EYE
271. Anne-Sofie Helvik: COPING AND EVERYDAY LIFE IN A POPULATION OF ADULTS WITH HEARING IMPAIRMENT
272. Therese Standal: MULTIPLE MYELOMA: THE INTERPLAY BETWEEN MALIGNANT PLASMA CELLS AND THE BONE MARROW MICROENVIRONMENT
273. Ingvild Saltvedt: TREATMENT OF ACUTELY SICK, FRAIL ELDERLY PATIENTS IN A GERIATRIC EVALUATION AND MANAGEMENT UNIT – RESULTS FROM A PROSPECTIVE RANDOMISED TRIAL
274. Birger Henning Endreseth: STRATEGIES IN RECTAL CANCER TREATMENT – FOCUS ON EARLY RECTAL CANCER AND THE INFLUENCE OF AGE ON PROGNOSIS
275. Anne Mari Aukan Rokstad: ALGINATE CAPSULES AS BIOREACTORS FOR CELL THERAPY
276. Mansour Akbari: HUMAN BASE EXCISION REPAIR FOR PRESERVATION OF GENOMIC STABILITY
277. Stein Sundstrøm: IMPROVING TREATMENT IN PATIENTS WITH LUNG CANCER – RESULTS FROM TWO MULITCENTRE RANDOMISED STUDIES
278. Hilde Pleym: BLEEDING AFTER CORONARY ARTERY BYPASS SURGERY - STUDIES ON HEMOSTATIC MECHANISMS, PROPHYLACTIC DRUG TREATMENT AND EFFECTS OF AUTOTRANSFUSION
279. Line Merethe Oldervoll: PHYSICAL ACTIVITY AND EXERCISE INTERVENTIONS IN CANCER PATIENTS

280. Boye Welde: THE SIGNIFICANCE OF ENDURANCE TRAINING, RESISTANCE TRAINING AND MOTIVATIONAL STYLES IN ATHLETIC PERFORMANCE AMONG ELITE JUNIOR CROSS-COUNTRY SKIERS
281. Per Olav Vandvik: IRRITABLE BOWEL SYNDROME IN NORWAY, STUDIES OF PREVALENCE, DIAGNOSIS AND CHARACTERISTICS IN GENERAL PRACTICE AND IN THE POPULATION
282. Idar Kirkeby-Garstad: CLINICAL PHYSIOLOGY OF EARLY MOBILIZATION AFTER CARDIAC SURGERY
283. Linn Getz: SUSTAINABLE AND RESPONSIBLE PREVENTIVE MEDICINE. CONCEPTUALISING ETHICAL DILEMMAS ARISING FROM CLINICAL IMPLEMENTATION OF ADVANCING MEDICAL TECHNOLOGY
284. Eva Tegnander: DETECTION OF CONGENITAL HEART DEFECTS IN A NON-SELECTED POPULATION OF 42,381 FETUSES
285. Kristin Gabestad Nørsett: GENE EXPRESSION STUDIES IN GASTROINTESTINAL PATHOPHYSIOLOGY AND NEOPLASIA
286. Per Magnus Haram: GENETIC VS. AQUIRED FITNESS: METABOLIC, VASCULAR AND CARDIOMYOCYTE ADAPTATIONS
287. Agneta Johansson: GENERAL RISK FACTORS FOR GAMBLING PROBLEMS AND THE PREVALENCE OG PATHOLOGICAL GAMBLING IN NORWAY
288. Svein Artur Jensen: THE PREVALENCE OF SYMPTOMATIC ARTERIAL DISEASE OF THE LOWER LIMB
289. Charlotte Björk Ingul: QUANITIFICATION OF REGIONAL MYOCARDIAL FUNCTION BY STRAIN RATE AND STRAIN FOR EVALUATION OF CORONARY ARTERY DISEASE. AUTOMATED VERSUS MANUAL ANALYSIS DURING ACUTE MYOCARDIAL INFARCTION AND DOBUTAMINE STRESS ECHOCARDIOGRAPHY
290. Jakob Nakling: RESULTS AND CONSEQUENCES OF ROUTINE ULTRASOUND SCREENING IN PREGNANCY – A GEOGRAPHIC BASED POPULATION STUDY
291. Anne Engum: DEPRESSION AND ANXIETY – THEIR RELATIONS TO THYROID DYSFUNCTION AND DIABETES IN A LARGE EPIDEMIOLOGICAL STUDY
292. Ottar Bjerkeset: ANXIETY AND DEPRESSION IN THE GENERAL POPULATION: RISK FACTORS, INTERVENTION AND OUTCOME – THE NORD-TRØNDELAG HEALTH STUDY (HUNT)
293. Jon Olav Drogset: RESULTS AFTER SURGICAL TREATMENT OF ANTERIOR CRUCIATE LIGAMENT INJURIES – A CLINICAL STUDY
294. Lars Fosse: MECHANICAL BEHAVIOUR OF COMPACTED MORSELLISED BONE – AN EXPERIMENTAL IN VITRO STUDY
295. Gunilla Klensmeden Fosse: MENTAL HEALTH OF PSYCHIATRIC OUTPATIENTS BULLIED IN CHILDHOOD
296. Paul Jarle Mork: MUSCLE ACTIVITY IN WORK AND LEISURE AND ITS ASSOCIATION TO MUSCULOSKELETAL PAIN
297. Björn Stenström: LESSONS FROM RODENTS: I: MECHANISMS OF OBESITY SURGERY – ROLE OF STOMACH. II: CARCINOGENIC EFFECTS OF *HELICOBACTER PYLORI* AND SNUS IN THE STOMACH

2007

298. Haakon R. Skogseth: INVASIVE PROPERTIES OF CANCER – A TREATMENT TARGET ? IN VITRO STUDIES IN HUMAN PROSTATE CANCER CELL LINES
299. Janniche Hammer: GLUTAMATE METABOLISM AND CYCLING IN MESIAL TEMPORAL LOBE EPILEPSY
300. May Britt Drugli: YOUNG CHILDREN TREATED BECAUSE OF ODD/CD: CONDUCT PROBLEMS AND SOCIAL COMPETENCIES IN DAY-CARE AND SCHOOL SETTINGS
301. Arne Skjold: MAGNETIC RESONANCE KINETICS OF MANGANESE DIPYRIDOXYL DIPHOSPHATE (MnDPDP) IN HUMAN MYOCARDIUM. STUDIES IN HEALTHY VOLUNTEERS AND IN PATIENTS WITH RECENT MYOCARDIAL INFARCTION
302. Siri Malm: LEFT VENTRICULAR SYSTOLIC FUNCTION AND MYOCARDIAL PERFUSION ASSESSED BY CONTRAST ECHOCARDIOGRAPHY
303. Valentina Maria do Rosario Cabral Iversen: MENTAL HEALTH AND PSYCHOLOGICAL ADAPTATION OF CLINICAL AND NON-CLINICAL MIGRANT GROUPS
304. Lasse Løvstakken: SIGNAL PROCESSING IN DIAGNOSTIC ULTRASOUND: ALGORITHMS FOR REAL-TIME ESTIMATION AND VISUALIZATION OF BLOOD FLOW VELOCITY

305. Elisabeth Olstad: GLUTAMATE AND GABA: MAJOR PLAYERS IN NEURONAL METABOLISM
306. Lilian Leistad: THE ROLE OF CYTOKINES AND PHOSPHOLIPASE A_2S IN ARTICULAR CARTILAGE CHONDROCYTES IN RHEUMATOID ARTHRITIS AND OSTEOARTHRITIS
307. Arne Vaaler: EFFECTS OF PSYCHIATRIC INTENSIVE CARE UNIT IN AN ACUTE PSYCIATHRIC WARD
308. Mathias Toft: GENETIC STUDIES OF LRRK2 AND PINK1 IN PARKINSON'S DISEASE
309. Ingrid Løvold Mostad: IMPACT OF DIETARY FAT QUANTITY AND QUALITY IN TYPE 2 DIABETES WITH EMPHASIS ON MARINE N-3 FATTY ACIDS
310. Torill Eidhammer Sjøbakk: MR DETERMINED BRAIN METABOLIC PATTERN IN PATIENTS WITH BRAIN METASTASES AND ADOLESCENTS WITH LOW BIRTH WEIGHT
311. Vidar Beisvåg: PHYSIOLOGICAL GENOMICS OF HEART FAILURE: FROM TECHNOLOGY TO PHYSIOLOGY
312. Olav Magnus Søndenå Fredheim: HEALTH RELATED QUALITY OF LIFE ASSESSMENT AND ASPECTS OF THE CLINICAL PHARMACOLOGY OF METHADONE IN PATIENTS WITH CHRONIC NON-MALIGNANT PAIN
313. Anne Brantberg: FETAL AND PERINATAL IMPLICATIONS OF ANOMALIES IN THE GASTROINTESTINAL TRACT AND THE ABDOMINAL WALL
314. Erik Solligård: GUT LUMINAL MICRODIALYSIS
315. Elin Tollefsen: RESPIRATORY SYMPTOMS IN A COMPREHENSIVE POPULATION BASED STUDY AMONG ADOLESCENTS 13-19 YEARS. YOUNG-HUNT 1995-97 AND 2000-01; THE NORD-TRØNDELAG HEALTH STUDIES (HUNT)
316. Anne-Tove Brenne: GROWTH REGULATION OF MYELOMA CELLS
317. Heidi Knobel: FATIGUE IN CANCER TREATMENT – ASSESSMENT, COURSE AND ETIOLOGY
318. Torbjørn Dahl: CAROTID ARTERY STENOSIS. DIAGNOSTIC AND THERAPEUTIC ASPECTS
319. Inge-Andre Rasmussen jr.: FUNCTIONAL AND DIFFUSION TENSOR MAGNETIC RESONANCE IMAGING IN NEUROSURGICAL PATIENTS
320. Grete Helen Bratberg: PUBERTAL TIMING – ANTECEDENT TO RISK OR RESILIENCE ? EPIDEMIOLOGICAL STUDIES ON GROWTH, MATURATION AND HEALTH RISK BEHAVIOURS; THE YOUNG HUNT STUDY, NORD-TRØNDELAG, NORWAY
321. Sveinung Sørhaug: THE PULMONARY NEUROENDOCRINE SYSTEM. PHYSIOLOGICAL, PATHOLOGICAL AND TUMOURIGENIC ASPECTS
322. Olav Sande Eftedal: ULTRASONIC DETECTION OF DECOMPRESSION INDUCED VASCULAR MICROBUBBLES
323. Rune Bang Leistad: PAIN, AUTONOMIC ACTIVATION AND MUSCULAR ACTIVITY RELATED TO EXPERIMENTALLY-INDUCED COGNITIVE STRESS IN HEADACHE PATIENTS
324. Svein Brekke: TECHNIQUES FOR ENHANCEMENT OF TEMPORAL RESOLUTION IN THREE-DIMENSIONAL ECHOCARDIOGRAPHY
325. Kristian Bernhard Nilsen: AUTONOMIC ACTIVATION AND MUSCLE ACTIVITY IN RELATION TO MUSCULOSKELETAL PAIN
326. Anne Irene Hagen: HEREDITARY BREAST CANCER IN NORWAY. DETECTION AND PROGNOSIS OF BREAST CANCER IN FAMILIES WITH *BRCA1*GENE MUTATION
327. Ingebjørg S. Juel : INTESTINAL INJURY AND RECOVERY AFTER ISCHEMIA. AN EXPERIMENTAL STUDY ON RESTITUTION OF THE SURFACE EPITHELIUM, INTESTINAL PERMEABILITY, AND RELEASE OF BIOMARKERS FROM THE MUCOSA
328. Runa Heimstad: POST-TERM PREGNANCY
329. Jan Egil Afset: ROLE OF ENTEROPATHOGENIC *ESCHERICHIA COLI* IN CHILDHOOD DIARRHOEA IN NORWAY
330. Bent Håvard Hellum: *IN VITRO* INTERACTIONS BETWEEN MEDICINAL DRUGS AND HERBS ON CYTOCHROME P-450 METABOLISM AND P-GLYCOPROTEIN TRANSPORT
331. Morten André Høydal: CARDIAC DYSFUNCTION AND MAXIMAL OXYGEN UPTAKE MYOCARDIAL ADAPTATION TO ENDURANCE TRAINING

2008

332. Andreas Møllerløkken: REDUCTION OF VASCULAR BUBBLES: METHODS TO PREVENT THE ADVERSE EFFECTS OF DECOMPRESSION

333. Anne Hege Aamodt: COMORBIDITY OF HEADACHE AND MIGRAINE IN THE NORD-TRØNDELAG HEALTH STUDY 1995-97
334. Brage Høyem Amundsen: MYOCARDIAL FUNCTION QUANTIFIED BY SPECKLE TRACKING AND TISSUE DOPPLER ECHOCARDIOGRAPHY – VALIDATION AND APPLICATION IN EXERCISE TESTING AND TRAINING